Fall 12-17-2011

Mineralogy and Geochemistry of Anorogenic Granitic Miarolitic Pegmatites Associated with the White Mountain Intrusive Suite, New Hampshire

Kristen F. Camp
University of New Orleans, kfcamp@uno.edu

Mineralogy and Geochemistry of Anorogenic Granitic Miarolitic Pegmatites Associated with the White Mountain Intrusive Suite, New Hampshire

A Thesis

Submitted to the Graduate Faculty of the

University of New Orleans

in partial fulfillment of the

requirements for the degree of

Master of Science

in Earth and Environmental Sciences

by

Kristen Camp

B.S., University of New Orleans, 2009

December 2011

This thesis is dedicated to my mother

and the greatest influence on my life,

Cynthia Camp.

ACKNOWLEDGEMENTS

This research would not have been possible without the assistance of numerous people over the past 2 years. I wish to express my undying gratitude to my thesis committee, William B. Simmons, Alexander U. Falster, and Karen Webber, for providing invaluable guidance, support, and wisdom. Deepest gratitude is also due to the pegmatite enthusiasts, Bob Whitmore, Donald Dallaire, Gordon Jackson, and Carlton Holt, who aided in the sample collection and my survival in the White Mountains of New Hampshire. Also, gratitude is due to my colleague and best friend, Gordon Borne Jr., for assisting with the sample collection and his ability to use a sledgehammer far better than myself. Appreciation is also extended to Gordon and Pam Jackson for opening her home and hearts to me during my stay in New Hampshire.

This paper and the analyses have benefitted from the multiple, constructive reviews and suggestions by Alexander U. Falster and William B. Simmons. Their leadership, attention to detail, and scholarship has inspired me to do my best in many aspects of my life. Finally, I am thankful to the University of New Orleans, the Capital Mineral Club of New Hampshire, and the Hew Hampshire Geological Survey who financially contributed to the research and travel costs associated with this thesis.

TABLE OF CONTENTS

LIST OF FIGURES

LIST OF TABLES

ABSTRACT

Subvolcanically emplaced granitic, miarolitic pegmatites associated with the White Mountain Igneous Province (WMIP), New Hampshire, were sampled and analyzed using modern analytical techniques including X-ray fluorescence, electron microprobe, scanning electron microscopy, and direct-coupled plasma spectrophotometry. Analytical results suggest that all the sampled miarolitic pegmatites from this study are petrogenetically related to the same intrusive suite, the WMIP. Based on the geochemical data, all the samples formed in an anorogenic tectonic setting and are rift-related. They are classified as NYF-type and plot in the "within plate granite" field on tectonic discrimination diagrams. The majority of the samples are peraluminous, A_1-type granites. The trace element abundances on the spider diagram and chondrite-normalized diagram, which include a pronounced negative Eu anomaly and REE enrichments, are consistent with these miarolitic pegmatites resulting from a strongly fractionated granitic parental melts, but less fractionated than the classic NYF-systems such as South Platte (Simmons et al. 1987) and the Wausau Syenite Complex (Meyers et al. 1984).

Keywords: NYF-pegmatite, White Mountain batholith, geochemical fractionation, igneous petrology, New Hampshire geochemistry

INTRODUCTION

The primary objective of this study was to interpret the spatial, temporal, and geochemical relationships between multiple NYF-type miarolitic pegmatites petrogenetically associated with the WMIP, New Hampshire (Figure 1). This was accomplished by field collecting samples from the miarolitic pegmatites' non-miarolitic granite and "*wall zone analogue*" granite, which is a term that will be used to describe the granite between miaroles.

The collected samples were prepared for the different analytical techniques, and the results were plotted on various diagrams to show the chemical relationships between these petrogenetically related miarolitic pegmatites. Previous research on the various magma series of the WMIP has been published in a number of scientific papers; however those studies only concentrated on a specific aspect of an individual miarolitic pegmatite. This study represents the first detailed geochemical study of the whole rock chemistry and mineral chemistry of multiple miarolitic pegmatites from all over the WMIP. The results of this study will be a useful addition to the database of knowledge for similar igneous environments.

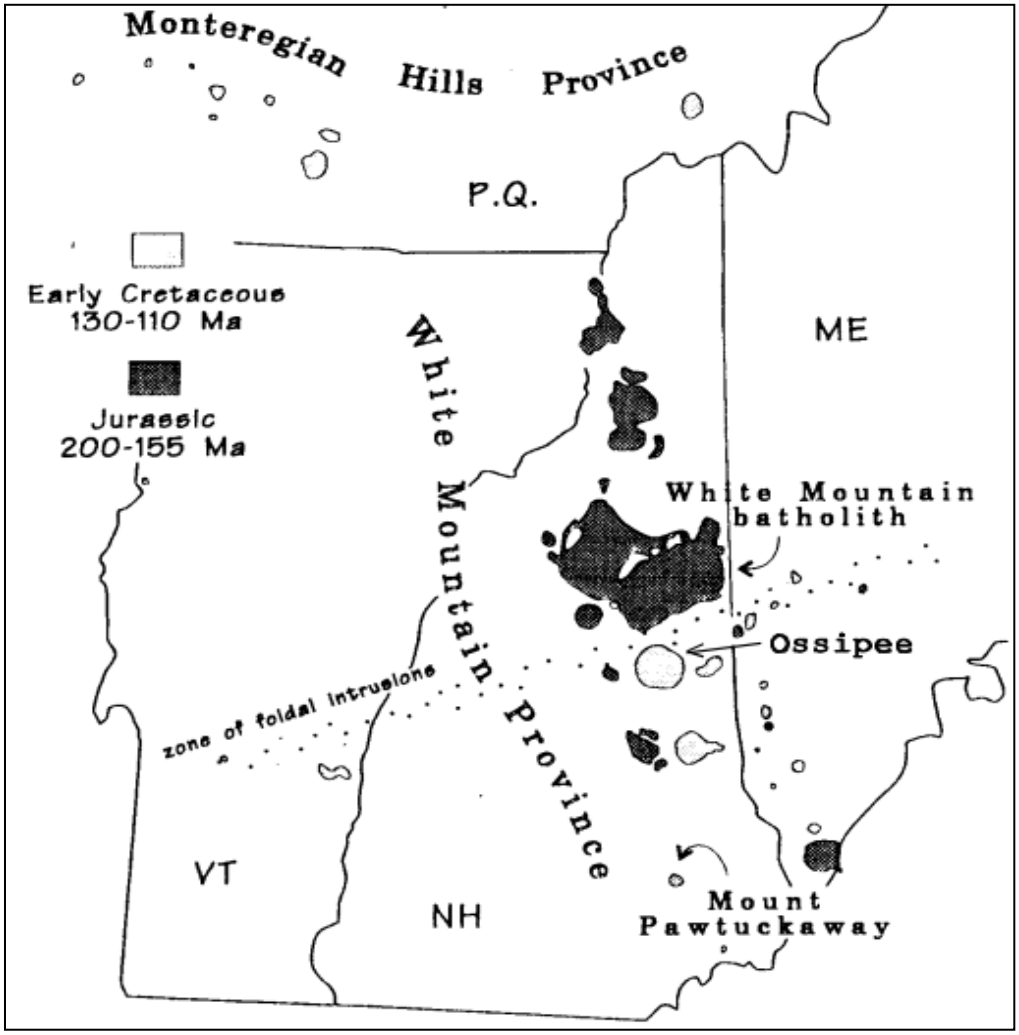

Figure 1. Geologic map of the WMIP (older magma series is indicated in black and the younger magma series is indicated by the white shapes) (Creasy & Eby 1993).

GENERAL GEOLOGY

The Jurassic period was a geologically active time in present day New Hampshire. The WMIP marks the areas where magma came close to the surface and either crystallized intrusively or erupted volcanically. This area is geologically well known for its classic, nearly concentric ring dike complexes, such as the Ossipee. The WMIP is dominantly located in central New Hampshire and is part of the New England-Quebec Province (Eby 1995).

The WMIP is represented by two periods of igneous activity, referred to as the older magma series and the younger magma series. The older magma series, which is volumetrically the larger of the two, was emplaced 200-155 Ma. The largest intrusive unit within the WMIP is the White Mountain batholith (WMB) which belongs to the older magma series (Eby 1995) (Figure 2). The younger magma series was emplaced 130-110 Ma and consists of small pluton plugs and the famous ring-like structures (Eby 2002) (Figure 3). These two periods of igneous activity are related to the rifting event responsible for the opening of the North Atlantic Ocean post Pangaea collisions (McHone and Butler 1984).

All lithologies within the WMIP are silica-saturated to silica-oversaturated, with silica-undersaturated rocks found at only two localities, neither of which are included in this study (Eby 1995). The differences in magma composition depend on the degree of melting in the source region and the amount of crustal interaction (Eby 2002).

White Mountain batholith geology

The WMB is the largest intrusive complex in the WMIP with an aerial extent of 1,000 km^2 (Figure 2). It comprises 50% of the total older magma series and is located in central New Hampshire (Eby & Krueger 1992). The majority of the samples for this thesis were collected from all over WMB. The batholith consists of numerous overlapping centers of felsic magmatism and thick sections of rhyolitic crystal tuffs, breccias, and subvolcanic granite porphyry, which are all bordered by porphyritic quartz syenite ring dikes (Creasy and Eby 1993). The major rock types that account for 97% of the WMB are granites, syenites, and quartz syenites; volcanic rocks of similar composition account for the remainder of the rocks. All of the units were emplaced into Lower Paleozoic schists, gneisses, and granites, which are locally preserved as screens within the WMB (Creasy & Eby 1993).

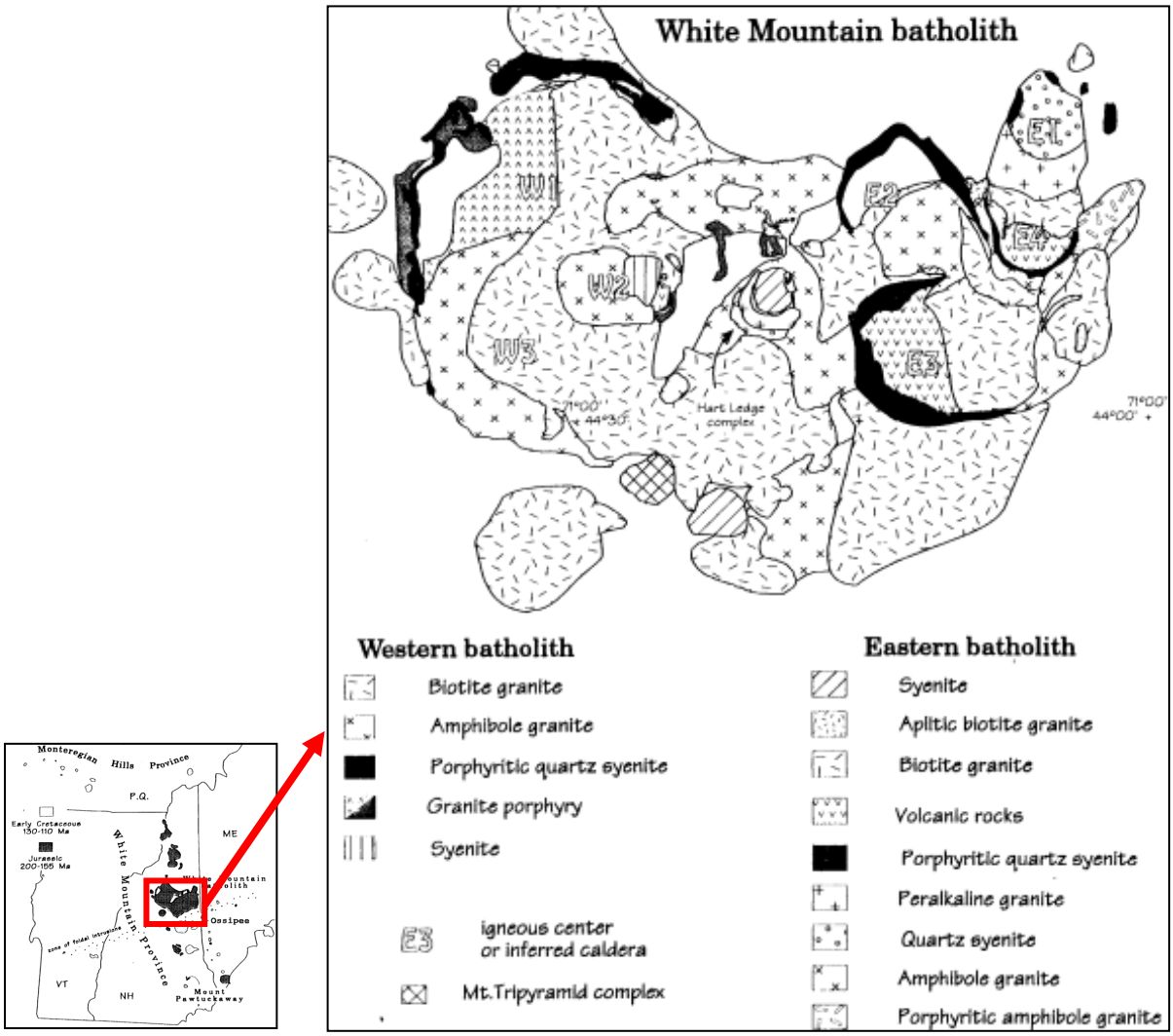

Figure 2. Geologic map of the WMB (Creasy & Eby 1993).

Two distinct medium-grained granites comprise approximately 80% of the WMB. The first is the Mount Osceola Granite, which is a green, subalkaline to peralkaline amphibole granite tending to be uniform in texture, chemistry, and radiometric age (~187 Ma) (Eby 1995). The second is the Conway Granite, which is a pink, subalkaline biotite granite that shows wide ranges and variations in texture, chemistry, and radiometric age (183-155 Ma) (Eby 1995). The second most abundant lithologies that make up the WMB are the syenite and quartz-syenite porphyries which comprise the ring dikes as well as several small plugs. The remaining 3% of the batholith is comprised by volcanic rocks of similar composition that mainly lie in the eastern portion of the batholith. This volcanic sequence consists of tuff, trachyte, breccia, rhyolite, and comendite (Creasy & Eby 1993).

Radiometric ages indicate igneous activity started in the western portion of the batholith with the intrusion of several ring dikes and granite porphyries between 200-190 Ma (Creasy & Eby 1993). These intrusive events were followed by the emplacement of the Mount Osceola Granite and then the Conway granite plutons throughout the entire batholith. Simultaneously, the porphyritic quartz syenite ring-dikes were emplaced as volcanic eruptions occurred in the eastern portion of the batholith (173-168 Ma) (Eby & Creasy 1992). The igneous activity ended with the emplacement of a small Conway Granite pluton at 155 Ma (Eby 1995). The batholith has been interpreted as a subhorizontal slice through a caldera field at a depth of 1-2 km below the original land surface (Creasy & Eby, 1993).

Ossipee complex geology

The younger magma series is volumetrically smaller than the older series, but unlike the older series, it has a significant amount of mafic rocks. This complex is 14 km in diameter and is considered to be a classic example of a ring-dike complex (Billings 1943; Chapman 1976). Only one sample was collected from the younger magma series for this study, and that sample came from the Ossipee ring-dike complex (Figure 3), which is located just south of the WMB in central New Hampshire. The rock types that comprise this complex are quartz syenite, Conway granite, and an abundance of mafic rocks (Creasy & Eby 1993).

The outer ring dike is an almost complete circle and forms a topographically elevated ridge around the inner basin which is underlain by granite. The outer ring-dike consists primarily of medium to coarse-grained quartz syentite, some pink granite, and porphyritic rhyolite (Creasy & Eby 1993). Whereas mafic rocks are scarce in the older White Mountain magma series, they are relatively abundant in the younger magma series and are most significant in the Ossipee ring structure. Geophysical data helps explain why the Ossipee complex is the only mafic structure in the WMIP as mafic rocks were abundant in the conduit that fed the structure (Eby 2002). The majority of these mafic rocks are basalts, and the basalt generally occurs as blocks within rhyolite suggesting that basaltic and rhyolitic volcanism was contemporaneous (Eby & Kennedy 2004). Both subvolcanically intrusive and erupted rhyolitic phases have been identified, and there are also thinly laminated beds of andesitic and basaltic

ash in the northeastern portion of the complex. The eastern portion of the complex is underlain by Conway Granite (Creasy & Eby 1993). Gravity and magnetic data indicate that the complex has a vertical core of mafic rock with a thin granitic carapace (Sharp & Simmons, 1978).

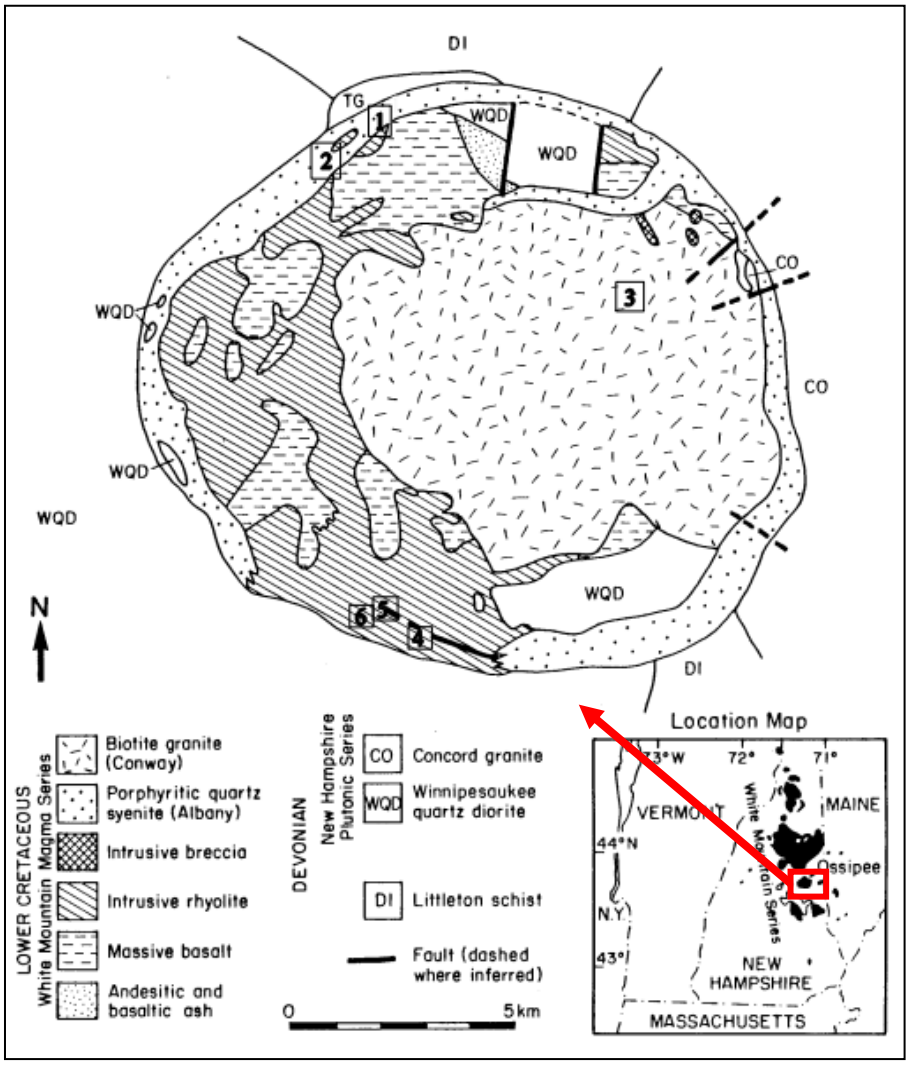

Figure 3. Geologic map of the Ossipee complex (Creasy & Eby 1993)

INDIVIDUAL SAMPLE LOCATIONS

In order to understand the overall geochemistry of the entire WMIP, samples were taken from numerous miarolitic pegmatites that geographically range all over the province (Figure 4). The miarolitic pegmatites sampled in this study include North Percy Peak, North Sugarloaf, West Hurricane, East Hurricane, Blackcap, Redstone Quarry, Government Pit, Brook Diggings, Ravine, Mousetrap, Oliver Trench, Oliver Diggings, Large Boulder near Oliver Diggings, Eastman Topaz, and Raccoon Gulch. The geospatial coordinates for each of these locations were taken onsite and then plotted using Google Earth overtop a lithologic map of New Hampshire provided by the USGS (Figure 4).

The sample locations geographically range from the biotite granites in north New Hampshire to the quartz syenite Ossipee complex in south central New Hampshire. Thus, this study represents a complete sampling of the WMIP. For plotting purposes, the sample locations were grouped together lithologically and then spatially (Figure 5).

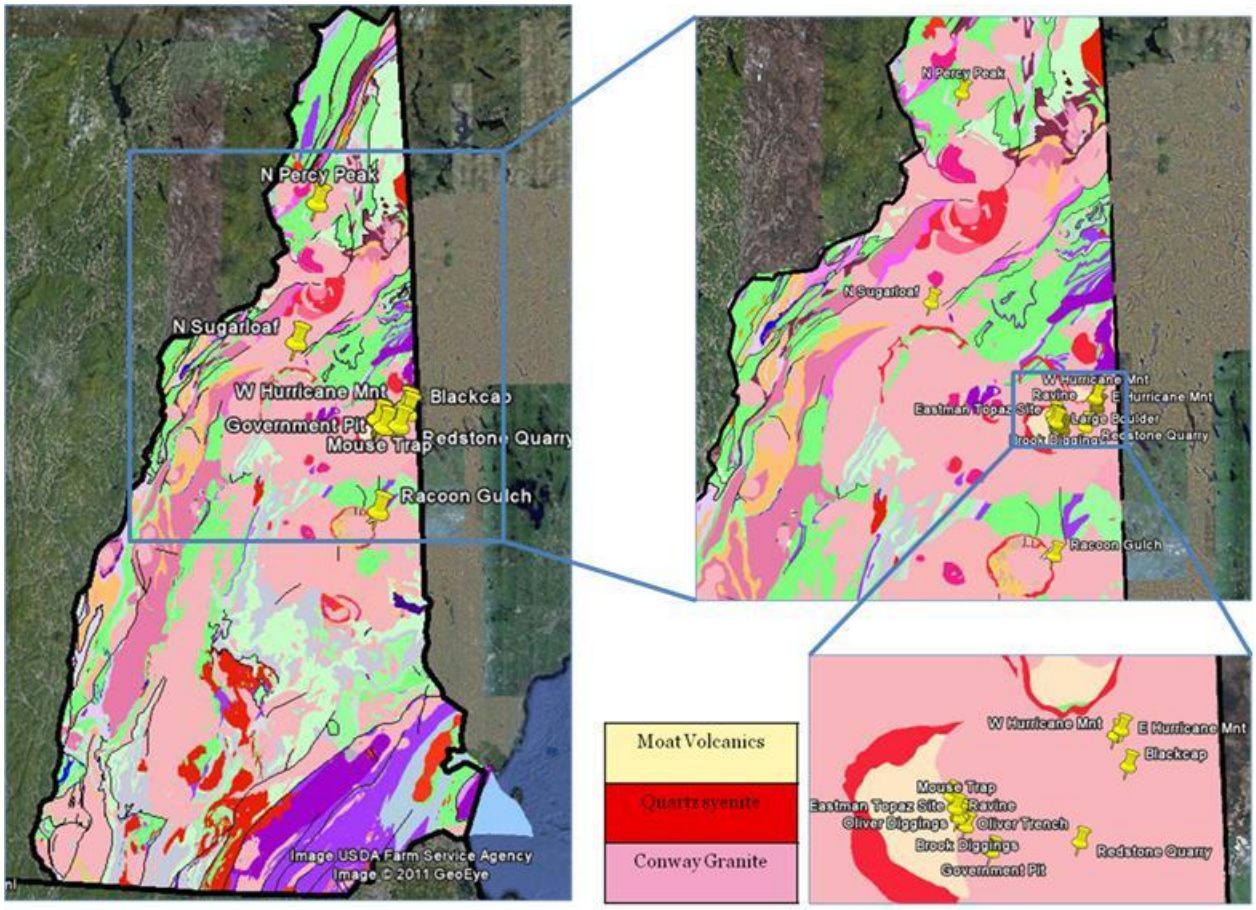

Figure 4. USGS lithologic map of New Hamsphire with sample locations marked using yellow pushpins and a key that represents the three lithologies represented by the samples (www.gelib.com).

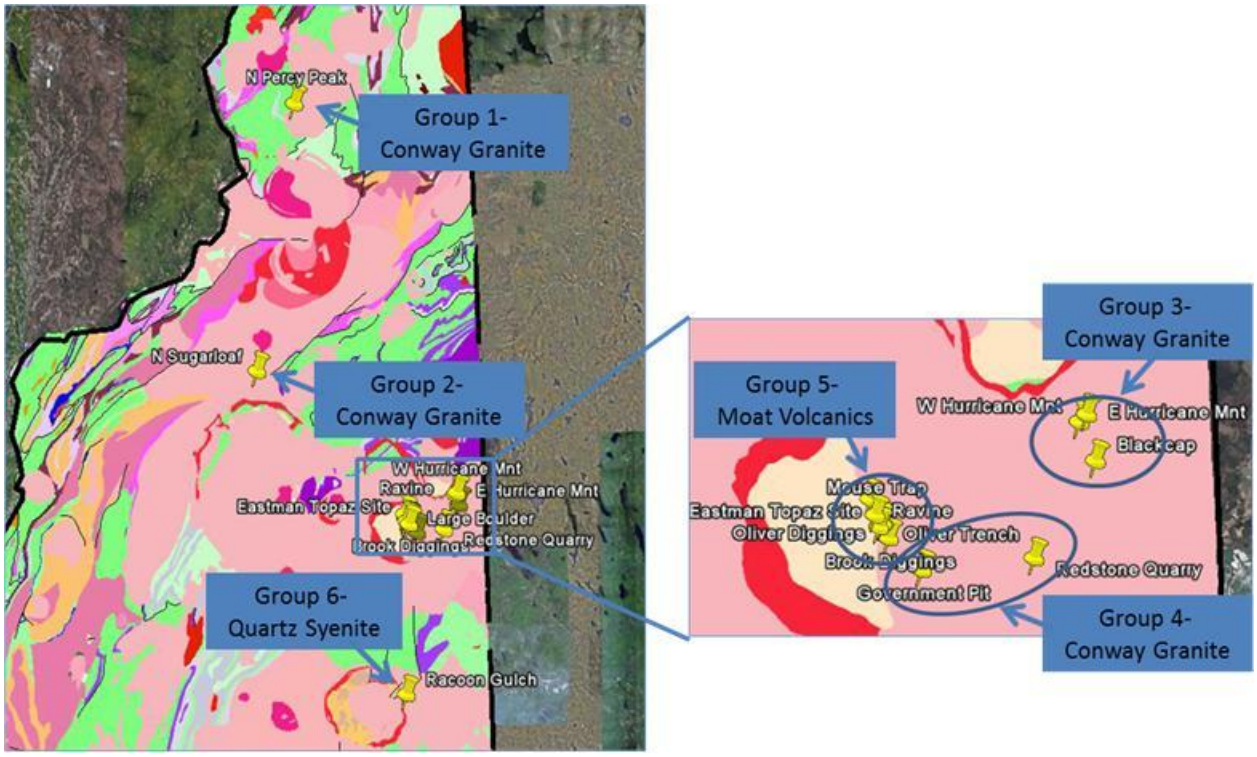

Figure 5. USGS lithologic map of New Hampshire showing the grouping of the sample locations (www.gelib.com).

PEGMATITE CLASSIFICATION

Černý & Ercit's (2005) classification scheme on pegmatites is widely accepted and categorizes pegmatites into four primary classes based on the depth of emplacement and the metamorphic grade of the igneous bodies. These classes are Abyssal, Muscovite, Rare-Element, and Miarolitic. The Rare-Element class is subdivided based on elemental abundances into NYF- (niobium, yttrium, fluorine) and LCT- (lithium, cesium, tantalum) families (Table 1) (Černý & Ercit 2005). This subclassification provides insight into the origin of the melts and their degree of crystal fractionation. All the WMIP samples collected for this thesis can be classified as Rare-Element Class based on their shallow emplacement, high REE-enrichment, and mineralogical diversity, and they can be further classified as NYF-type based on their elemental abundances of Nb, Y, and F.

These Rare-Element miarolitic pegmatites formed through a process called volatile decompression (Simmons 2007). After a pool of magma at the base of the lithosphere was fractionated to produce a more felsic, less dense melt, it began to rise through the lithosphere. As the melt rises to a shallow level, the pressure decreases causing the volatiles in the melt to quickly exsolve and form vapor filled bubbles. Minerals, highly concentrated in incompatible elements, can start to crystallize into the bubbles forming the euhedral crystals and rare minerals commonly seen in these miarolitic pegmatites (Simmons 2007).

THE FAMILY SYSTEM OF PETROGENETIC CLASSIFICATION OF GRANITIC PEGMATITES OF PLUTONIC DERIVATION Černý & Ercit 2005

Family	Pegmatite subclass	Geochemical signature	Pegmatite bulk composition	Associated granites	Granite bulk composition*	Source lithologies**
LCT	REL-Li MI-Li	Li, Rb, Cs, Be, Sn, Ga, Ta>Nb, (B, P, F)	peraluminous to subaluminous	**synorogenic to late-orogenic (to anorogenic);** largely heterogeneous	peraluminous, S, I or mixed S+I types	Undepleted upper- to middle-crust supracrustals and basement gneisses
NYF	REL -REE MI-REE	Nb>Ta, Ti Y, Sc, REE, Zr, U, Th, F	subaluminous to metaluminous (to subalkaline)	**syn-, late, post- to mainly anorogenic;** quasi-homogeneous	pera!uminous to subaluminous and metaluminous; A and I types	depleted middle to lower crustal granulites, or juvenile granitoids
Mixed	Cross-bred: LCT & NYF	mixed	metaluminous to moderately peraluminous	**postorogenic to anorogenic;** heterogeneous	subaluminous to slightly peraluminous	mixed protoliths or assimilation of supracrustals by NYF granites

Table 1. The Family System of Petrogenetic Classification of Granitic Pegmatites of Plutonic Derivation (Černý & Ercit 2005).

In 1999, Wise expanded the classification of NYF-type pegmatites using key mineralogical assemblages. He subdivided them into 3 groups: peralkaline, metaluminous, and peraluminous (Table 2). All the samples for this thesis are peraluminous, or Al-rich, which is supported by the Shand's Index (Figure 58) and the abundance of topaz, which typically occurs in Al-rich environments, in these locations.

Wise related NYF-type pegmatites to A-type granites, which are igneous bodies associated with an anorogenic origin (Wise 1999). A-type granites are subdivided into A_1-type granites and A_2-type granites (Eby 2006). A_1-type granites are consistently associated with true anorogenic rift zone, within-plate granite settings. They are differentiates of basaltic magma derived from an ocean island basalt (OIB)-like source (Figure 6) (Eby 2002). A_2-type granites are associated with post-collisional settings that originated by melting of mantle material followed by crustal contamination in some areas (Loiselle & Wones 1979). All of the miarolitic pegmatites sampled for this study are A_1-type granites.

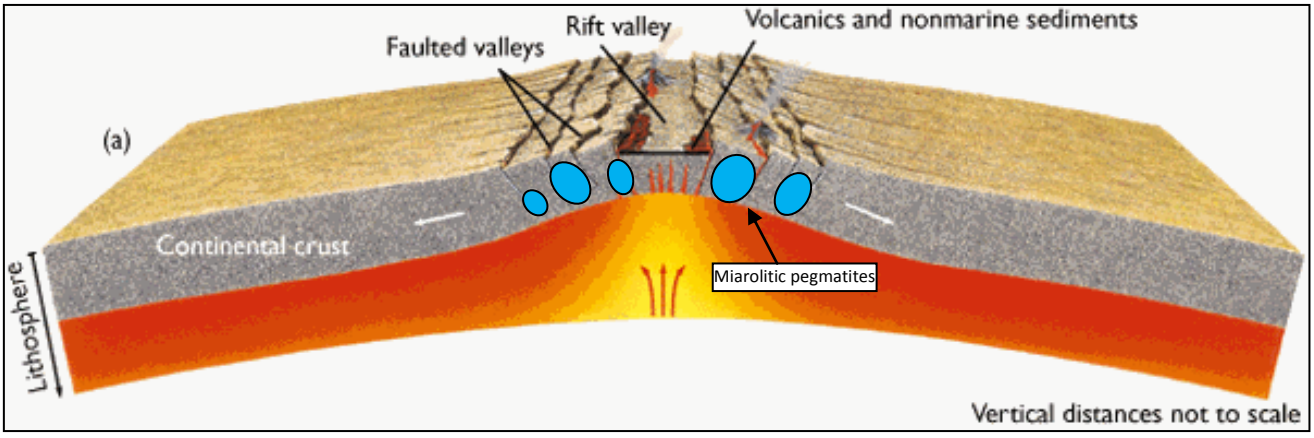

Figure 6. A_1-type granite, NYF tectonic setting (Modified from www.northwestern.edu).

CLASSIFICATION OF NYF-TYPE PEGMATITES MIKE WISE (1999)				
PEGMATITE TYPE	**PEGMATITE SUBTYPE**	**ASSOCIATED ACCESSORY MINERALS**	**GEO-CHEMICAL SIGNATURE**	**EXAMPLES**
PERALKALINE GROUP				
Fayalite		magnetite, (hematite, ilmenite, epidote, titanite, allanite)	Fe (Ti, Ca)	Velence Mtns., Hungary; Sawtooth batholith, Idaho; Rockport, Massachusetts; Strzegom-Sobotka, Poland; Mt. Perdosu, Sardinia
Amphibole	Aegirine-Arfvedsonite	fluorite, allanite, zircon (columbite fergusonite, monazite, pyrochlore)	Na, Fe, Zr, F (± Ti, REE, Nb)	Zomba, Malawi ; Strange Lake Complex, Quebec ; Stettin Complex, Wisconsin
	Riebeckite	zircon, fluorite, (magnetite, rutile, ilmenite, monazite, columbite, pyrochlore)		Mt. Rosa (St Peter's Dome), Colorado; Quincy, Massachussetts; Hurricane Mtn., New Hampshire; Granite Peak, Franklin Mtns., Texas
	Allanite	zircon, (beryl, apatite)		Pacoima Canyon, California
METALUMINOUS GROUP				
Allanite	Allanite	(fluorite, magnetite, monazite, zircon, ilmenite, rutile)	LREE (± Ti, Zr, F)	South Platte (south), Colorado Red Rock, Nevada; Gold Butte, Clark Co., Nevada; Amherst Co., Virginia
	Euxenite (Polycrase)	monazite, zircon, xenotime, ilmenite, (fergusonite, aeschynite, rutile, tourmaline)	LREE→HREE Nb > Ta, Ti, Zr, Y, P	Trout Creek, Colorado; Gloserheia, Norway; West Portland, Quebec; Evans-Lou, Quebec
	Gadolinite	fergusonite, xenotime, samarskite, zircon, (euxenite, ilmenite, rutile, magnetite, fluorite)	Y+HREE, Nb > Ta, Be, Ti, Zr, P, (F)	South Platte (north), Colorado Pyörönmaa, Finland Ytterby Sweden; Barringer Hill, Texas; Clear Creek, Texas
PERALUMINOUS GROUP				
Beryl	Beryl	zinnwaldite, spessartine, fluorite, hematite, muscovite	Be (Li, F)	Mt. Antero, Colorado Sawtooth batholith, Idaho
	Tourmaline	topaz, lepidolite, fluorite. danburite, hambergite	Be, B, Li, F	Leduc, Quebec, Rangkul, Pamirs, Tadjikistan, Russia; Borshchovochny, Transbaikalia, Russia
	Topaz	muscovite, monazite, euxenite, fluorite, columbite,	Be, F (± B, Li)	Luumäki, Finland; Klein Spitzkoppe, Namibia; Tordal, Norway; Volhynia, Ukraine;
		zinnwaldite (phenakite, lepidolite, schorl, zircon, cassiterite)		Morefield-Rutherford-Herbb #2, Virginia
Phenakite		muscovite, fluorite, (topaz, beryl, bertrandite, ilmenite, zircon)	Be, F	Mt. Antero, Colorado; Pikes Peak, Colorado; South Baldface Mtn., New Hampshire; Nine Mile Pluton, Wisconsin
Topaz		zinnwaldite, muscovite, fluorite, hematite, spessartine, cassiterite	F, (Be, Li, Sn)	Mt. Antero, Colorado; Sawtooth batholith, Idaho
Fluorite		calcite, hematite	F	Khantau massif, Kazakhstan

Table 2. Classification of NYF pegmatites (Wise 1999).

METHODOLOGY

Field Methods

Field sampling of the WMIP was performed in June, 2010. With the help of local friends who happened to be finely seasoned pegmatite enthusiasts, locating the multiple areas of interests was much easier than expected. Upon arriving at each location, geospatial coordinates were instrumentally taken, if service permitted. Once the exposed area of interest was located, it was photographed with a pen or chisel for scale and then, using a sledge hammer, rock hammer, and/or chisel, a freshly exposed piece of the rock was sampled (Figure 7). These samples were stored in plastic bags labeled with the sample location and details.

Once sampling of the WMIP was complete, the pegmatite "*wall zone analogue*" samples were brought back to the MP^2 lab at the University of New Orleans. The samples were then photographed individually with a scale and stored in plastic shoe box containers, which were labeled with sample location and details. Each sample was then divided into a few large pieces that would later be used to make thin sections and conduct analyses using a direct-coupled plasma spectrophotometer, scanning electron microscope, electron microprobe, and X-ray fluorescence spectrometer.

Figure 7. Miarolitic pegmatite "*wall zone analogue*" (22 cm chisel for scale).

Thin Sections

To prepare the samples for thin section analysis, a 27x46 mm rectangle was taken from each rock using a diamond blade rock saw cooled with cold water (Figure 8). These rectangular subsamples were labeled, packaged into individual plastic bags, and shipped to National Petrographic Services Inc. for completion. There, the samples were mounted on glass slides and ground smooth using progressively finer abrasive grit until the sample was 30 microns thick. Upon return, the thin sections were photographed and examined using a petrographic microscope.

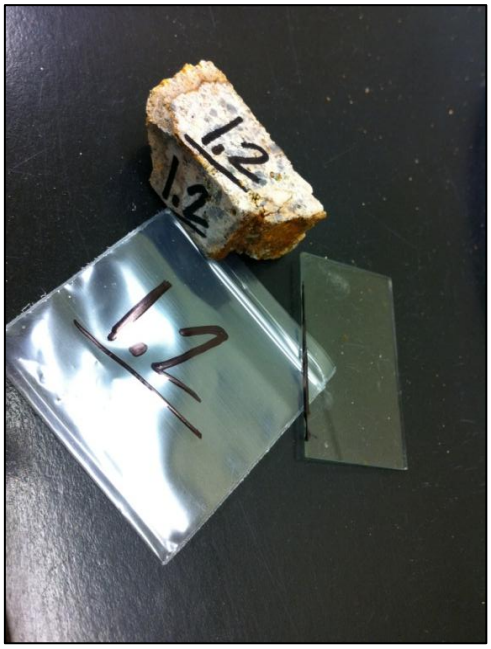

Figure 8. Sample prepared for thin section completion.

XRF

X-ray fluorescence (XRF) is a bulk analysis technique used for the identification and quantification of major and trace elements in whole rock samples. To prepare each sample, the rocks were broken with a hammer into small pieces under a piece of thick paper to ensure no contamination occurred with the metal alloys of the hammer. A handful of the broken pieces were put into a ceramic-walled container with a ceramic puck and a ceramic lid (Figure 9). This container was secured into an 8510 Shatter Box and milled for a minimum of 20 minutes or until the rock was ground to a fine enough powder for XRF analysis. The grinding container and puck were cleaned thoroughly using warm running water, a toothbrush, and ethanol. It should be noted that a pre-contamination run was performed on an aliquot of the actual sample, the material was disregarded, and the sample container and puck were cleaned before milling for XRF. The milled samples for XRF were stored in 50 ml standard, plastic vials and sent to Michigan State University for analysis. The XRF laboratory at Michigan State University used a Bruker S4 Pioneer X-ray fluorescence spectrometer along with SPECTRAplus software (Figure 10). All major elements and 29 trace elements were analyzed (Table 11).

Figure 9. Sample milled and prepared for XRF.

Figure 10. X-ray fluorescence spectrometer (XRF) used for the identification and quantification of major and trace elements in the samples.

DCP

At the University of New Orleans, a Beckman Spectraspan V, Direct-Coupled Plasma Spectrophotometer (DCP) was used for trace element and whole rock analyses (Figure 11). To prepare each sample for trace element analysis, a piece of the rock was broken with a hammer then crushed even finer with a SPEX 4200 Jaw Crusher into less than 6 mm pieces. Using tweezers and stereomicroscope, approximately 0.2 g of the following minerals were extracted, when available, from each sample: K-feldspar, biotite, amphibole, and fluorite. The feldspars, micas, and amphiboles were digested in 5-10 ml of 51% hydrofluoric acid at room temperature for approximately 2 days or until dissolved. The fluorites were digested in 5-10 ml of 98% sulphuric acid at 80 degrees for approximately 36 hours or until dissolved. The samples were diluted to a volume of 35 ml and were then ready for DCP analysis.

For whole rock analysis, 0.2 g of the unused, milled whole rock material from the XRF analysis preparation was dissolved in 51% hydrofluoric acid and diluted to a volume of 35 ml and was then ready for DCP analysis.

Figure 11. Direct-Coupled Plasma Spectrophotometer (DCP) used for trace element analyses.

Heavy Mineral Separation

To isolate the heavy minerals, a large chunk of each rock sample was broken with a hammer then crushed finer with a SPEX 4200 Jaw Crusher into less than 6 mm pieces. The crushed portion was then sieved under running water and the grains smaller than 1 mm were collected in 50 ml standard, plastic sample vials. After drying, the grains were gravity separated using lithium metatungstate liquid adjusted to a density of 2.95 g/cm^3 forcing the heavy minerals with a density higher than 2.95 g/cm^3 to settle at the bottom and the less dense minerals to float to the top. The heavy mineral separates at the bottom were frozen using liquid nitrogen and the unwanted light minerals floating on top were discarded. Once the frozen heavy minerals in the metatungstate thawed, they were rinsed repeatedly with running water and dried to be later used for scanning electron microscope and electron microprobe analysis (Figure 12).

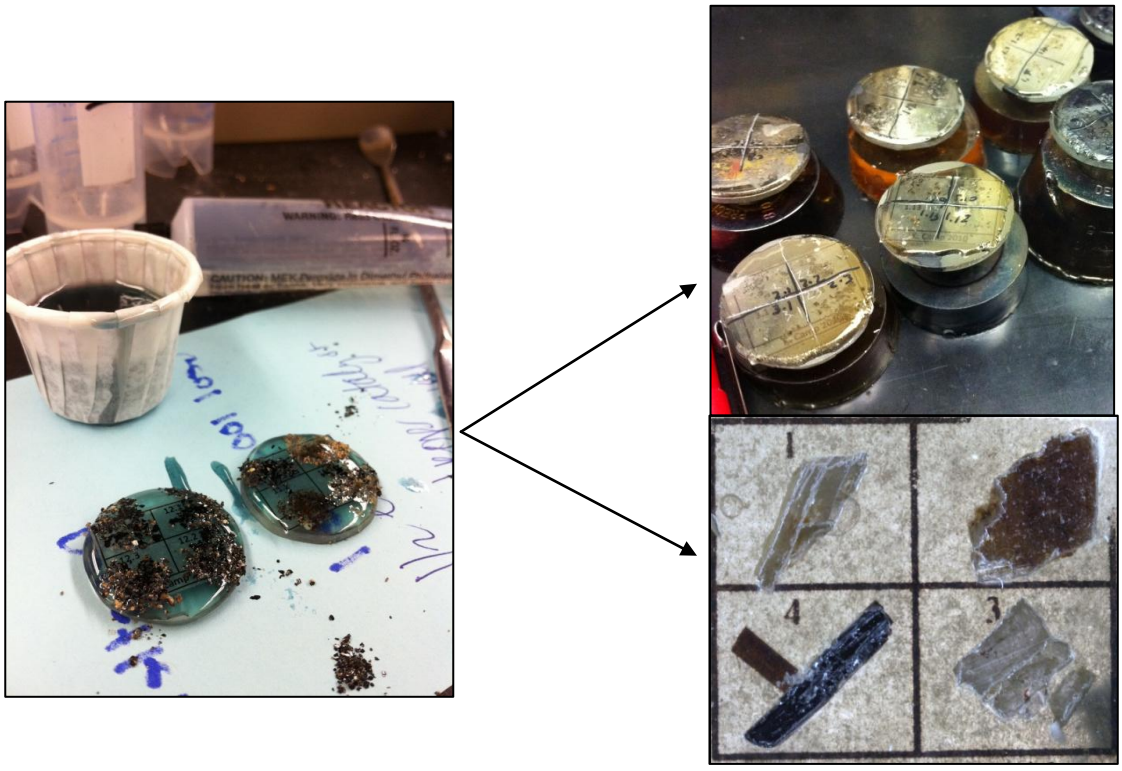

Figure 12. Preparation of heavy separates for analysis on the SEM and EMP.

SEM

At the University of New Orleans, an AMRAY 1820 Digital Scanning Electron Microscope (SEM) was used for spot chemical analysis, acquisition of elemental maps, and mineral identification using the EDS 2009 system (Figure 13). A small scoop of heavy separates from each sample were encased in epoxy using Elmer's All-Purpose Fiberglass Resin on glass sample dishes (Figure 12). Once cured, the mounts were ground down to expose the mineral grains and then polished with 1 micron, 0.3 micron and finally, 0.05 micron alumina grit to polish the grain surfaces. Between each polishing step, the sample mounts were cleaned under running water and then put in an ultrasonic cleaner for 10 minutes. The mounts were then dried and coated with 250 Ångstroms of carbon under a vacuum of $1x10^{-5}$ torr and were ready for SEM analysis (Figure 12).

Figure 13. Scanning Electron Microscope (SEM) used for spot chemical analysis, acquisition of elemental maps, and mineral identification.

EMP

At the University of New Orleans, a fully-automated, nine-spectrometer ARL SEMQ Electron Microprobe (EMP) was used for major and minor element analysis of minerals on microprobe mounts (Figure 14). Minerals were handpicked from the crushed whole rock and also from the heavy mineral separates. The following minerals were extracted, when available, from each sample: feldspar, mica, amphibole, zircon, monazite, bastnasite, xenotime, ilmenite, ferrocolumbite, and thorite. For the process of preparing the grains on sample mounts refer to the SEM section (Figure 12).

Figure 14. Electron Microprobe (EMP) was used for major and minor element analysis of minerals on microprobe mounts.

Standards

Standards for EMP analysis for feldspars and micas
Acceleration potential: 15-20 kV
Beam current: 15-22 nA
Count times: 45 seconds per spot

Albite, Tiburen	($Si_{K\alpha}$, $Al_{K\alpha}$, $Na_{K\alpha}$)
Adularia, Fibbia	($K_{K\alpha}$, $Al_{K\alpha}$, $Si_{K\alpha}$)
An50, Larne	($Ca_{K\alpha}$, $Al_{K\alpha}$)
Clinopyroxene	($Fe_{K\alpha}$, $Mg_{K\alpha}$)
$BaSO_4$, Synthetic	($Ba_{L\alpha}$)
$SrSO_4$, Synthetic	($Sr_{L\alpha}$)
Fluorphlogopite, Synthetic	($F_{K\alpha}$, $K_{K\alpha}$, $Al_{K\alpha}$, $Si_{K\alpha}$)
Rutile, Synthetic	($Ti_{K\alpha}$)
Spessartine, Little 3 Pegmatite	($Mn_{K\alpha}$)

Other MAN standards used as well as the main ones as applicable:

Corundum
Quartz
Hematite
Periclase
PbO, Synthetic
ZrO_2, Synthetic
V_2O_5, Synthetic
Sillimanite
Zinc Oxide, Synthetic

Standards for EMP analysis for zircons
Acceleration potential: 15-20 kV
Beam current: 15-22 nA
Count times: 45 seconds per spot

Microlite, Harding	($Ca_{K\alpha}$, $Ta_{K\alpha}$)
$YNbO_4$, Synthetic	($Nb_{L\alpha}$, $Y_{L\alpha}$)
SnO_2, Synthetic	($Sn_{L\alpha}$)
$CaWO_4$, Synthetic	($W_{L\alpha}$)
Manganotantalite, RGN	($Mn_{K\alpha}$, $Ta_{M\alpha}$)
Rutile, Synthetic	($Ti_{K\alpha}$)
Hematite, Elba	($Fe_{K\alpha}$)
ZrO_2, Synthetic	($Zr_{L\alpha}$)
HfO_2, Synthetic	($Hf_{L\alpha}$)
UO_2, Synthetic	($U_{M\alpha}$)
ThO_2, Synthetic	($Th_{M\alpha}$)
PbO, Synthetic	($Pb_{M\alpha}$)

Other MAN standards used as well as the main ones as applicable:

Corundum
Quartz
Hematite
Periclase
PbO, Synthetic
ZrO_2, Synthetic
V_2O_5, Synthetic
Sillimanite
Zinc Oxide, Synthetic

Data Plotting

The data obtained from the DCP, XRF, SEM, and EMP analyses were incorporated into a number of different diagrams including alkali versus silica diagram, Shand's Index, R_1, R_2 discrimination diagram, Calc-Alkalic/Tholeiitic affiliation plot, K/Rb versus Rb plot, various ternaries, Chondrite-normalized REE diagram, Spider diagram, tectonic discrimination diagrams, and tectonic discrimination ternaries (Figures 57-72). These diagrams were generated using Microsoft Excel and Igpet, and were used to discuss the mineralogy and geochemical fractionation of the miarolitic pegmatites associated with the WMIP.

RESULTS AND DISCUSSION

Mineralogy

Table 3. List of all minerals identified in the samples.	
"Allanite"	Magnetite
"Amphibole"	"Monazite"
Apatite	Muscovite
"Bastnaesite"	Plagioclase
Biotite	Potassium feldspar
"Columbite"	Rutile
"Euxenite/aeschynite"	Quartz
Ferberite/huebnerite series	"Samarskite"
"Fergusonite"	Thorite/thorogummite
Fluorite	Thorogummite
Almanditic garnet	"Xenotime"
Ilmenite series	Zircon
Ilmenite/pyrophanite series	

Allanite-(Ce)

"Allanite" (Figure 15) is exceedingly rare in all the whole rock samples; however, grains of allanite-(Ce) were identified in the heavy separates from Redstone Quarry and the Large Boulder near Oliver Diggings. The grains of allanite-(Ce) are brownish black in color, and its accessory minerals include zircon, apatite, and fluorite. The morphology could not be determined because the grains were crushed and incorporated into the heavy separates. Oxide weight percent from EMP data was used to calculate ion proportions on the basis of 13 O per formula unit (Table 3). The allanite-(Ce) from the Large Boulder locality is more Mg-rich (0.4-0.7 wt.% MgO) compared to the allanite-(Ce) from the Redstone Quarry locality is more Mn-rich (1.2-1.7 wt.% MnO) (Figure 28). Both "allanite" samples are Ce-dominant with a significant Nd concentration ranging from 0.2-0.3 apfu and a very low La concentration <0.1 apfu (Figure 29). Allanite-(Ce) is a good indicator of a high degree of geochemical evolution in these miarolitic pegmatites.

Figure 15 shows a representative EDS analysis of allanite-(Ce) within the energy range 1-15 keV showing the family of various X-ray lines for its essential elements.

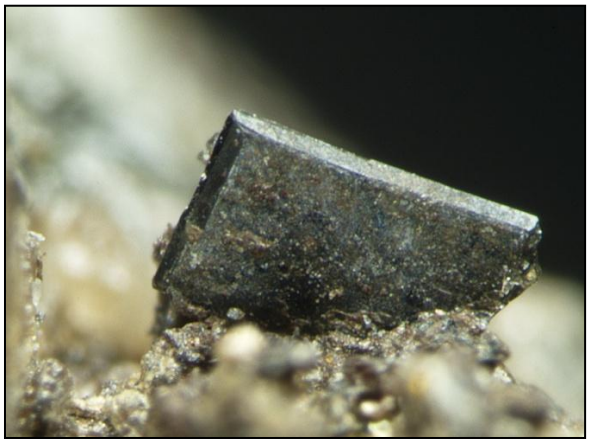

Figure 15. Allanite-(Ce)→ $(Ca,Ce,La)_2(Al,Fe^{2+},Fe^{3+})_3Si_3O_{12}(OH)$

Simplified Formula → $A_2M_3T_3O_{12}(OH)$

1 mm crystal (mindat.org)

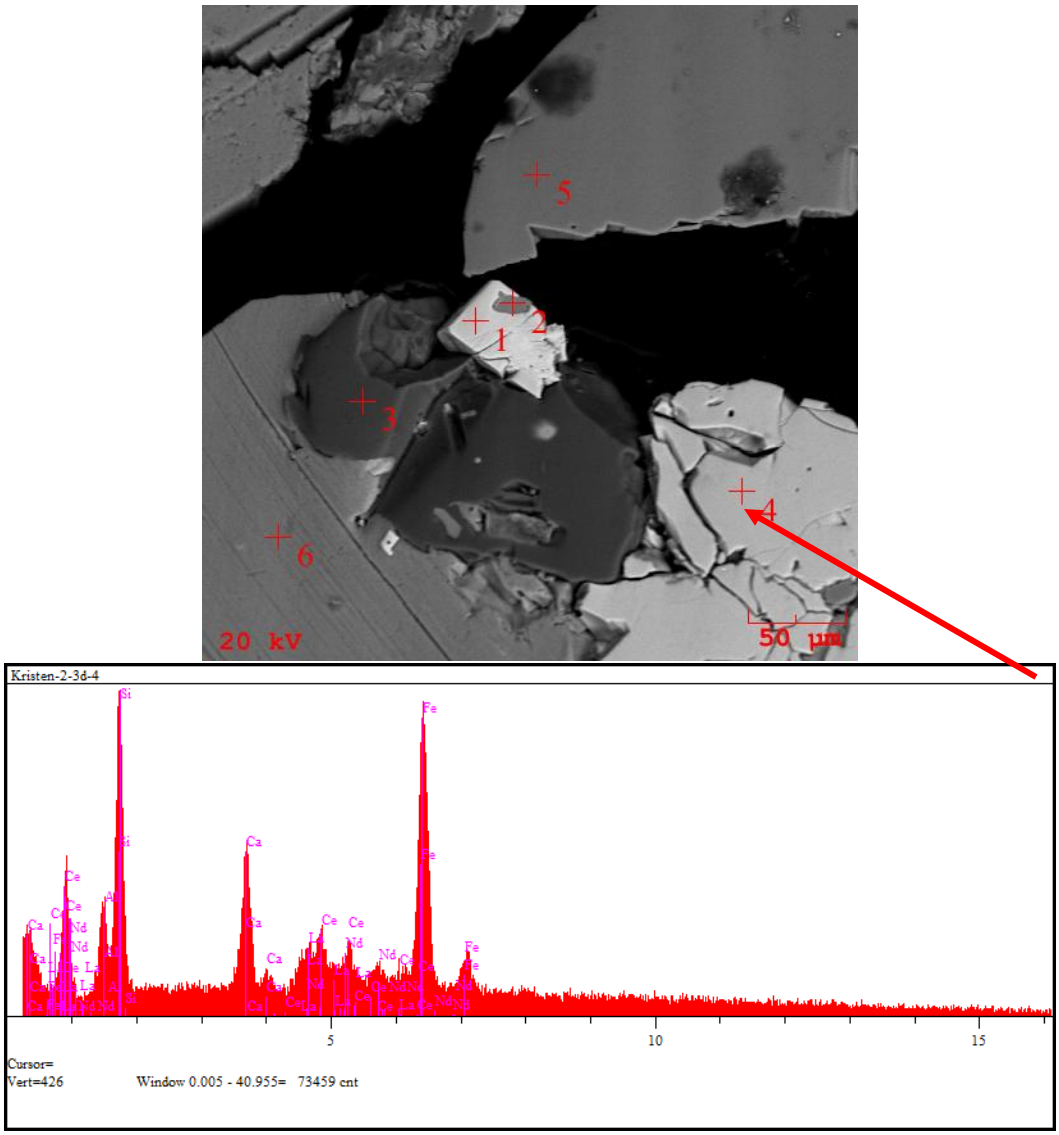

Figure 16. Photomicrograph and an EDS analysis of "allanite" from West Hurricane.

Table 3. Electron microprobe analysis of allanite-Ce.

	Large boulder near Oliver Diggings					Redstone Quarry				
Wt. % oxides										
SiO2	30.121	30.673	30.522	30.434	29.882	30.112	30.093	30.233	30.175	29.887
TiO2	0.654	0.700	0.634	0.445	0.512	0.677	0.676	0.834	0.779	0.444
ThO2	0.089	0.112	0.091	0.083	0.032	0.121	0.145	0.144	0.141	0.156
UO2	0.000	0.009	0.015	0.000	0.000	0.009	0.027	0.011	0.010	0.014
Al2O3	13.114	12.982	13.873	13.272	13.554	13.778	13.698	13.770	13.789	13.900
Y2O3	0.005	0.011	0.045	0.043	0.015	0.034	0.031	0.038	0.044	0.041
Ce2O3	6.985	7.112	7.456	6.983	7.043	7.985	7.883	7.734	7.800	7.834
Pr2O3	1.334	1.400	1.323	1.267	1.221	1.678	1.874	1.677	1.814	1.800
La2O3	2.761	2.612	2.331	2.772	2.753	3.093	3.232	3.227	3.200	3.167
Nd2O3	6.985	6.336	6.316	6.136	5.983	6.554	6.233	6.554	6.458	6.400
Sm2O3	1.811	1.945	1.012	1.783	1.650	1.345	1.733	1.556	1.612	1.650
FeO	17.943	18.232	18.130	18.078	18.312	18.678	18.930	18.554	18.723	18.560
MnO	1.101	1.001	0.914	0.955	1.134	1.223	1.267	1.540	1.670	1.650
CaO	11.091	10.781	11.212	11.433	11.495	11.478	11.877	11.785	11.556	11.676
MgO	0.554	0.510	0.681	0.457	0.445	0.334	0.356	0.332	0.345	0.342
Total	94.548	94.416	94.555	94.141	94.031	97.099	98.055	97.989	98.116	97.521
Ions on the basis of 13 O + F										
Th	0.002	0.003	0.002	0.002	0.001	0.003	0.003	0.003	0.003	0.004
U	0.000	0.000	0.000	0.000	0.000	0.000	0.001	0.000	0.000	0.000
Y	0.000	0.001	0.002	0.002	0.001	0.002	0.002	0.002	0.002	0.002
Ce	0.268	0.272	0.283	0.268	0.271	0.301	0.295	0.289	0.292	0.295
Pr	0.051	0.053	0.050	0.048	0.047	0.063	0.070	0.062	0.067	0.067
La	0.107	0.101	0.089	0.107	0.107	0.117	0.122	0.121	0.121	0.120
Nd	0.262	0.237	0.233	0.229	0.224	0.241	0.228	0.239	0.235	0.235
Sm	0.065	0.070	0.036	0.064	0.060	0.048	0.061	0.055	0.057	0.058
Mn	0.098	0.089	0.080	0.085	0.101	0.107	0.110	0.133	0.144	0.144
Ca	1.247	1.208	1.244	1.282	1.292	1.265	1.302	1.289	1.264	1.287
Sum of A-Site	2.101	2.033	2.020	2.088	2.102	2.146	2.193	2.194	2.186	2.213
Al	1.622	1.600	1.692	1.637	1.676	1.670	1.652	1.656	1.659	1.685
Fe+2	1.575	1.594	1.569	1.582	1.607	1.607	1.620	1.584	1.599	1.596
Ti	0.052	0.055	0.049	0.035	0.040	0.052	0.052	0.064	0.060	0.034
Mg	0.087	0.079	0.105	0.071	0.070	0.051	0.054	0.051	0.053	0.052
Sum of M-Site	3.335	3.328	3.416	3.326	3.393	3.381	3.378	3.354	3.370	3.368
Si **(T-site)**	3.161	3.207	3.160	3.186	3.136	3.098	3.079	3.086	3.082	3.075

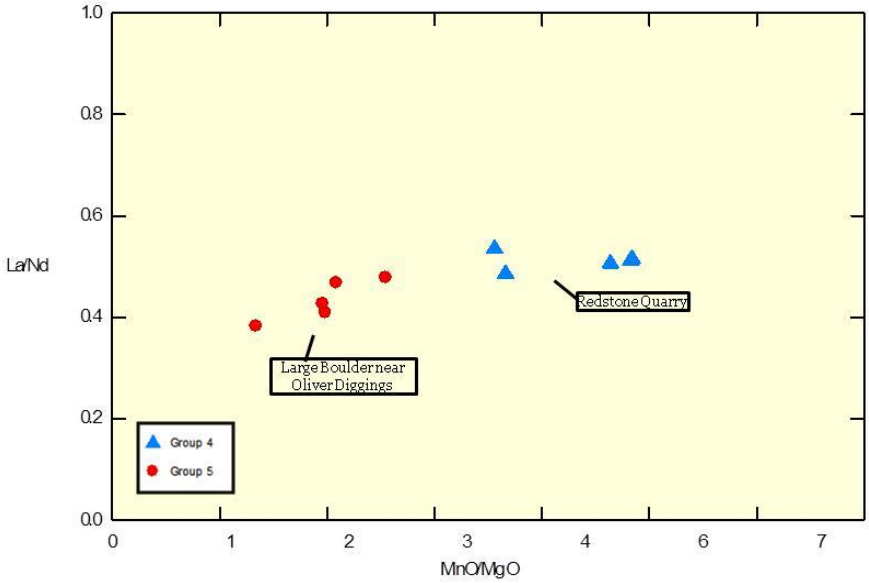

Figure 17. X/Y plot of La/Nd apfu versus MnO/MgO wt.% for allanite-(Ce).

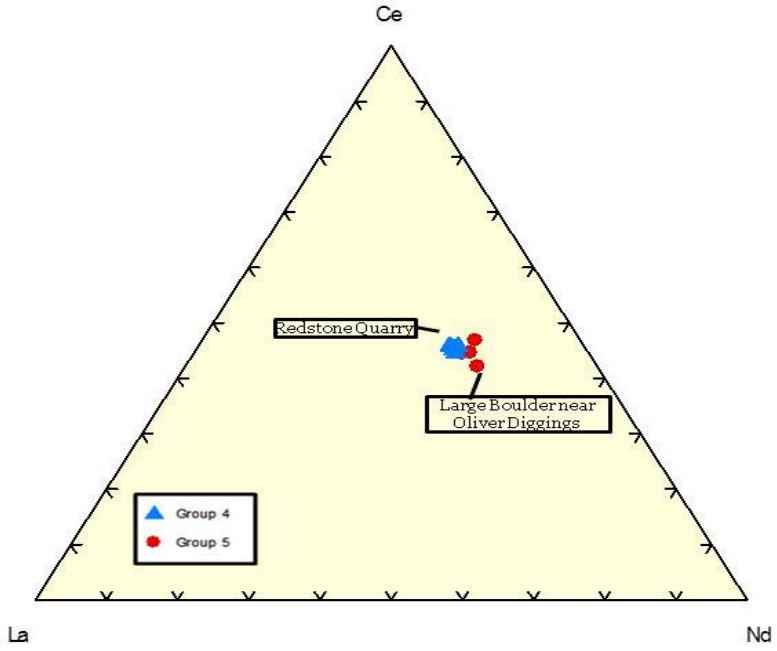

Figure 18. La-Ce-Nd ternary diagram for allanite-(Ce) based on apfu.

"Bastnaesite"

"Bastnaesite" (Figure 19) was found in the heavy mineral separates from Raccoon Gulch, West Hurricane, East Hurricane, North Sugarloaf, and North Percy Peak. Figure 20 shows a representative EDS analysis of "bastnaesite" within the energy range 1-15 keV showing the family of various X-ray lines for the essential elements.

Figure 19. "Bastnaesite" → (Ce, La,Y)(CO_3)F
2 mm crystal (mindat.org)

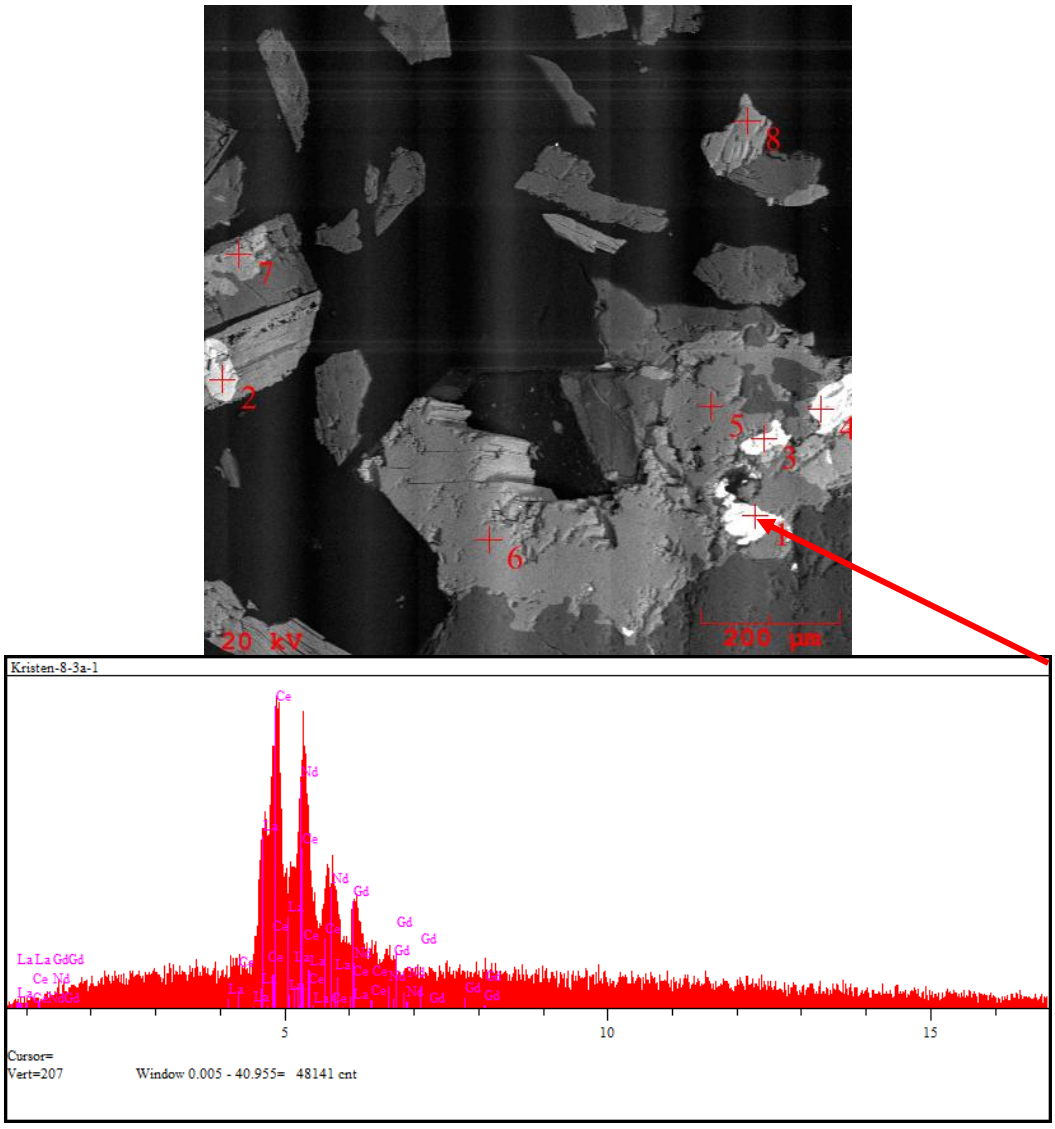

Figure 20. Photomicrograph and an EDS analysis of "bastnaesite" from West Hurricane.

Biotite

Biotite (Figure 21) was found and analyzed in all of the samples except Blackcap and Raccoon Gulch because the quantities were insufficient for analysis. Accessory minerals associated with the biotite include allanite-(Ce), apatite, "bastnaesite", "euxenite/aeschynite", ferberite/huebnerite series, ferrocolumbite, fergusonite-(Y), fluorite, almanditic garnet, members of the ilmenite series, members of the ilmenite/pyrophanite series, magnetite, "monazite", rutile, "samarskite", thorite, thorogummite, and zircon. Biotite is relatively abundant in all of the samples analyzed. Morphologically, the grains are black and anhedral. Oxide weight percent from EMP data was used to calculate ion proportions on the basis of 12 O per formula unit (Table 4). With the exception of Mousetrap which is Fe-rich but F-poor (F<0.4 apfu), the majority of the analyses are both Fe- (Fe/(Fe+Mg) ratio = 0.72-0.99 apfu) and F-enriched (F = 1.0-1.8 apfu) (Figure 22). This enrichment in both Fe and F undoubtedly reflects the character of melts that typically form miarolitic pegmatites.

Figure 21. Biotite→ $K(Fe, Mg)_3AlSi_3O_{10}(OH)_2$

Simplified Formula → $A_1B_3T_4O_{10}(OH)_2$

3.5 mm crystal (mindat.org)

Table 4. Electron microprobe analysis of biotite.

	Government Pit									Oliver Trench				
Wt. % oxides														
SiO2	35.495	35.755	36.112	35.895	36.098	36.118	36.078	36.055	36.100	35.985	35.893	36.004	36.121	36.093
TiO2	2.887	2.595	3.095	3.004	2.433	2.511	2.487	2.399	2.513	2.344	2.423	2.484	2.652	2.663
Al2O3	15.996	16.094	16.225	15.984	16.232	16.188	16.433	16.338	16.232	15.445	15.445	14.984	15.556	15.334
Fe2O3	1.278	1.281	1.239	1.266	1.303	1.301	1.308	1.303	1.297	1.353	1.343	1.361	1.362	1.376
FeO	27.609	27.664	26.766	27.339	28.141	28.086	28.246	28.139	28.003	29.212	28.996	29.383	29.404	29.718
MnO	1.145	1.212	1.119	1.093	0.890	0.876	0.760	0.776	0.906	0.751	0.809	0.778	0.807	0.785
MgO	1.004	1.255	1.312	1.184	1.228	1.187	1.276	1.109	1.219	0.332	0.319	0.299	0.347	0.300
CaO	0.323	0.198	0.225	0.291	0.035	0.038	0.033	0.045	0.031	0.262	0.227	0.267	0.265	0.309
Na2O	0.267	0.344	0.219	0.236	0.390	0.044	0.032	0.035	0.033	0.056	0.054	0.034	0.045	0.056
K2O	8.834	8.889	9.055	9.321	8.887	8.679	9.009	8.785	8.556	5.895	6.223	6.985	8.344	8.876
H2O+	2.550	2.560	2.670	2.540	2.490	2.420	2.460	2.390	2.430	2.480	2.640	2.590	2.470	2.500
F	2.445	2.454	2.334	2.568	2.677	2.800	2.769	2.880	2.776	2.445	2.121	2.236	2.566	2.565
Subtotal	99.833	100.301	100.371	100.721	100.804	100.248	100.891	100.254	100.096	96.560	96.493	97.405	99.939	100.575
-O=F	1.029	1.033	0.983	1.081	1.127	1.179	1.166	1.213	1.169	1.029	0.893	0.941	1.080	1.080
Total	98.804	99.268	99.388	99.640	99.677	99.069	99.725	99.041	98.927	95.531	95.600	96.464	98.859	99.495
Based on normalization to 22 cation charges														
Ca	0.020	0.028	0.017	0.019	0.025	0.003	0.003	0.003	0.004	0.003	0.023	0.018	0.023	0.023
Na	0.055	0.042	0.053	0.034	0.036	0.060	0.007	0.005	0.005	0.005	0.009	0.009	0.005	0.007
K	0.913	0.905	0.906	0.917	0.947	0.901	0.884	0.913	0.895	0.871	0.617	0.651	0.730	0.856
Sum A site	0.988	0.975	0.976	0.970	1.008	0.965	0.894	0.920	0.904	0.879	0.649	0.678	0.758	0.886
Al(vi)	0.367	0.365	0.373	0.384	0.358	0.392	0.405	0.403	0.418	0.410	0.445	0.440	0.394	0.378
Ti(vi)	0.176	0.174	0.156	0.185	0.180	0.145	0.151	0.149	0.144	0.151	0.145	0.150	0.153	0.160
Fe3	0.076	0.078	0.077	0.074	0.076	0.078	0.078	0.079	0.079	0.078	0.084	0.083	0.084	0.083
Fe2	1.836	1.863	1.857	1.785	1.829	1.880	1.883	1.884	1.888	1.878	2.013	1.999	2.021	1.986
Mn	0.080	0.078	0.082	0.075	0.074	0.060	0.059	0.051	0.053	0.061	0.052	0.056	0.054	0.055
Mg	0.133	0.120	0.149	0.155	0.140	0.146	0.141	0.151	0.132	0.145	0.041	0.039	0.036	0.042
Vacancy(vi)	0.331	0.322	0.306	0.342	0.343	0.299	0.282	0.283	0.287	0.277	0.221	0.234	0.257	0.297
Sum B-Site	3.000	3.000	3.000	3.000	3.000	3.000	3.000	3.000	3.000	3.000	3.000	3.000	3.000	3.000
Si	2.857	2.851	2.857	2.866	2.858	2.870	2.882	2.865	2.880	2.882	2.952	2.945	2.948	2.904
Al(iv)	1.143	1.149	1.143	1.134	1.142	1.130	1.118	1.135	1.120	1.118	1.048	1.055	1.052	1.096
Sum of T-Site	4.000	4.000	4.000	4.000	4.000	4.000	4.000	4.000	4.000	4.000	4.000	4.000	4.000	4.000
F	0.667	0.621	0.620	0.586	0.647	0.673	0.707	0.695	0.727	0.701	0.634	0.550	0.579	0.652
OH	1.333	1.379	1.380	1.414	1.353	1.327	1.293	1.305	1.273	1.299	1.366	1.450	1.421	1.348
Sum OH-site	2.000	2.000	2.000	2.000	2.000	2.000	2.000	2.000	2.000	2.000	2.000	2.000	2.000	2.000
	Fe+2/Fe+3 ratio = .96		H2O determined from stoichiometry.											

Table 4. Electron microprobe analysis of biotite (continued).

	Oliver Diggings					Large boulder near Oliver Diggings					Brook Diggings			
Wt. % oxides														
SiO2	36.554	36.521	36.874	36.723	36.689	37.000	36.896	36.776	37.008	36.634	36.565	36.667	36.723	36.778
TiO2	1.555	1.480	1.560	1.444	1.645	2.783	2.898	3.007	2.784	2.856	1.857	1.800	1.781	1.872
Al2O3	17.766	17.988	18.009	17.566	17.598	15.099	15.008	14.899	14.223	14.655	14.566	14.211	14.005	13.893
Fe2O3	1.234	1.225	1.214	1.228	1.239	1.372	1.375	1.375	1.406	1.381	1.416	1.411	1.416	1.397
FeO	26.643	26.459	26.219	26.528	26.759	29.637	29.692	29.690	30.354	29.830	30.572	30.463	30.590	30.159
MnO	0.785	0.754	0.834	0.675	0.665	0.722	0.678	0.712	0.675	0.657	0.581	0.609	0.563	0.533
MgO	0.219	0.211	0.194	0.231	0.244	0.189	0.200	0.211	0.189	0.200	0.499	0.509	0.533	0.498
CaO	0.355	0.432	0.342	0.299	0.334	0.076	0.045	0.044	0.063	0.034	0.213	0.211	0.198	0.187
Na2O	0.147	0.166	0.134	0.143	0.112	0.167	0.211	0.187	0.165	0.183	0.367	0.354	0.299	0.339
K2O	8.773	8.556	8.876	8.454	8.334	8.320	8.099	8.656	8.554	8.322	9.007	9.056	9.111	9.078
H2O+	2.350	2.650	2.630	2.670	2.720	2.610	2.400	2.500	2.440	2.530	2.250	2.140	2.250	2.180
F	2.889	2.223	2.300	2.211	2.099	2.333	2.787	2.564	2.700	2.488	3.098	3.332	3.098	3.234
Subtotal	99.270	98.665	99.186	98.172	98.438	100.308	100.289	100.621	2.700	99.770	100.991	100.763	100.567	100.148
-O=F	1.216	0.936	0.968	0.931	0.884	0.982	1.173	1.080	2.700	1.048	1.304	1.403	1.304	1.362
Total	98.054	97.729	98.218	97.241	97.554	99.326	99.116	99.541	2.700	98.722	99.687	99.360	99.263	98.786
Based on normalization to 22 cation charges														
Ca	0.030	0.037	0.029	0.026	0.029	0.007	0.004	0.004	0.005	0.003	0.018	0.018	0.017	0.016
Na	0.023	0.026	0.021	0.022	0.017	0.026	0.033	0.029	0.026	0.029	0.057	0.056	0.047	0.053
K	0.894	0.872	0.899	0.865	0.850	0.847	0.827	0.883	0.876	0.856	0.926	0.935	0.942	0.941
Sum A site	0.947	0.934	0.949	0.913	0.896	0.880	0.863	0.916	0.907	0.887	1.002	1.008	1.006	1.011
Al(vi)	0.591	0.611	0.615	0.607	0.593	0.375	0.368	0.344	0.318	0.345	0.329	0.321	0.313	0.319
Ti(vi)	0.093	0.089	0.093	0.087	0.099	0.167	0.174	0.181	0.168	0.173	0.113	0.110	0.109	0.114
Fe3	0.074	0.074	0.073	0.074	0.075	0.083	0.083	0.083	0.085	0.084	0.086	0.086	0.087	0.086
Fe2	1.787	1.775	1.749	1.788	1.797	1.988	1.996	1.994	2.048	2.020	2.069	2.070	2.082	2.059
Mn	0.053	0.051	0.056	0.046	0.045	0.049	0.046	0.048	0.046	0.045	0.040	0.042	0.039	0.037
Mg	0.026	0.025	0.023	0.028	0.029	0.022	0.024	0.025	0.023	0.024	0.060	0.061	0.064	0.060
Vacancy(vi)	0.374	0.375	0.391	0.370	0.362	0.316	0.309	0.324	0.312	0.309	0.303	0.310	0.307	0.325
Sum B-Site	3.000	3.000	3.000	3.000	3.000	3.000	3.000	3.000	3.000	3.000	3.000	3.000	3.000	3.000
Si	2.919	2.917	2.929	2.946	2.934	2.954	2.952	2.940	2.972	2.953	2.946	2.966	2.975	2.988
Al(iv)	1.081	1.083	1.071	1.054	1.066	1.046	1.048	1.060	1.028	1.047	1.054	1.034	1.025	1.012
Sum of T-Site	4.000	4.000	4.000	4.000	4.000	4.000	4.000	4.000	4.000	4.000	4.000	4.000	4.000	4.000
F	0.730	0.562	0.578	0.561	0.531	0.589	0.705	0.648	0.686	0.634	0.789	0.852	0.794	0.831
OH	1.270	1.438	1.422	1.439	1.469	1.411	1.295	1.352	1.314	1.366	1.211	1.148	1.206	1.169
Sum OH-site	2.000	2.000	2.000	2.000	2.000	2.000	2.000	2.000	2.000	2.000	2.000	2.000	2.000	2.000
	Fe+2/Fe+3 ratio = .96		H2O determined from stoichiometry.											

Table 4. Electron microprobe analysis of biotite (continued).

	Brook Diggings						Redstone Quarry					West Hurricane		
Wt. % oxides														
SiO2	36.783	36.556	36.484	36.557	36.593	36.583	36.776	37.034	36.894	36.922	36.823	36.344	36.334	36.422
TiO2	1.900	2.123	2.221	2.198	2.322	2.198	3.837	3.783	3.903	3.892	3.872	4.766	4.673	4.559
Al2O3	14.145	14.556	13.067	12.877	12.211	12.455	15.655	15.556	15.493	15.500	15.502	13.121	13.221	13.412
Fe2O3	1.406	1.431	1.411	1.419	1.434	1.415	1.106	1.107	1.099	1.103	1.101	1.365	1.362	1.372
FeO	30.360	30.903	30.481	30.636	30.977	30.547	23.878	23.897	23.735	23.820	23.772	29.468	29.421	29.629
MnO	0.519	0.562	0.557	0.674	0.558	0.512	0.703	0.657	0.712	0.702	0.675	0.814	0.783	0.803
MgO	0.478	2.123	2.332	2.121	2.344	2.345	4.055	4.221	4.094	3.993	4.442	0.244	0.231	0.202
CaO	0.222	0.312	0.278	0.322	0.309	0.298	0.073	0.089	0.072	0.062	0.072	0.147	0.145	0.183
Na2O	0.376	0.670	0.773	0.734	0.673	0.773	0.320	0.333	0.343	0.345	0.360	0.222	0.234	0.195
K2O	9.006	7.768	7.997	8.006	8.456	8.099	8.887	8.605	8.455	8.856	8.442	8.944	9.005	9.112
H2O+	2.240	2.610	2.610	2.720	2.710	2.770	2.350	2.290	2.350	2.350	2.460	2.500	2.490	2.560
F	3.098	2.332	2.331	2.092	2.119	2.004	2.872	3.003	2.892	2.872	2.663	2.562	2.600	2.434
Subtotal	100.533	101.946	100.542	100.356	100.706	99.999	100.512	100.575	100.042	100.417	100.184	100.497	100.499	100.883
-O=F	1.304	0.982	0.981	0.881	0.892	0.844	1.209	1.264	1.218	1.209	1.121	1.079	1.095	1.025
Total	99.229	100.964	99.561	99.475	99.814	99.155	99.303	99.311	98.824	99.208	99.063	99.418	99.404	99.858
Based on normalization to 22 cation charges														
Ca	0.019	0.026	0.024	0.028	0.027	0.026	0.006	0.007	0.006	0.005	0.006	0.013	0.018	0.016
Na	0.059	0.103	0.121	0.115	0.105	0.121	0.048	0.050	0.052	0.052	0.054	0.035	0.037	0.030
K	0.929	0.783	0.821	0.824	0.871	0.836	0.884	0.854	0.843	0.882	0.840	0.920	0.926	0.933
Sum A site	1.007	0.912	0.965	0.966	1.003	0.983	0.939	0.912	0.901	0.939	0.900	0.967	0.981	0.979
Al(vi)	0.323	0.245	0.175	0.171	0.116	0.149	0.308	0.309	0.311	0.307	0.295	0.176	0.185	0.193
Ti(vi)	0.116	0.126	0.134	0.133	0.141	0.134	0.225	0.221	0.229	0.228	0.227	0.289	0.283	0.275
Fe3	0.086	0.085	0.086	0.086	0.088	0.087	0.065	0.065	0.065	0.065	0.065	0.083	0.083	0.083
Fe2	2.062	2.051	2.060	2.075	2.101	2.077	1.565	1.562	1.558	1.561	1.557	1.995	1.992	1.998
Mn	0.036	0.038	0.038	0.046	0.038	0.035	0.046	0.043	0.047	0.046	0.045	0.056	0.053	0.055
Mg	0.058	0.250	0.280	0.255	0.282	0.283	0.471	0.490	0.477	0.464	0.516	0.029	0.028	0.024
Vacancy(vi)	0.320	0.205	0.227	0.233	0.235	0.236	0.319	0.309	0.313	0.327	0.295	0.373	0.375	0.372
Sum B-Site	3.000	3.000	3.000	3.000	3.000	3.000	3.000	3.000	3.000	3.000	3.000	3.000	3.000	3.000
Si	2.974	2.889	2.935	2.947	2.954	2.961	2.869	2.882	2.883	2.881	2.871	2.929	2.929	2.923
Al(iv)	1.026	1.111	1.065	1.053	1.046	1.039	1.131	1.118	1.117	1.119	1.129	1.071	1.071	1.077
Sum of T-Site	4.000	4.000	4.000	4.000	4.000	4.000	4.000	4.000	4.000	4.000	4.000	4.000	4.000	4.000
F	0.792	0.583	0.593	0.533	0.541	0.513	0.709	0.739	0.715	0.709	0.657	0.653	0.663	0.618
OH	1.208	1.417	1.407	1.467	1.459	1.487	1.291	1.261	1.285	1.291	1.343	1.347	1.337	1.382
Sum OH-site	2.000	2.000	2.000	2.000	2.000	2.000	2.000	2.000	2.000	2.000	2.000	2.000	2.000	2.000
	Fe+2/Fe+3 ratio = .96		H2O determined from stoichiometry.											

Table 4. Electron microprobe analysis of biotite (continued).

	West Hurricane												East Hurricane	
Wt. % oxides														
SiO2	36.512	36.393	36.455	36.512	36.593	36.412	36.667	36.877	36.903	36.884	36.783	36.900	37.112	36.985
TiO2	4.783	4.634	3.650	3.499	3.783	3.620	3.455	2.998	2.982	2.782	3.092	3.122	3.069	3.112
Al2O3	13.226	13.094	13.870	13.545	13.448	13.412	13.367	13.566	13.521	13.343	13.556	13.632	13.883	13.983
Fe2O3	1.369	1.367	1.337	1.353	1.360	1.357	1.352	1.333	1.324	1.329	1.333	1.325	1.304	1.303
FeO	29.565	29.526	28.884	29.213	29.374	29.316	29.203	28.789	28.599	28.705	28.788	28.609	28.150	28.140
MnO	0.783	0.777	0.894	0.902	0.921	0.823	0.872	1.202	1.211	1.309	1.198	1.223	1.100	1.009
MgO	0.198	0.255	0.462	0.383	0.412	0.455	0.412	0.368	0.400	0.366	0.334	0.339	0.185	0.212
CaO	0.143	0.112	0.365	0.343	0.432	0.315	0.345	0.110	0.133	0.092	0.114	0.145	0.060	0.056
Na2O	0.215	0.236	0.330	0.298	0.345	0.283	0.322	0.302	0.343	0.295	0.355	0.412	0.556	0.061
K2O	8.782	8.882	9.076	8.454	8.883	9.003	8.734	9.223	8.775	8.923	9.112	9.055	9.610	9.322
H2O+	2.590	2.550	2.250	2.470	2.350	2.510	2.370	2.160	2.300	2.400	2.300	2.350	2.030	2.140
F	2.366	2.455	3.078	2.623	2.872	2.556	2.834	3.265	2.992	2.778	2.982	2.892	3.544	3.334
Subtotal	100.532	100.281	100.651	99.595	100.773	100.062	99.933	100.193	99.483	99.206	99.947	100.004	100.603	99.657
-O=F	0.996	1.034	1.296	1.104	1.209	1.076	1.193	1.375	1.260	1.170	1.256	1.218	1.492	1.404
Total	99.536	99.247	99.355	98.491	99.564	98.986	98.740	98.818	98.223	98.036	98.691	98.786	99.111	98.253
Based on normalization to 22 cation charges														
Ca	0.012	0.010	0.031	0.030	0.037	0.027	0.030	0.010	0.012	0.008	0.010	0.013	0.005	0.018
Na	0.033	0.037	0.052	0.047	0.054	0.044	0.051	0.047	0.054	0.047	0.056	0.065	0.087	0.010
K	0.900	0.914	0.932	0.874	0.912	0.930	0.902	0.953	0.909	0.928	0.943	0.934	0.988	0.964
Sum A site	0.946	0.961	1.015	0.951	1.003	1.002	0.983	1.010	0.975	0.983	1.008	1.011	1.080	0.991
Al(vi)	0.186	0.182	0.251	0.254	0.219	0.228	0.245	0.282	0.292	0.290	0.278	0.284	0.311	0.333
Ti(vi)	0.289	0.281	0.221	0.213	0.229	0.220	0.210	0.183	0.182	0.171	0.189	0.190	0.186	0.190
Fe3	0.083	0.083	0.081	0.083	0.083	0.083	0.083	0.082	0.081	0.082	0.082	0.081	0.079	0.080
Fe2	1.995	2.001	1.953	1.989	1.985	1.994	1.987	1.959	1.951	1.966	1.961	1.944	1.906	1.916
Mn	0.053	0.053	0.061	0.062	0.063	0.056	0.060	0.082	0.083	0.090	0.082	0.084	0.075	0.069
Mg	0.024	0.031	0.055	0.046	0.049	0.055	0.050	0.044	0.048	0.044	0.040	0.041	0.022	0.026
Vacancy(vi)	0.369	0.368	0.377	0.352	0.372	0.364	0.365	0.368	0.361	0.356	0.369	0.377	0.420	0.387
Sum B-Site	3.000	3.000	3.000	3.000	3.000	3.000	3.000	3.000	3.000	3.000	3.000	3.000	3.000	3.000
Si	2.933	2.937	2.934	2.960	2.944	2.948	2.969	2.987	2.998	3.008	2.982	2.984	2.992	2.997
Al(iv)	1.067	1.063	1.066	1.040	1.056	1.052	1.031	1.013	1.002	0.992	1.018	1.016	1.008	1.003
Sum of T-Site	4.000	4.000	4.000	4.000	4.000	4.000	4.000	4.000	4.000	4.000	4.000	4.000	4.000	4.000
F	0.601	0.627	0.784	0.672	0.731	0.654	0.726	0.836	0.769	0.716	0.765	0.740	0.904	0.855
OH	1.399	1.373	1.216	1.328	1.269	1.346	1.274	1.164	1.231	1.284	1.235	1.260	1.096	1.145
Sum OH-site	2.000	2.000	2.000	2.000	2.000	2.000	2.000	2.000	2.000	2.000	2.000	2.000	2.000	2.000
	Fe+2/Fe+3 ratio = .96		H2O determined from stoichiometry.											

Table 4. Electron microprobe analysis of biotite (continued).

	East Hurricane			North Sugarloaf									
Wt. % oxides													
SiO2	36.734	36.932	36.967	37.094	37.111	37.045	36.895	36.966	37.322	37.198	37.218	37.009	37.105
TiO2	3.023	2.982	3.093	3.117	3.187	3.200	3.096	3.222	2.785	2.679	2.558	2.765	2.833
Al2O3	13.988	13.878	13.801	14.445	14.344	14.456	14.554	14.488	15.987	16.219	16.655	16.544	16.500
Fe2O3	1.298	1.297	1.309	1.254	1.264	1.274	1.275	1.293	1.258	1.257	1.263	1.278	1.270
FeO	28.020	28.004	28.258	27.090	27.303	27.513	27.545	27.918	27.177	27.155	27.281	27.595	27.430
MnO	0.923	1.034	1.112	0.617	0.556	0.633	0.612	0.733	0.431	0.419	0.398	0.411	0.439
MgO	0.236	0.309	0.255	0.709	0.722	0.729	0.674	0.688	0.359	0.351	0.409	0.443	0.418
CaO	0.063	0.073	0.056	0.877	0.767	0.845	0.777	0.763	0.007	0.009	0.000	0.000	0.007
Na2O	0.121	0.144	0.103	0.750	0.765	0.687	0.733	0.700	0.054	0.055	0.053	0.045	0.062
K2O	9.343	9.455	9.334	8.655	8.098	8.634	8.554	8.600	9.000	8.945	9.211	9.067	9.117
H2O+	2.200	2.170	2.190	2.660	2.720	2.570	2.620	2.670	2.400	2.520	2.410	2.430	2.370
F	3.212	3.256	3.223	2.232	2.098	2.423	2.300	2.216	2.765	2.539	2.768	2.700	2.845
Subtotal	99.161	99.534	99.701	99.500	98.935	100.009	99.635	100.257	99.545	99.346	100.224	100.287	100.396
-O=F	1.352	1.371	1.357	0.940	0.883	1.020	0.968	0.933	1.164	1.069	1.165	1.137	1.198
Total	97.809	98.163	98.344	98.560	98.052	98.989	98.667	99.324	98.381	98.277	99.059	99.150	99.198
Based on normalization to 22 cation charges													
Ca	0.005	0.006	0.005	0.075	0.066	0.072	0.067	0.065	0.001	0.001	0.000	0.000	0.001
Na	0.019	0.023	0.016	0.116	0.119	0.106	0.114	0.108	0.008	0.009	0.008	0.007	0.010
K	0.971	0.979	0.966	0.884	0.829	0.880	0.874	0.875	0.915	0.910	0.930	0.916	0.920
Sum A site	0.996	1.008	0.987	1.076	1.014	1.058	1.055	1.048	0.924	0.919	0.938	0.923	0.931
Al(vi)	0.336	0.327	0.317	0.334	0.337	0.320	0.331	0.310	0.475	0.489	0.500	0.476	0.475
Ti(vi)	0.185	0.182	0.189	0.188	0.192	0.192	0.187	0.193	0.167	0.161	0.152	0.165	0.169
Fe3	0.080	0.080	0.080	0.076	0.077	0.077	0.077	0.078	0.076	0.076	0.076	0.076	0.076
Fe2	1.917	1.910	1.925	1.822	1.841	1.846	1.854	1.870	1.819	1.818	1.814	1.836	1.823
Mn	0.064	0.071	0.076	0.042	0.038	0.043	0.042	0.050	0.029	0.028	0.027	0.028	0.029
Mg	0.029	0.037	0.031	0.085	0.086	0.087	0.080	0.082	0.043	0.042	0.048	0.052	0.049
Vacancy(vi)	0.390	0.392	0.382	0.454	0.429	0.435	0.429	0.418	0.391	0.386	0.383	0.368	0.378
Sum B-Site	3.000	3.000	3.000	3.000	3.000	3.000	3.000	3.000	3.000	3.000	3.000	3.000	3.000
Si	2.992	2.999	2.998	2.970	2.979	2.959	2.956	2.948	2.974	2.965	2.946	2.931	2.936
Al(iv)	1.008	1.001	1.002	1.030	1.021	1.041	1.044	1.052	1.026	1.035	1.054	1.069	1.064
Sum of T-Site	4.000	4.000	4.000	4.000	4.000	4.000	4.000	4.000	4.000	4.000	4.000	4.000	4.000
F	0.827	0.836	0.827	0.565	0.533	0.612	0.583	0.559	0.697	0.640	0.693	0.676	0.712
OH	1.173	1.164	1.173	1.435	1.467	1.388	1.417	1.441	1.303	1.360	1.307	1.324	1.288
Sum OH-site	2.000	2.000	2.000	2.000	2.000	2.000	2.000	2.000	2.000	2.000	2.000	2.000	2.000
	Fe+2/Fe+3 ratio = .96		H2O determined from stoichiometry.										

Table 4. Electron microprobe analysis of biotite (continued).

	North Percy Peak										Ravine				
Wt. % oxides															
SiO2	36.985	36.876	36.794	36.784	36.934	36.788	36.845	36.778	36.912	36.810	37.167	37.232	37.123	37.312	37.343
TiO2	1.760	1.556	1.677	1.810	1.782	2.111	2.221	2.091	2.145	2.166	3.690	3.722	3.612	3.555	3.609
Al2O3	16.877	17.004	16.845	16.783	16.930	15.877	15.783	15.660	15.734	15.782	15.433	15.445	15.395	15.412	15.445
Fe2O3	1.229	1.216	1.223	1.220	1.222	1.141	1.131	1.135	1.136	1.134	0.983	0.998	0.993	0.988	0.978
FeO	26.537	26.261	26.411	26.346	26.390	24.637	24.414	24.519	24.541	24.489	21.230	21.546	21.440	21.346	21.120
MnO	0.655	0.712	0.672	0.566	0.612	4.176	4.112	4.312	4.156	4.332	1.400	1.432	1.350	1.411	1.222
MgO	0.500	0.523	0.456	0.426	0.634	0.120	0.134	0.119	0.132	0.113	4.758	4.880	4.754	4.688	4.885
CaO	0.677	0.710	0.723	0.654	0.584	0.000	0.000	0.000	0.000	0.008	0.100	0.098	0.128	0.107	0.118
Na2O	0.561	0.513	0.456	0.650	0.623	0.380	0.410	0.344	0.412	0.398	0.330	0.232	0.311	0.300	0.288
K2O	9.665	9.544	9.433	9.422	9.344	9.654	9.453	9.600	9.342	9.006	9.566	9.877	9.766	9.639	9.766
H2O+	2.670	2.470	2.500	2.550	2.590	2.140	2.200	2.180	2.100	2.150	2.350	2.400	2.460	2.440	2.370
F	2.221	2.623	2.566	2.455	2.385	3.322	3.212	3.223	3.412	3.334	2.887	2.784	2.655	2.700	2.845
Subtotal	100.337	100.008	99.756	99.666	100.030	100.346	99.915	99.961	100.022	99.722	99.894	100.646	99.987	99.898	99.989
-O=F	0.935	1.104	1.080	1.034	1.004	1.399	1.352	1.357	1.437	1.404	1.216	1.172	1.118	1.137	1.198
Total	99.402	98.904	98.676	98.632	99.026	98.947	98.563	98.604	98.585	98.318	98.678	99.474	98.869	98.761	98.791
Based on normalization to 22 cation charges															
Ca	0.057	0.018	0.062	0.056	0.050	0.000	0.000	0.000	0.000	0.001	0.008	0.008	0.011	0.009	0.010
Na	0.086	0.079	0.070	0.101	0.096	0.059	0.064	0.054	0.064	0.062	0.050	0.035	0.047	0.045	0.043
K	0.977	0.968	0.960	0.959	0.945	0.988	0.969	0.987	0.958	0.925	0.953	0.978	0.972	0.959	0.970
Sum A site	1.120	1.065	1.092	1.115	1.091	1.048	1.033	1.040	1.022	0.988	1.011	1.021	1.030	1.014	1.024
Al(vi)	0.505	0.526	0.517	0.511	0.512	0.455	0.457	0.449	0.458	0.462	0.321	0.303	0.314	0.328	0.327
Ti(vi)	0.105	0.093	0.101	0.109	0.106	0.127	0.134	0.127	0.130	0.131	0.217	0.217	0.212	0.209	0.211
Fe3	0.074	0.073	0.074	0.074	0.073	0.069	0.069	0.069	0.069	0.069	0.058	0.059	0.059	0.058	0.058
Fe2	1.766	1.754	1.769	1.765	1.758	1.661	1.649	1.659	1.657	1.656	1.392	1.405	1.406	1.399	1.382
Mn	0.044	0.048	0.045	0.038	0.041	0.284	0.280	0.294	0.283	0.295	0.093	0.094	0.089	0.093	0.081
Mg	0.059	0.062	0.054	0.051	0.075	0.014	0.016	0.014	0.016	0.014	0.553	0.564	0.553	0.545	0.567
Vacancy(vi)	0.448	0.443	0.440	0.453	0.434	0.389	0.395	0.387	0.388	0.373	0.366	0.358	0.367	0.368	0.375
Sum B-Site	3.000	3.000	3.000	3.000	3.000	3.000	3.000	3.000	3.000	3.000	3.000	3.000	3.000	3.000	3.000
Si	2.929	2.932	2.934	2.933	2.929	2.952	2.962	2.962	2.967	2.964	2.901	2.890	2.897	2.911	2.909
Al(iv)	1.071	1.068	1.066	1.067	1.071	1.048	1.038	1.038	1.033	1.036	1.099	1.110	1.103	1.089	1.091
Sum of T-Site	4.000	4.000	4.000	4.000	4.000	4.000	4.000	4.000	4.000	4.000	4.000	4.000	4.000	4.000	4.000
F	0.556	0.660	0.647	0.619	0.598	0.843	0.817	0.821	0.867	0.849	0.713	0.683	0.655	0.666	0.701
OH	1.444	1.340	1.353	1.381	1.402	1.157	1.183	1.179	1.133	1.151	1.287	1.317	1.345	1.334	1.299
Sum OH-site	2.000	2.000	2.000	2.000	2.000	2.000	2.000	2.000	2.000	2.000	2.000	2.000	2.000	2.000	2.000
	Fe+2/Fe+3 ratio = .96		H2O determined from stoichiometry.												

Table 4. Electron microprobe analysis of biotite (continued).

	Mouse trap					Eastman Topaz				
Wt. % oxides										
SiO2	37.776	37.540	36.899	37.321	37.654	37.554	37.512	37.565	37.800	37.623
TiO2	0.076	0.045	0.094	0.220	0.255	0.044	0.054	0.065	0.045	0.065
Al2O3	18.676	18.900	19.023	17.889	18.655	18.093	18.222	18.093	18.233	18.333
Fe2O3	1.185	1.229	1.181	1.196	1.199	1.200	1.205	1.214	1.209	1.199
FeO	25.591	26.546	25.495	25.827	25.901	25.922	26.027	26.219	26.102	25.896
MnO	0.600	0.544	0.567	0.560	0.622	0.189	0.200	0.198	0.177	0.211
MgO	0.223	0.220	0.214	0.210	0.235	0.228	0.218	0.209	0.233	0.199
CaO	0.118	0.114	0.094	0.099	0.234	0.000	0.000	0.000	0.000	0.000
Na2O	0.080	0.033	0.094	0.112	0.023	0.170	0.200	0.167	0.211	0.165
K2O	1.098	1.345	1.455	1.233	1.322	7.233	7.322	7.099	7.009	6.887
H2O+	3.350	3.450	3.510	3.550	3.620	2.710	2.770	2.780	2.820	2.820
F	0.776	0.566	0.434	0.334	0.211	2.122	2.001	1.983	1.889	1.887
Subtotal	89.549	90.532	89.060	88.551	89.931	95.465	95.731	95.592	95.728	95.285
-O=F	0.327	0.238	0.183	0.141	0.089	0.893	0.843	0.835	0.795	0.795
Total	89.222	90.294	88.877	88.410	89.842	94.572	94.888	94.757	94.933	94.490
Based on normalization to 22 cation charges										
Ca	0.010	0.018	0.008	0.009	0.021	0.000	0.000	0.000	0.000	0.000
Na	0.013	0.005	0.015	0.018	0.004	0.027	0.031	0.026	0.033	0.026
K	0.116	0.141	0.154	0.132	0.139	0.749	0.756	0.734	0.721	0.711
Sum A site	0.139	0.164	0.178	0.159	0.163	0.775	0.787	0.760	0.754	0.737
Al(vi)	0.935	0.908	0.934	0.888	0.904	0.777	0.774	0.771	0.783	0.794
Ti(vi)	0.005	0.003	0.006	0.014	0.016	0.003	0.003	0.004	0.003	0.004
Fe3	0.074	0.076	0.074	0.076	0.075	0.074	0.074	0.074	0.074	0.073
Fe2	1.774	1.830	1.781	1.816	1.789	1.767	1.769	1.784	1.769	1.761
Mn	0.042	0.038	0.040	0.040	0.043	0.013	0.014	0.014	0.012	0.014
Mg	0.027	0.027	0.027	0.026	0.029	0.028	0.026	0.025	0.028	0.024
Vacancy(vi)	0.143	0.118	0.138	0.141	0.145	0.339	0.339	0.328	0.332	0.329
Sum B-Site	3.000	3.000	3.000	3.000	3.000	3.000	3.000	3.000	3.000	3.000
Si	3.118	3.080	3.069	3.123	3.096	3.047	3.036	3.043	3.049	3.045
Al(iv)	0.882	0.920	0.931	0.877	0.904	0.953	0.964	0.957	0.951	0.955
Sum of T-Site	4.000	4.000	4.000	4.000	4.000	4.000	4.000	4.000	4.000	4.000
F	0.203	0.147	0.114	0.088	0.055	0.544	0.512	0.508	0.482	0.483
OH	1.797	1.853	1.886	1.912	1.945	1.456	1.488	1.492	1.518	1.517
Sum OH-site	2.000	2.000	2.000	2.000	2.000	2.000	2.000	2.000	2.000	2.000
	Fe+2/Fe+3 ratio = .96		H2O determined from stoichiometry.							

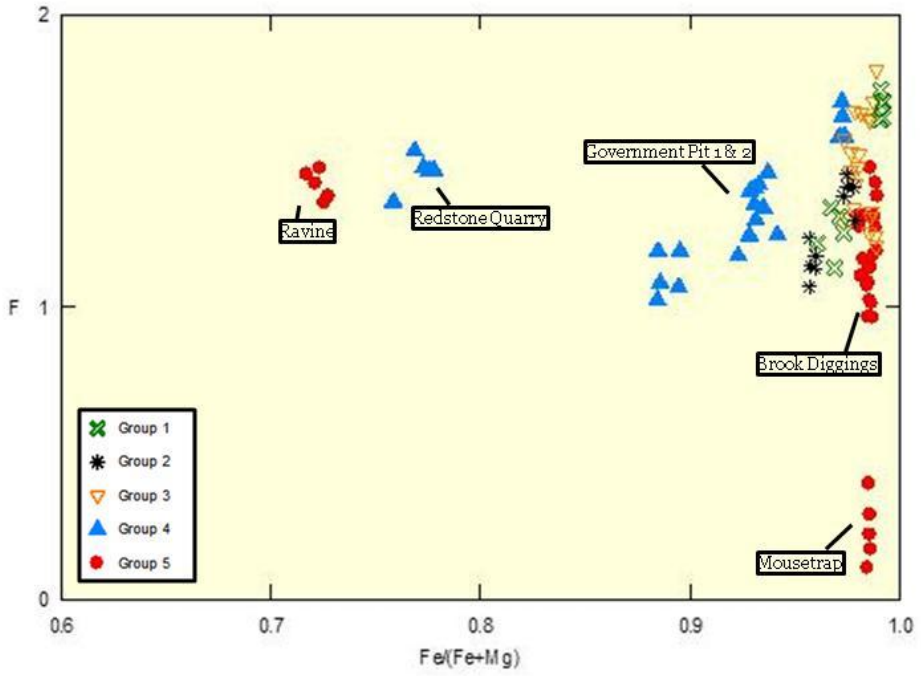

Figure 22. X/Y plot of F versus Fe/(Fe+Mg) for biotite based on apfu.

"Euxenite/aeschynite"

"Euxenite/aeschynite" (Figure 23) is extremely rare in the miarolitic pegmatite samples; although two grains were found in the heavy mineral separates from Government Pit. Figure 24 shows a representative EDS analysis of "euxenite/aeschynite" within the energy range 1-15 keV showing the family of various X-ray lines for its essential elements.

Figure 23. "Euxenite/aeschynite"→

(Y, Ca, Ce, U, Th)(Nb, Ta, Ti)$2O_6$/(Y, Ca, Fe, Th)$(Ti, Nb)_2(O, OH)_6$

25 mm Euxenite-(Y) crystal (mindat.org)

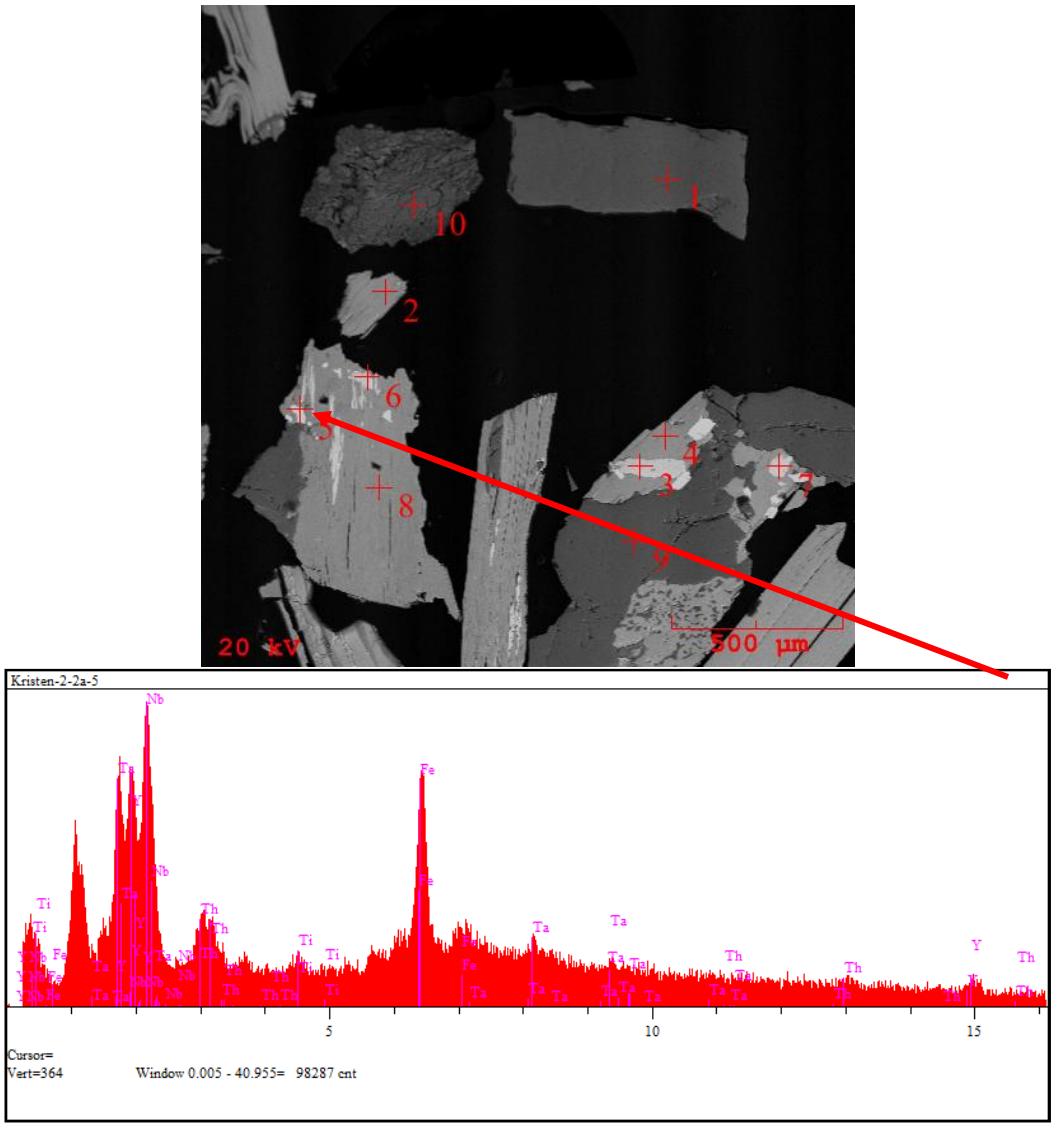

Figure 24. Photomicrograph and an EDS analysis of "euxenite/aeschynite" from Government Pit.

Ferberite/huebnerite series

"Ferberite/huebnerite" (Figure 25) series minerals are exceedingly rare in these miarolitic pegmatite samples, although one grain was analyzed in the heavy mineral separates from Raccoon Gulch. Figure 26 shows the EDS analysis of the "ferberite/huebnerite" series mineral within the energy range 1-15 keV showing the family of various X-ray lines for its essential elements.

Figure 25. Ferberite/huebnerite series→ $(Fe,Mn)WO_4$
60 mm wolframite crystals (mindat.org)

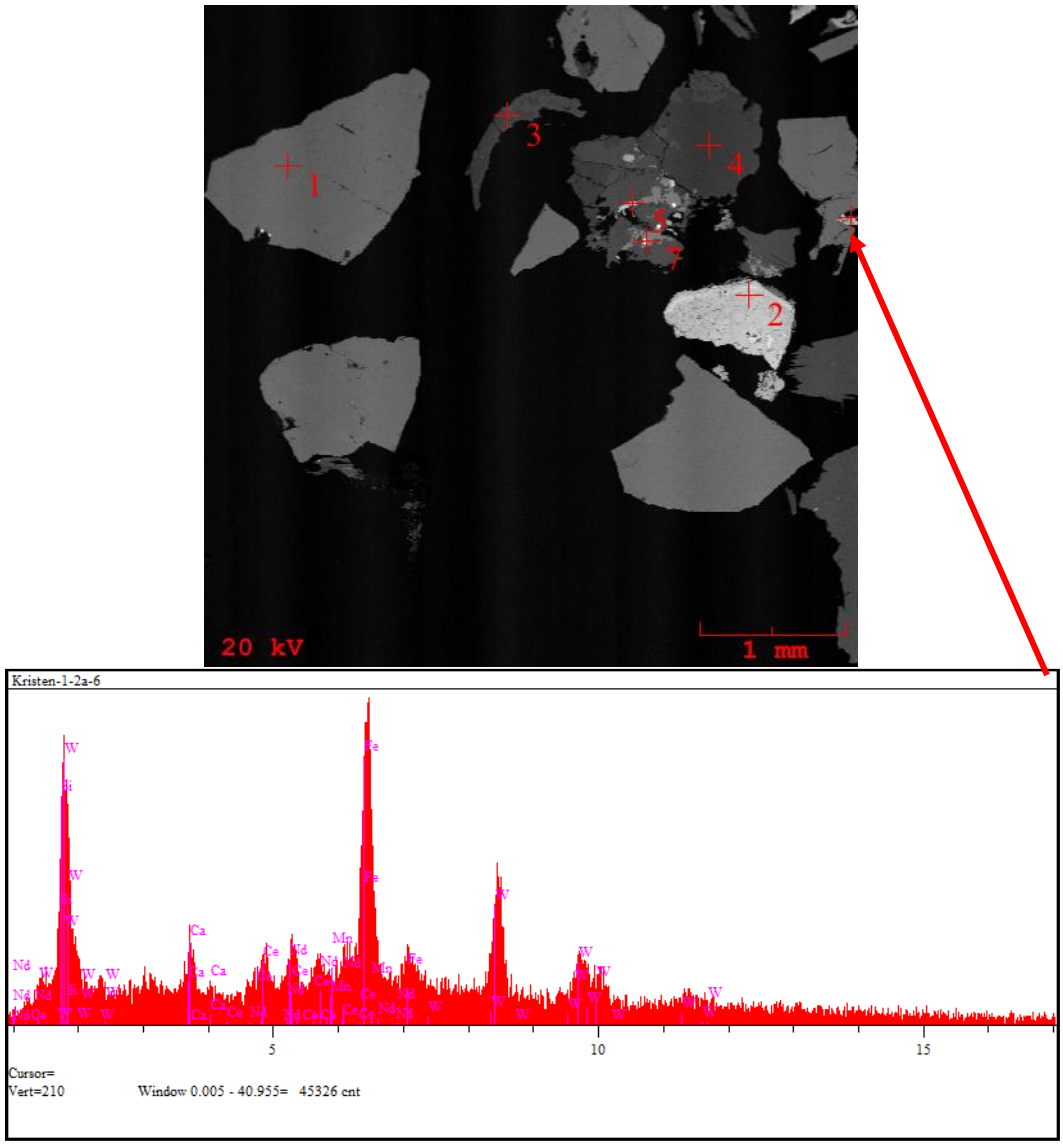

Figure 26. Photomicrograph and an EDS analysis of a member from the ferberite/huebnerite series from Raccoon Gulch.

Fergusonite-(Y)

"Fergusonite" (Figure 27) is exceedingly rare in the miarolitic pegmatites sampled. A few grains were identified in the heavy mineral separates from Oliver Trench, which serves as the first confirmed finding by a member of the MP^2 research group. Oxide weight percent from EMP data was used to calculate ion proportions on the basis of 4 O per formula unit (Table 5). Accessory minerals associated with "fergusonite" include "bastnaesite", members of the ilmenite series, members of the ilmenite/pyrophanite series, "monazite", "samarskite", thorite, and zircon. The morphology could not be determined because the grains were crushed and incorporated into the heavy mineral separates. The grain is identified as fergusonite-(Y) considering the concentration of Y (0.55 apfu) is greater than that of Ce and Nd. The fergusonite-(Y) is Nb-dominant (0.90 apfu) with low Ta enrichment (0.13 apfu) (Figure 29). The presence of Fergusonite-(Y) in these miarolitic pegmatites indicates a higher degree of geochemical evolution.

Figure 28 shows a representative EDS analysis of fergusonite-(Y) within the energy range 1-15 keV showing the family of various X-ray lines for its essential elements.

Figure 27. Fergusonite-(Y)→ $YNbO_4$

3 mm crystal (mindat.org)

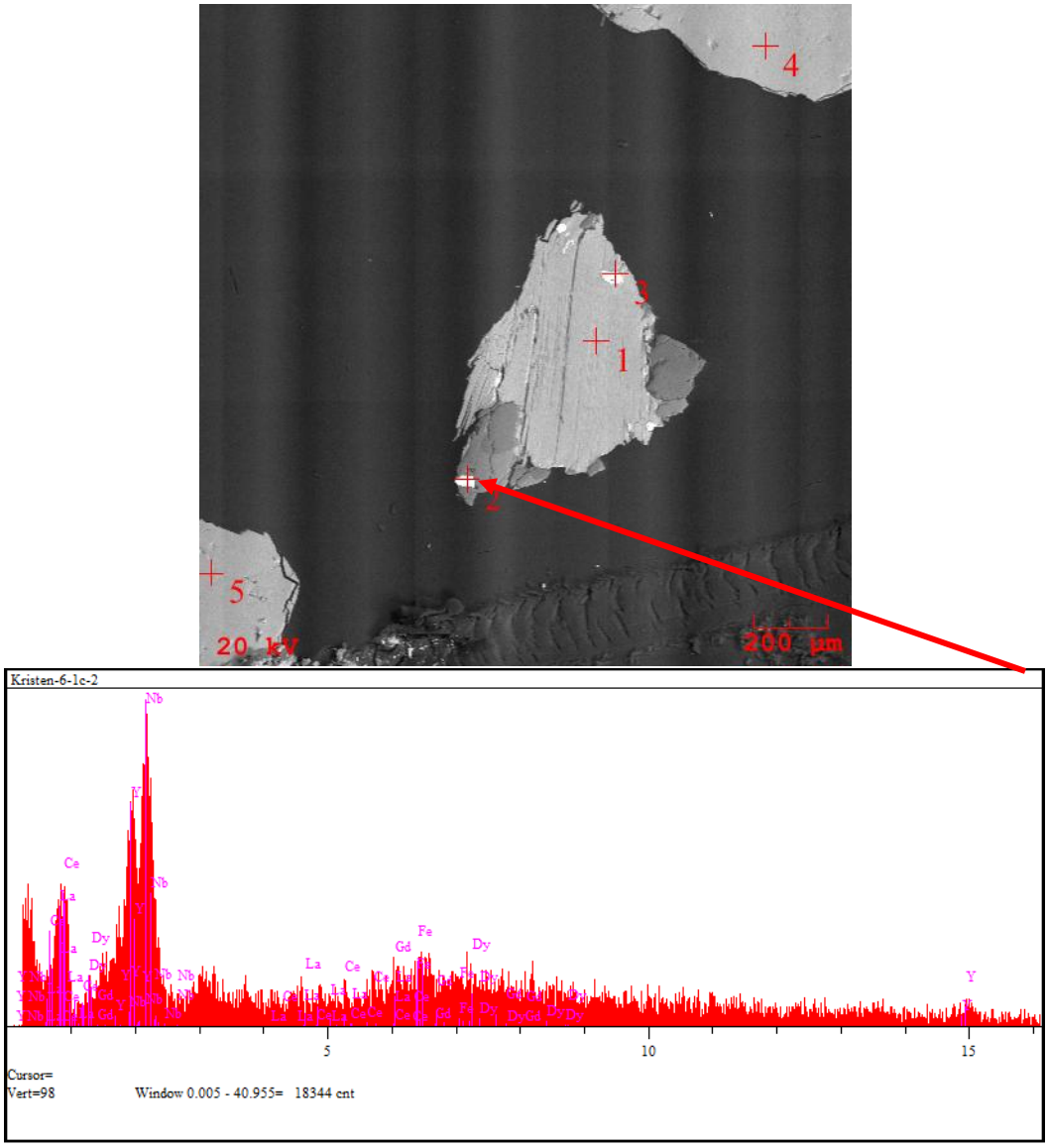

Figure 28. Photomicrograph and an EDS analysis of "fergusonite" from Brook Diggings.

Table 5. Electron microprobe analysis of fergusonite-(Y).

	Oliver Trench				
Wt. % oxides					
UO2	0.954	1.043	1.004	0.934	0.984
Nb2O5	44.700	44.565	45.003	44.673	44.511
Ta2O5	10.800	11.001	10.673	10.912	10.992
Ce2O3	5.451	4.994	4.893	4.845	5.332
TiO2	0.667	0.700	0.682	0.672	0.722
ZrO2	0.455	0.377	0.404	0.422	0.385
ThO2	0.322	0.267	0.342	0.309	0.294
FeO	0.800	0.902	0.992	0.872	0.772
MnO	0.500	0.545	0.482	0.457	0.432
Al2O3	0.600	0.485	0.611	0.581	0.456
La2O3	2.091	2.156	2.167	2.002	2.054
Yb2O3	3.983	4.123	4.235	4.443	3.993
Er2O3	2.082	2.100	2.009	2.112	1.933
Y2O3	23.034	22.892	23.133	23.110	23.092
CaO	2.555	2.774	2.292	2.612	2.335
ZnO	0.233	0.232	0.245	0.225	0.215
MgO	0.009	0.008	0.013	0.011	0.008
Total	99.236	99.164	99.180	99.192	98.510
Ions on the basis of 4 O					
U	0.009	0.010	0.010	0.009	0.010
Ce	0.088	0.081	0.079	0.079	0.087
Zr	0.010	0.008	0.009	0.009	0.008
Th	0.003	0.003	0.003	0.003	0.003
Fe	0.030	0.033	0.037	0.032	0.029
Mn	0.019	0.020	0.018	0.017	0.016
Al	0.031	0.025	0.032	0.030	0.024
La	0.034	0.035	0.035	0.033	0.034
Yb	0.054	0.056	0.057	0.060	0.054
Er	0.029	0.029	0.028	0.029	0.027
Y	0.543	0.540	0.545	0.545	0.549
Ca	0.121	0.132	0.109	0.124	0.112
Zn	0.008	0.008	0.008	0.007	0.007
Mg	0.001	0.001	0.001	0.001	0.001
Sum of A-site	0.980	0.982	0.971	0.979	0.961
Ti	0.022	0.023	0.023	0.022	0.024
Nb	0.895	0.894	0.901	0.895	0.899
Ta	0.130	0.133	0.128	0.132	0.134
Sum of B-site	1.048	1.050	1.052	1.049	1.057

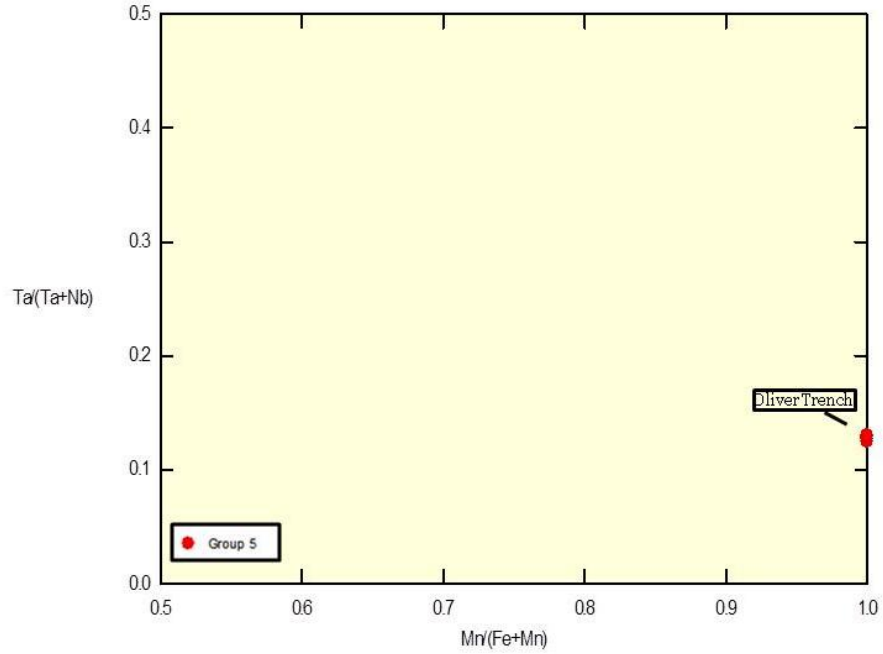

Figure 29. Ta/(Ta+Nb) versus Mn/(Fe+Mn) for fergusonite-(Y) based on apfu.

Ferrocolumbite

"Columbite" (Figure 30) is rare in the whole rock samples; however, grains were identified in the heavy separates from Redstone Quarry and Blackcap. Oxide weight percent from EMP data was used to calculate ion proportions on the basis of 6 O per formula unit (Table 6). Both "columbite" grains plot in the ferrocolumbite, or iron niobium oxide, field of the "columbite" quadrilateral (Figure 32). These grains are associated with fluorite, members of the ilmenite/pyrophanite series, "monazite", thorite, and zircon. The morphology could not be determined because the grains were crushed and incorporated into the heavy separates. The ferrocolumbite from Redstone Quarry is more Ta-rich (Ta/(Ta+Nb) ratio >0.43 apfu) than the ferrocolumbite from Blackcap (Ta/(Ta+Nb) ratio <0.13 apfu), indicating late stage crystallization and consequently a higher degree of pegmatitic evolution of the former.

Figure 31 shows a representative EDS analysis of ferrocolumbite within the energy range 1-15 keV showing the family of various X-ray lines for its essential elements.

Figure 30. Ferrocolumbite → $Fe^{2+}Nb_2O_6$

Simplified Formula → AB_2O_6

13 mm crystal (mindat.org)

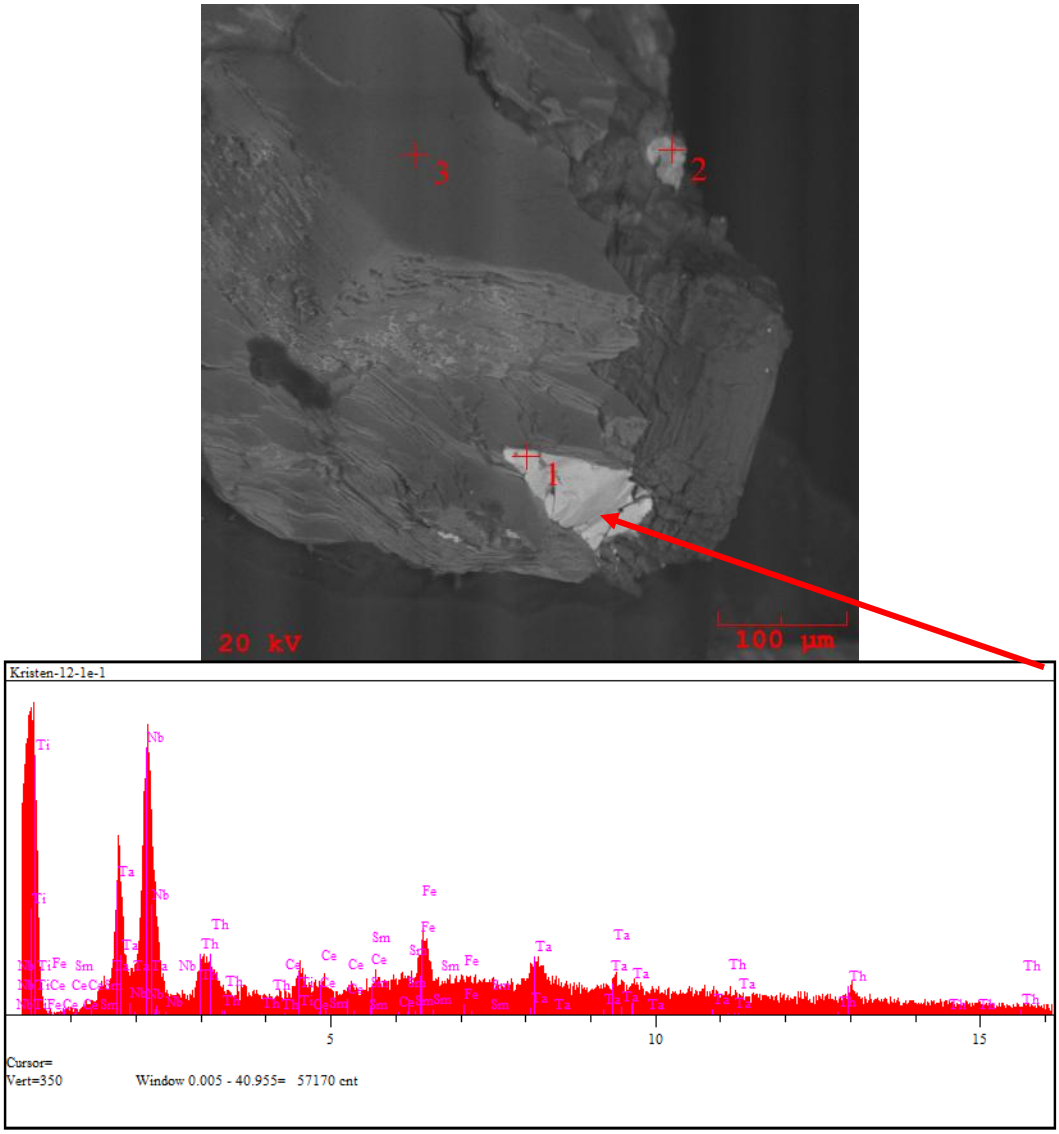

Figure 31. Photomicrograph and an EDS analysis of ferrocolumbite from North Percy Peak.

Table 6. Electron microprobe analysis of ferrocolumbite.

	Blackcap					Redstone Quarry				
Wt. % oxides										
Nb2O5	64.187	64.009	63.983	63.883	63.432	35.200	35.122	34.884	34.945	34.656
Ta2O5	14.662	14.812	14.943	15.093	15.334	44.310	44.210	44.784	44.894	45.122
SiO2	0.032	0.019	0.022	0.018	0.023	0.021	0.000	0.000	0.000	0.022
TiO2	0.731	0.712	0.672	0.647	0.623	2.677	2.334	2.345	2.440	2.223
UO2	0.009	0.000	0.000	0.011	0.013	0.043	0.055	0.032	0.028	0.035
SnO2	0.000	0.000	0.000	0.022	0.025	0.009	0.012	0.013	0.008	0.009
Al2O3	0.021	0.034	0.041	0.028	0.023	0.000	0.000	0.012	0.022	0.000
Sc2O3	0.009	0.021	0.016	0.011	0.031	0.021	0.011	0.014	0.009	0.008
FeO	12.916	12.892	12.672	12.233	12.821	10.991	10.332	9.882	9.774	9.433
MnO	6.935	7.122	7.398	7.773	7.093	6.698	7.322	7.984	8.112	8.454
CaO	0.009	0.012	0.008	0.024	0.023	0.000	0.000	0.008	0.000	0.009
MgO	0.007	0.000	0.000	0.000	0.000	0.000	0.000	0.000	0.000	0.000
Total	99.518	99.633	99.755	99.743	99.441	99.970	99.398	99.958	100.232	99.971
Ions on the basis of 6 O										
Si	0.002	0.001	0.001	0.001	0.001	0.001	0.000	0.000	0.000	0.001
U	0.000	0.000	0.000	0.000	0.000	0.001	0.001	0.000	0.000	0.001
Sn	0.000	0.000	0.000	0.001	0.001	0.000	0.000	0.000	0.000	0.000
Al	0.001	0.002	0.003	0.002	0.002	0.000	0.000	0.001	0.002	0.000
Sc	0.000	0.001	0.001	0.001	0.002	0.001	0.001	0.001	0.001	0.000
Fe	0.645	0.644	0.633	0.611	0.644	0.620	0.588	0.560	0.552	0.536
Mn	0.351	0.360	0.374	0.393	0.361	0.383	0.422	0.458	0.464	0.486
Ca	0.001	0.001	0.001	0.002	0.001	0.000	0.000	0.001	0.000	0.001
Mg	0.001	0.000	0.000	0.000	0.000	0.000	0.000	0.000	0.000	0.000
Sum A-Site	1.002	1.010	1.012	1.011	1.011	1.007	1.012	1.022	1.019	1.026
Nb	1.734	1.729	1.727	1.726	1.721	1.074	1.081	1.069	1.067	1.064
Ta	0.238	0.241	0.243	0.245	0.250	0.813	0.818	0.826	0.825	0.834
Ti	0.033	0.032	0.030	0.029	0.028	0.136	0.120	0.120	0.124	0.114
Sum B-Site	2.005	2.001	2.000	2.000	2.000	2.023	2.018	2.014	2.016	2.011

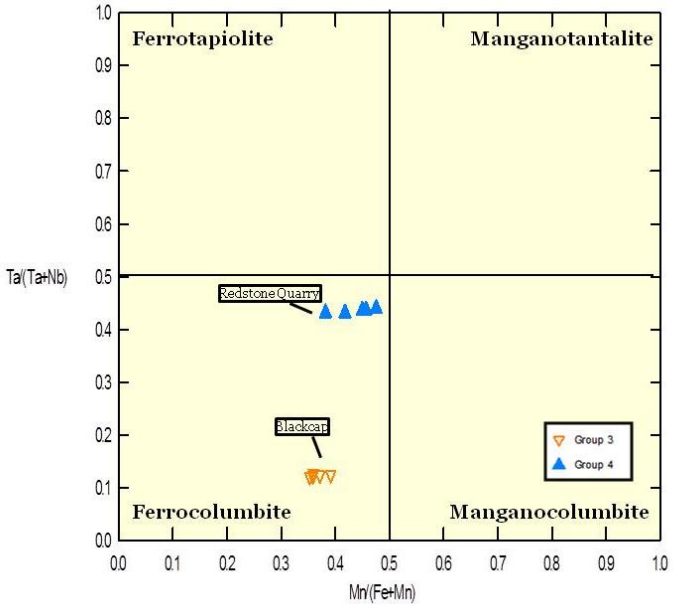

Figure 32. Columbite quadrilateral with Ta/(Ta+Nb) versus Mn/(Fe+Mn) for ferrocolumbite based on apfu.

Fluorite

Fluorite (Figure 33) was identified at North Sugarloaf, West Hurricane, East Hurricane, Redstone Quarry, Government Pit, Brook Diggings, Oliver Trench, Eastman Topaz, and Raccoon Gulch. The quantity needed for DCP analysis was large enough in only two localities, Oliver Trench and Sugarloaf. The results of the DCP analysis (Table 7) were compared to an analysis on the same two localities in a previous study in 2002 by Louise Totten (Figure 34). Overall, the new data from this thesis and the previous data show the same elemental patterns. They have a slight enrichment in Ce and Sm and a slight depletion in Nd and La. The only variance between the two is the exceedingly high Yb peak in the new Sugarloaf analysis. Further investigation is needed to fully explain this Yb enrichment. Accessory minerals associated with fluorite include allanite-(Ce), apatite, "bastnaesite", "euxenite/aeschynite", members of the ferberite/huebnerite series, ferrocolumbite, fergusonite-(Y), almanditic garnet, members of the ilmenite series, members of the ilmenite/pyrophanite series, magnetite, "monazite", rutile, "samarskite", thorite, thorogummite, and zircon.

Figure 33. Fluorite→ CaF_2

2.5 mm crystals (mindat.org)

Table 7. Direct-coupled plasma spectrophotometer chondrite-normalized analysis of fluorite based on apfu.

	Moat Mtn	Sugarloaf Mtn.	Moat Mtn. (previous)	Sugarloaf Mtn. (previous)
La	158.74	606.42	153.81	573.45
Ce	504.36	1348.63	552.29	887.49
Nd	189.67	556.27	153.84	440.55
Sm	235.288	482.95	249.38	435.54
Eu	46.83	53.64		
Gd	168.05	274.45	164.25	227.94
Dy	291.00	345.14	215.71	277.48
Yb	1008.10	8891.14	1067.23	1030.86
Y	567.00	524.05	652.93	562.35

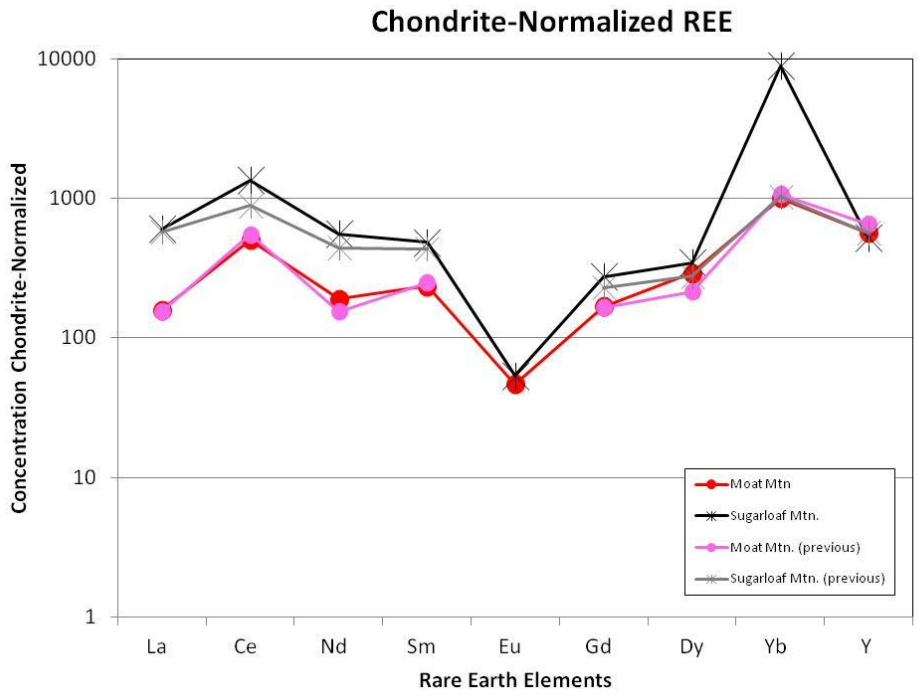

Figure 34. Chondrite-normalized REE diagram depicting the REE enrichments and depletions of fluorite samples from this thesis and previous work.

Ilmenite/pyrophanite series

Ilmenite/pyrophanite series (Figure 35) minerals were identified in the heavy mineral separates from Government Pit, Redstone Quarry, East Hurricane, North Percy Peak, Mousetrap, and Eastman Topaz. Figure 36 shows a representative EDS analysis of an ilmenite/pyrophanite series mineral within the energy range 1-15 keV showing the family of various X-ray lines for its essential elements.

Figure 35. Ilmenite/pyrophanite series→ $(Fe^{2+},Mn)TiO_3$ 3.5 mm crystals (mindat.org)

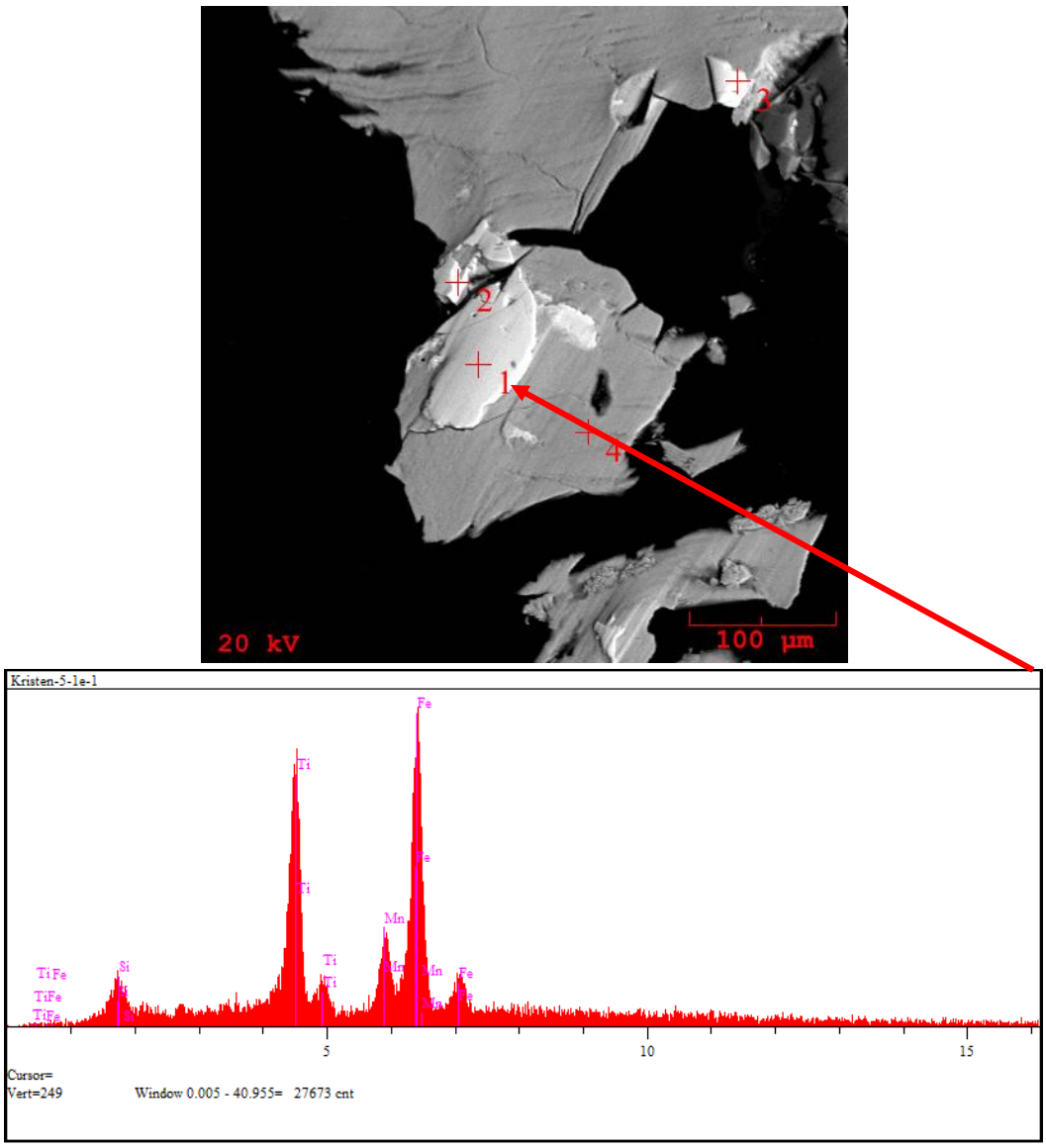

Figure 36. Photomicrograph and an EDS analysis of a member from the ilmenite/pyrophanite series from the Large Boulder near Oliver Diggings.

Table 8. Electron microprobe analysis of ilmenite and hematite.

	East Hurricane					Redstone					Raccoon Gulch					Ravine				
Wt. % oxides																				
SiO2	0.021	0.036	0.011	0.009	0.041	0.051	0.023	0.018	0.020	0.041	0.021	0.009	0.021	0.007	0.011	0.018	0.009	0.013	0.018	0.014
TiO2	50.009	49.876	49.856	50.055	50.008	49.876	50.008	49.845	49.774	50.121	0.312	0.400	0.322	0.355	0.289	0.309	0.298	0.310	0.289	0.303
Al2O3	0.211	0.198	0.166	0.177	0.194	0.332	0.412	0.387	0.405	0.389	0.022	0.032	0.024	0.025	0.028	0.018	0.020	0.023	0.026	0.011
FeO	46.211	47.099	47.104	44.006	43.211	46.877	45.983	46.664	45.098	45.000	88.098	87.967	87.988	88.065	88.034	88.005	88.114	87.984	87.666	87.675
MnO	2.610	2.556	2.764	4.887	4.953	2.223	2.870	2.472	3.987	3.778	0.976	1.121	1.091	1.054	0.983	0.958	0.983	1.112	1.092	1.076
CaO	0.080	0.111	0.095	0.106	0.087	0.411	0.342	0.412	0.443	0.412	0.023	0.021	0.018	0.015	0.026	0.043	0.033	0.039	0.028	0.032
MgO	0.600	0.499	0.645	0.541	0.539	0.387	0.412	0.376	0.454	0.554	0.008	0.007	0.000	0.000	0.006	0.000	0.000	0.000	0.006	0.007
Total	99.74	100.38	100.64	99.78	99.03	100.16	100.05	100.17	100.18	100.30	89.46	89.56	89.46	89.52	89.38	89.35	89.46	89.48	89.13	89.12
Ions on the basis of 3 O																				
Al	0.006	0.006	0.005	0.005	0.006	0.010	0.012	0.012	0.012	0.012	0.001	0.002	0.001	0.001	0.001	0.001	0.001	0.001	0.001	0.001
Fe	0.987	1.002	1.001	0.940	0.927	0.998	0.979	0.994	0.960	0.955	2.944	2.934	2.940	2.940	2.945	2.944	2.945	2.939	2.941	2.941
Mn	0.056	0.055	0.059	0.106	0.108	0.048	0.062	0.053	0.086	0.081	0.033	0.038	0.037	0.036	0.033	0.032	0.033	0.038	0.037	0.037
Ca	0.002	0.003	0.003	0.003	0.002	0.011	0.009	0.011	0.012	0.011	0.001	0.001	0.001	0.001	0.001	0.002	0.001	0.002	0.001	0.001
Mg	0.023	0.019	0.024	0.021	0.021	0.015	0.016	0.014	0.017	0.021	0.000	0.000	0.000	0.000	0.000	0.000	0.000	0.000	0.000	0.000
Sum of A-site	1.075	1.085	1.092	1.074	1.064	1.082	1.078	1.084	1.087	1.079	2.979	2.975	2.978	2.978	2.981	2.980	2.981	2.980	2.941	2.941
Si	0.001	0.001	0.000	0.000	0.001	0.001	0.001	0.000	0.001	0.001	0.001	0.000	0.001	0.000	0.000	0.001	0.000	0.001	0.001	0.001
Ti	0.961	0.955	0.953	0.961	0.965	0.955	0.957	0.955	0.953	0.956	0.009	0.012	0.010	0.011	0.009	0.009	0.009	0.009	0.009	0.009
Sum of B-Site	0.961	0.956	0.953	0.962	0.967	0.957	0.958	0.955	0.953	0.957	0.010	0.012	0.011	0.011	0.009	0.010	0.009	0.010	0.049	0.049

*The two samples on the left are ilmenite and the two on the right are hematite.

"Monazite"

"Monazite" (Figure 37) is an abundant accessory mineral in some of the miarolitic pegmatite locations including Raccoon Gulch, Redstone Quarry, West Hurricane, North Sugarloaf, and North Percy Peak. Figure 38 shows a representative EDS analysis of a "monazite" within the energy range 1-15 keV showing the family of various X-ray lines for its essential elements.

Figure 37. "Monazite"→ (Ce, La, Nd)PO_4

2 mm crystal (mindat.org)

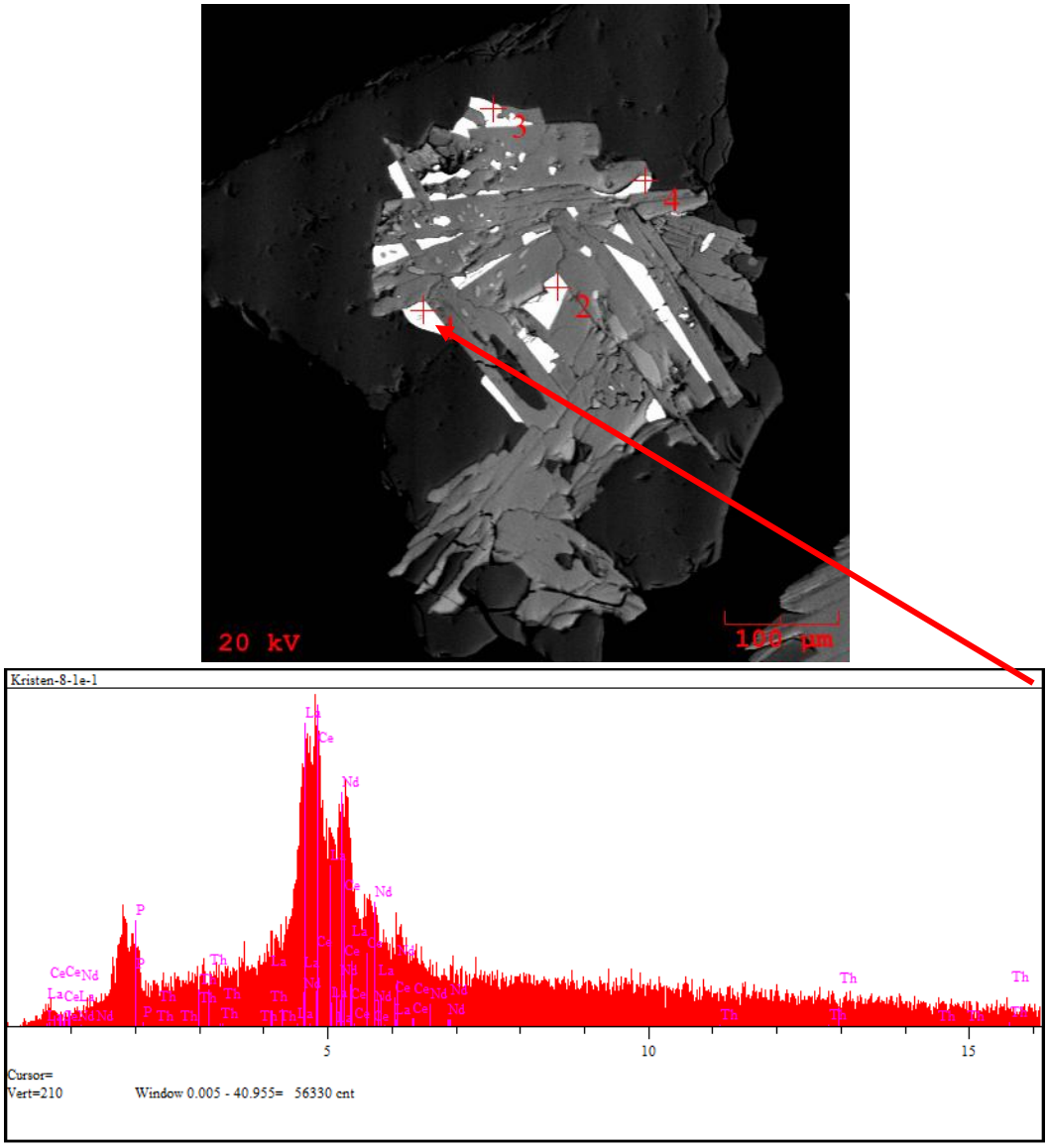

Figure 38. Photomicrograph and an EDS analysis of "monazite" from West Hurricane.

Rutile

Rutile (Figure 39) was identified in the heavy mineral separates from Raccoon Gulch. Figure 40 shows a representative EDS analysis of rutile within the energy range 1-15 keV showing the family of various X-ray lines for its essential elements

Figure 39. Rutile→ TiO_2

6 mm crystal (mindat.org)

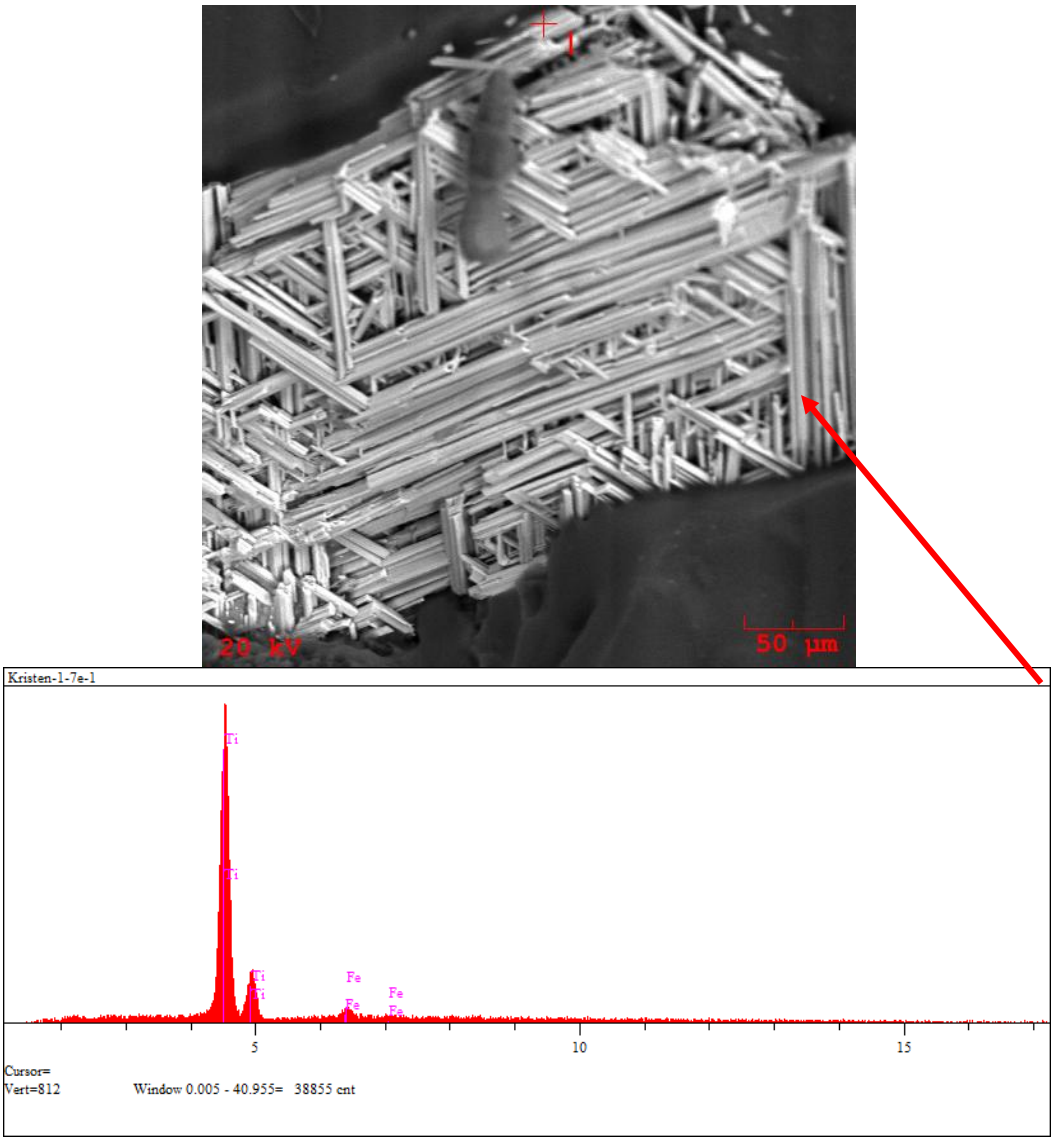

Figure 40. Photomicrograph and an EDS analysis of rutile showing sagenite twinning from Raccoon Gulch.

"Samarskite"

"Samarskite" (Figure 41) is exceedingly rare in these miarolitic pegmatite samples; although a few grains were identified in the heavy mineral separates from Oliver Trench. Figure 42 shows a representative EDS analysis of samarskite within the energy range 1-15 keV showing the family of various X-ray lines for its essential elements.

Figure 41. "Samarskite" → (Y+REE, Fe^{2+}, Fe^{3+}, U, Th, Ca)(Nb, Ta, Ti)O_4 3 mm crystal (mindat.org)

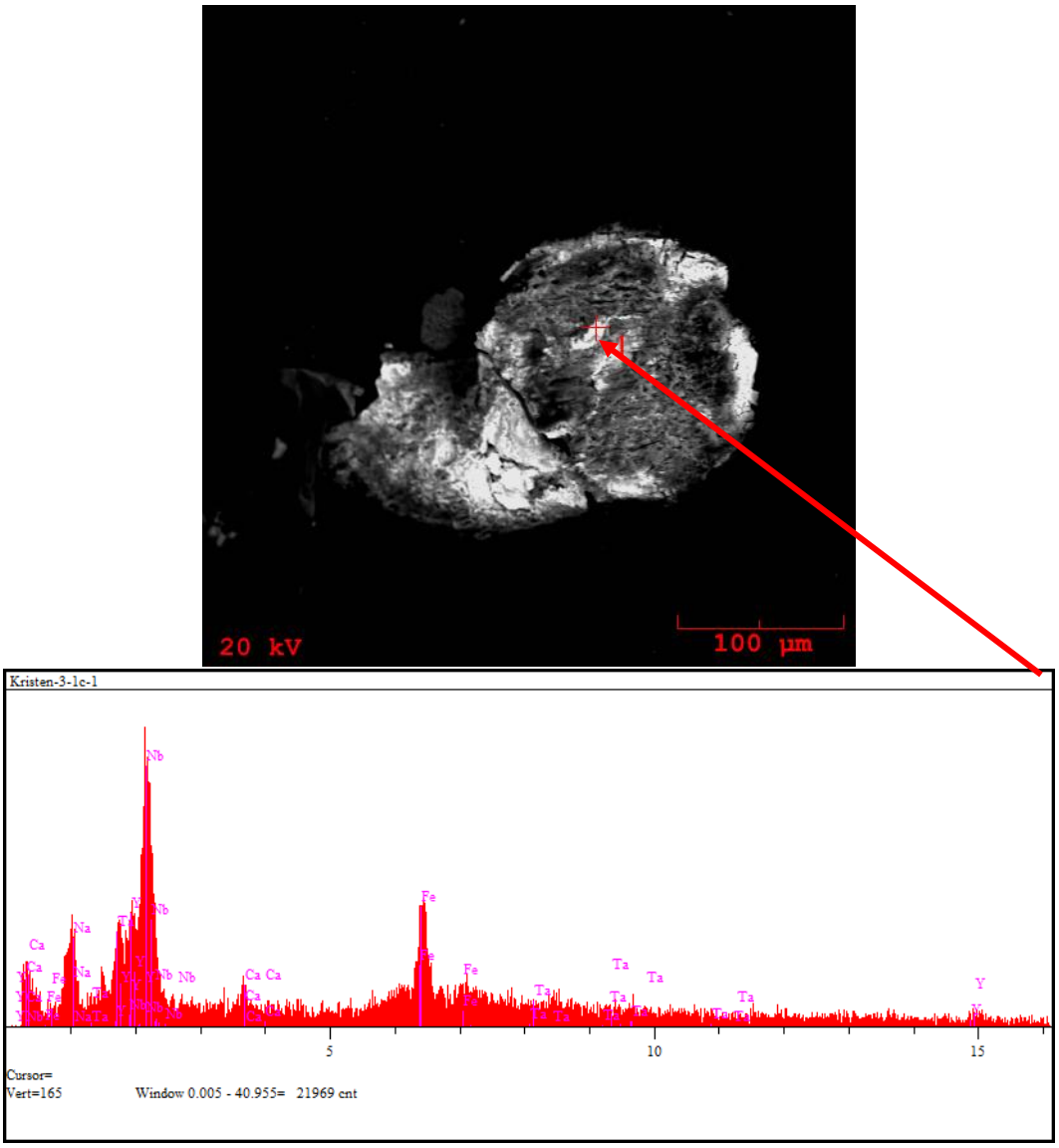

Figure 42. Photomicrograph and an EDS analysis of "samarskite" from Oliver Trench.

Thorite/thorogummite

Thorite/thorogummite (Figure 43) minerals are rare in the miarolitic pegmatites sampled' although a few grains were found in the heavy mineral separates from Oliver Trench, Redstone Quarry, North Sugarloaf, North Percy Peak, and Ravine. The sample from the Ravine was analyzed and oxide weight percent from EMP data was used to calculate ion proportions on the basis of 4 O per formula unit (Table 8). Figure 44 shows a representative EDS analysis of a thorite/thorogummite mineral within the energy range 1-15 keV showing the family of various X-ray lines for its essential elements.

Figure 43. Thorite/ Thorogummite→ $ThSiO_4$/ $(Th, U)_2SiO_4(OH)_4$

Simplified Formula → $ABO_4(OH)_4$

17 mm crystal of thorite (mindat.org)

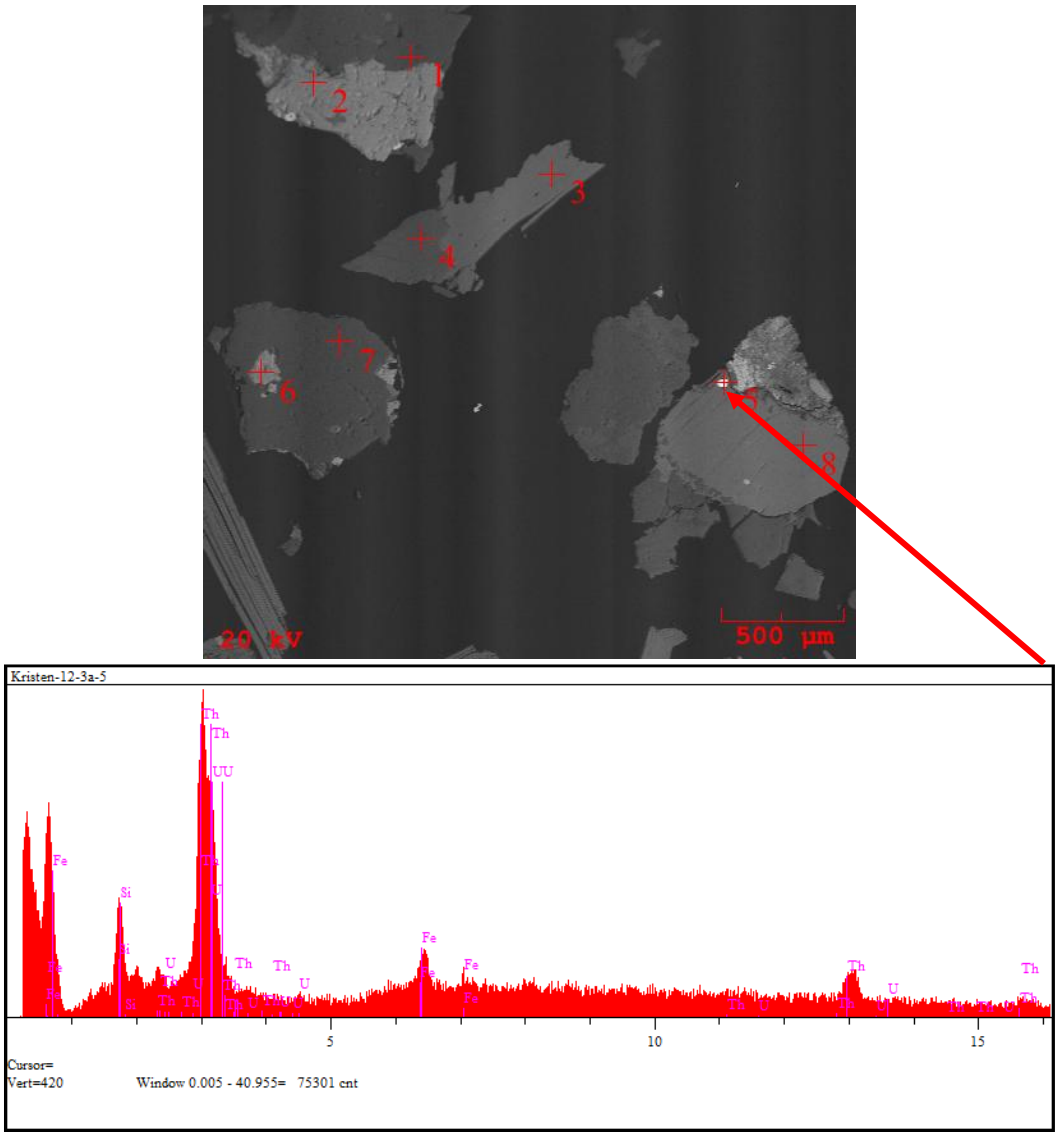

Figure 44. Photomicrograph and an EDS analysis of thorite/thorogummite from North Percy Peak.

Table 9. Electron microprobe analysis of thorite/thorogummite.

	Ravine				
Wt. % oxides					
UO2	2.333	2.304	1.891	2.002	1.671
ThO2	52.334	51.730	53.009	51.891	49.843
SiO2	12.872	12.344	12.455	12.820	13.092
TiO2	0.232	0.325	0.271	0.226	0.145
Al2O3	0.634	0.512	0.456	0.265	0.553
FeO	1.112	1.455	1.872	1.223	3.223
MnO	0.110	0.143	0.118	0.093	0.123
CeO2	1.778	1.983	1.671	1.455	1.001
PbO	0.711	0.683	0.692	0.634	0.455
CaO	0.236	0.345	0.229	0.198	0.434
H2O	27.648	28.176	27.336	29.193	29.460
Total	100.000	100.000	100.000	100.000	100.000
Ions on the basis of 4 O					
U	0.038	0.038	0.031	0.033	0.027
Th	0.870	0.873	0.888	0.884	0.826
Ti	0.013	0.018	0.015	0.013	0.008
Fe	0.068	0.090	0.115	0.077	0.196
Mn	0.007	0.009	0.007	0.006	0.008
Ce	0.045	0.051	0.043	0.038	0.025
Pb	0.014	0.014	0.014	0.013	0.009
Ca	0.018	0.027	0.018	0.016	0.034
Sum of A-Site	1.073	1.121	1.131	1.079	1.134
Si	0.940	0.916	0.917	0.959	0.954
Al	0.055	0.045	0.040	0.023	0.047
Sum of B-Site	0.995	0.960	0.956	0.983	1.002

"Xenotime"

"Xenotime" (Figure 45) was only found in the heavy separates from the Raccoon Gulch locality. Figure 46 shows a representative EDS analysis of "xenotime" within the energy range 1-15 keV showing the family of various X-ray lines for its essential elements.

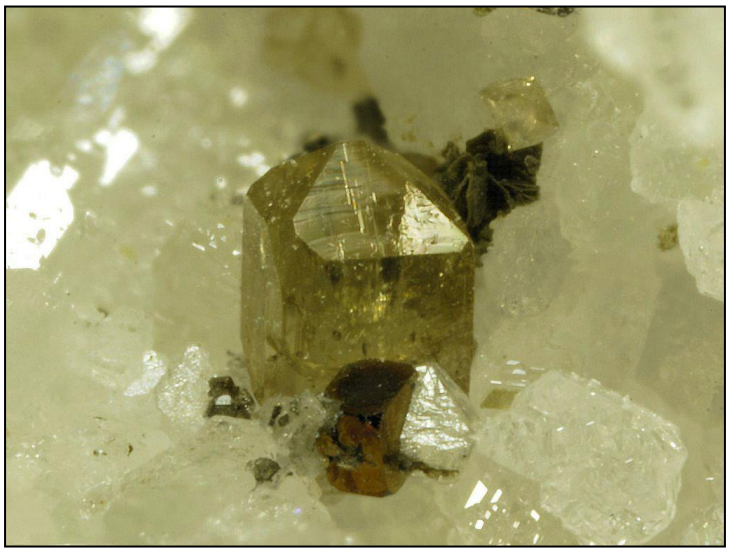

Figure 45. "Xenotime" → (Y, Yb)PO_4 8 mm crystal (mindat.org)

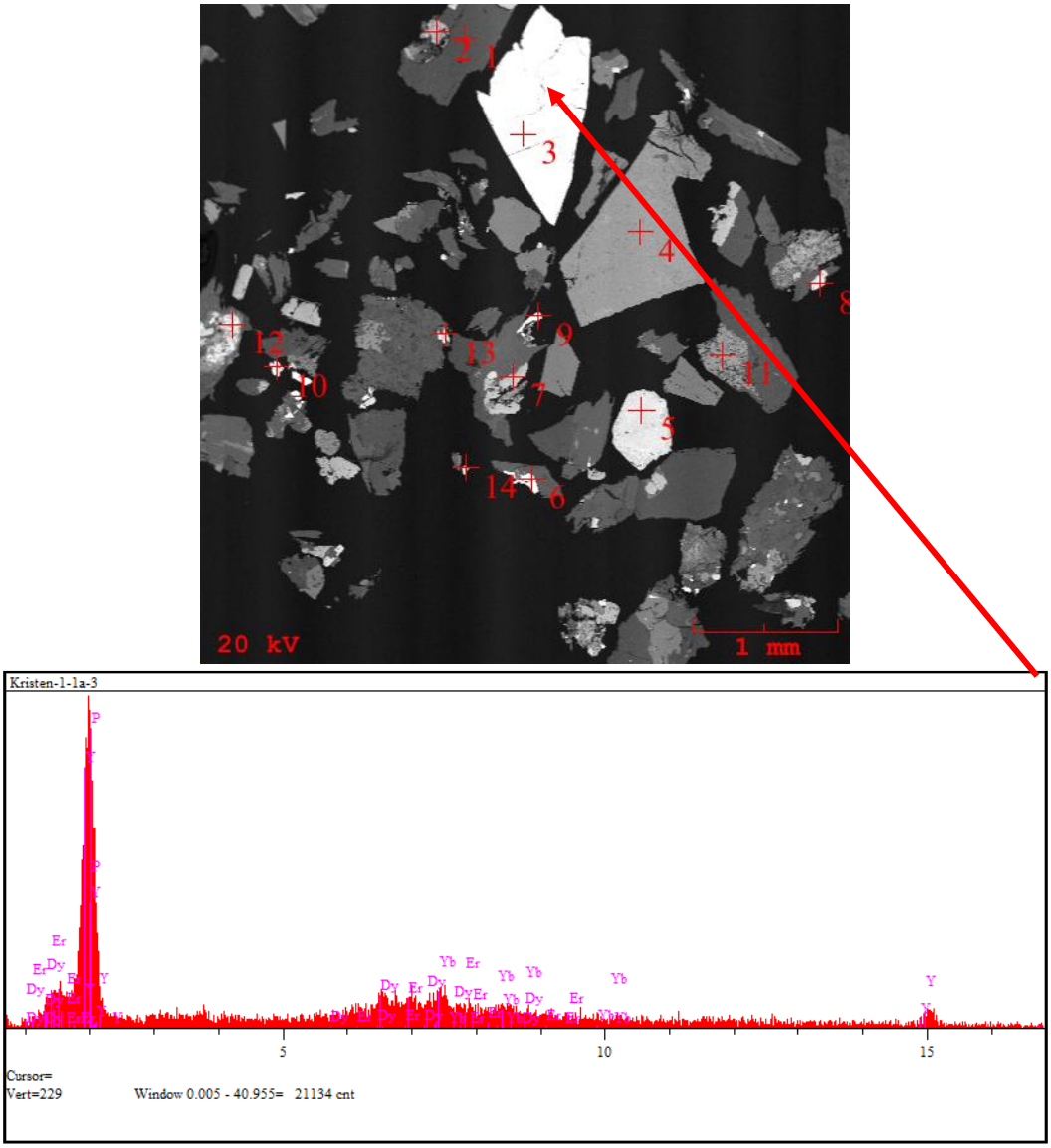

Figure 46. Photomicrograph and an EDS analysis of "xenotime" from Raccoon Gulch.

Zircon

Zircon (Figure 47) was identified in all the miarolitic pegmatites sampled and analyzed from Oliver Trench, Oliver Diggings, Eastman Topaz, Mousetrap, Ravine, Government Pit, Redstone Quarry, Blackcap, and North Percy Peak. The zircon grains range from colorless to yellow, and its accessory minerals include allanite-(Ce), apatite, "bastnaesite", "euxenite/aeschynite", members of the ferberite/huebnerite series, ferrocolumbite, fergusonite-(Y), fluorite, almanditic garnet, members of the ilmenite series, members of the ilmenite/pyrophanite series, magnetite, "monazite", rutile, "samarskite", thorite, and thorogummite. Oxide weight percent from EMP data was used to calculate ion proportions on the basis of 4 O per formula unit (Table 9). On the Zr/Hf versus HfO_2 plot, the data forms a uniformly, down sloping curve with the locations at the bottom of the curve having the highest HfO_2 concentration and the lowest Zr/Hf ratio (Figure 39). This plot suggests these miarolitic pegmatites are probable products of a differentiated granitic parental melt. The sample locations with the highest HfO_2 concentration (<4.50 wt.% HfO_2) have the highest degree of geochemical evolution. These samples include North Percy Peak, Ravine, Government Pit, and Oliver Trench.

Figure 48 shows a representative EDS analysis of zircon within the energy range 1-15 keV showing the family of various X-ray lines for its essential element.

Figure 47. Zircon → $ZrSiO_4$

Simplified Formula → ABO_4

2 mm crystal (mindat.org)

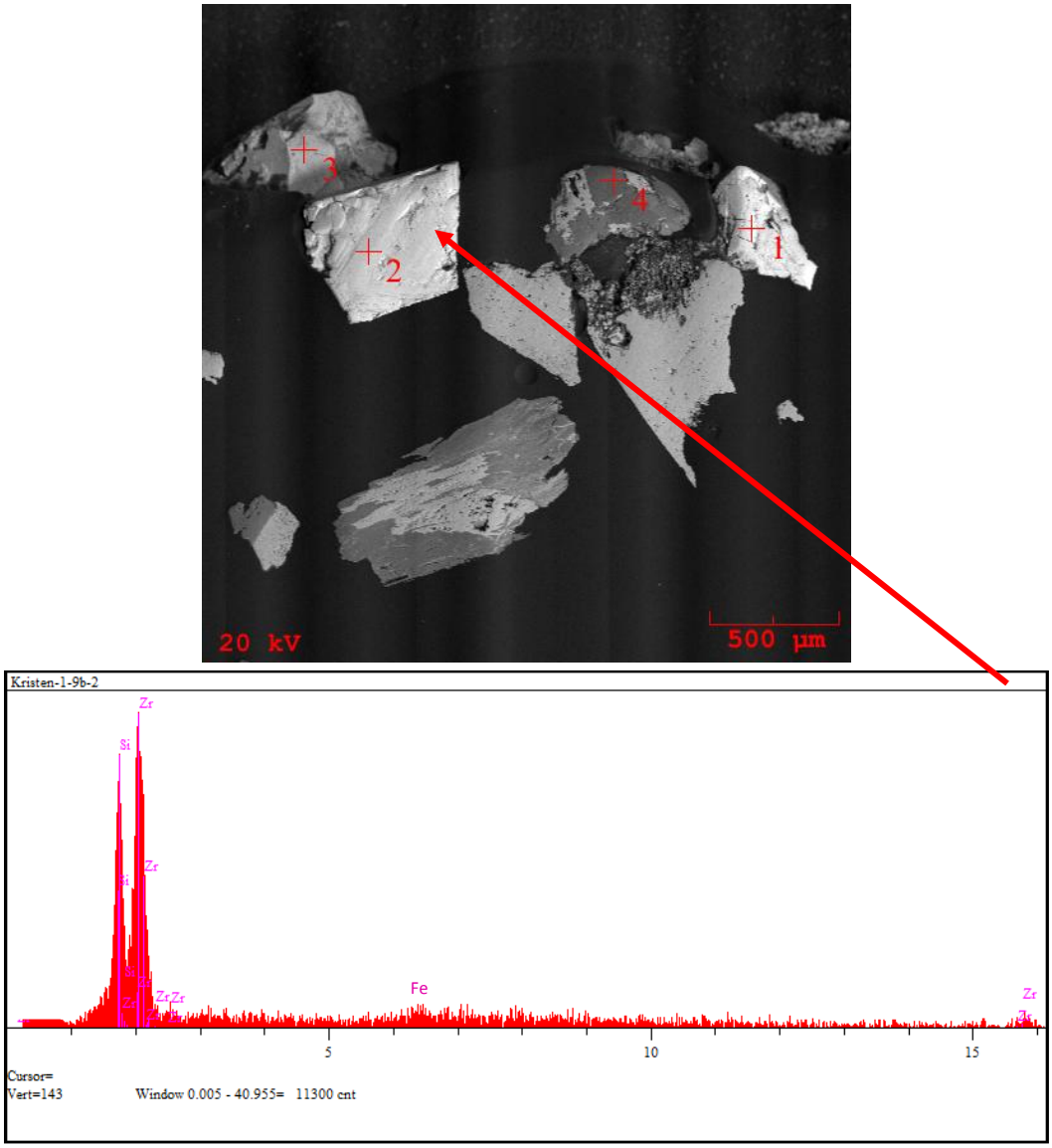

Figure 48. Photomicrograph and an EDS analysis of zircon from Raccoon Gulch.

Table 10. Electron microprobe analysis of zircon.

	Oliver Diggings					Oliver Trench										
Wt % oxides																
ZrO2	60.009	59.895	60.055	59.893	59.903	60.101	60.078	60.083	60.100	60.210	60.540	60.562	60.115	60.210	60.287	60.112
SiO2	31.788	31.723	31.811	31.612	31.613	31.981	31.983	31.991	31.933	31.657	31.840	31.560	21.677	31.657	31.455	31.671
TiO2	0.654	0.098	0.070	0.032	0.076	0.130	0.123	0.109	0.104	0.078	0.078	0.078	0.078	0.078	0.078	0.112
ThO2	0.898	1.001	1.054	0.933	0.984	1.004	0.982	1.005	0.993	0.365	0.235	0.294	0.345	0.365	0.341	0.256
UO2	0.033	0.054	0.024	0.037	0.033	0.095	0.093	0.093	0.098	0.083	0.070	0.055	0.060	0.083	0.078	0.101
HfO2	4.876	5.098	5.312	5.099	5.332	4.550	4.435	4.563	4.494	3.873	3.673	3.798	3.867	3.873	3.923	3.889
Al2O3	0.045	0.112	0.143	0.310	0.228	0.101	0.094	0.123	0.121	0.145	0.111	0.182	0.150	0.145	0.147	0.092
FeO	2.020	1.870	1.867	2.009	1.776	1.000	1.003	0.974	0.984	1.710	1.665	1.623	1.810	1.710	1.990	1.384
MnO	0.776	0.934	0.856	0.804	0.777	0.564	0.552	0.553	0.561	0.885	0.893	0.076	0.650	0.903	0.903	0.962
MgO	0.000	0.000	0.000	0.008	0.000	0.029	0.028	0.032	0.028	0.033	0.028	0.022	0.031	0.033	0.021	0.000
CaO	0.332	0.343	0.303	0.384	0.411	0.332	0.305	0.315	0.322	0.420	0.555	0.467	0.312	0.420	0.413	0.467
Total	101.431	101.128	101.495	101.121	101.133	99.887	99.676	99.841	99.738	99.459	99.688	98.717	89.095	99.477	99.636	99.046
Ions on the basis of 4 O																
Zr	0.907	0.910	0.910	0.910	0.911	0.918	0.918	0.917	0.919	0.921	0.922	0.931	1.094	0.921	0.923	0.914
Th	0.006	0.007	0.007	0.007	0.007	0.007	0.007	0.007	0.007	0.003	0.002	0.002	0.003	0.003	0.002	0.002
U	0.000	0.000	0.000	0.000	0.000	0.001	0.001	0.001	0.001	0.001	0.000	0.000	0.000	0.001	0.001	0.001
Hf	0.043	0.045	0.047	0.045	0.047	0.041	0.040	0.041	0.040	0.035	0.033	0.034	0.041	0.035	0.035	0.035
Al	0.002	0.004	0.005	0.011	0.008	0.004	0.003	0.005	0.004	0.005	0.004	0.007	0.007	0.005	0.005	0.003
Fe	0.052	0.049	0.049	0.052	0.046	0.026	0.026	0.026	0.026	0.045	0.043	0.043	0.056	0.045	0.052	0.036
Mn	0.020	0.025	0.023	0.021	0.021	0.015	0.015	0.015	0.015	0.024	0.024	0.002	0.021	0.024	0.024	0.025
Mg	0.000	0.000	0.000	0.000	0.000	0.001	0.001	0.001	0.001	0.002	0.001	0.001	0.002	0.002	0.001	0.000
Ca	0.011	0.011	0.010	0.013	0.014	0.011	0.010	0.011	0.011	0.014	0.019	0.016	0.012	0.014	0.014	0.016
Sum of A-Site	1.042	1.052	1.051	1.060	1.055	1.023	1.022	1.023	1.024	1.048	1.048	1.036	1.236	1.049	1.058	1.032
Si	0.985	0.989	0.989	0.985	0.986	1.001	1.003	1.002	1.001	0.993	0.995	0.995	0.809	0.993	0.988	0.988
Ti	0.015	0.002	0.002	0.001	0.002	0.003	0.003	0.003	0.002	0.002	0.002	0.002	0.002	0.002	0.002	0.003
Sum of B-Site	1.000	0.991	0.990	0.986	0.988	1.004	1.006	1.004	1.004	0.995	0.996	0.997	0.811	0.995	0.989	0.990

Table 10. Electron microprobe analysis of zircon (continued).

	Oliver Trench				Eastman Topaz					Mousetrap					Ravine	
Wt % oxides																
ZrO2	59.957	60.093	60.154	60.095	61.567	61.608	61.568	61.734	61.801	61.709	61.815	61.781	61.791	61.800	59.856	60.014
SiO2	31.700	31.598	31.712	31.566	31.987	31.922	31.891	32.002	31.984	32.009	31.981	31.945	32.011	31.964	31.728	31.811
TiO2	0.089	0.092	0.100	0.127	0.098	0.089	0.086	0.056	0.099	0.086	0.045	0.054	0.056	0.043	0.150	0.103
ThO2	0.283	0.274	0.319	0.322	0.211	0.189	0.183	0.178	0.173	0.234	0.192	0.216	0.195	0.189	0.887	0.923
UO2	0.089	0.082	0.089	0.098	0.056	0.045	0.063	0.030	0.045	0.087	0.056	0.062	0.072	0.045	0.132	0.115
HfO2	3.935	3.834	3.902	4.021	3.987	3.783	3.899	3.693	3.935	3.776	3.563	3.673	3.489	3.544	5.007	5.032
Al2O3	0.100	0.084	0.045	0.121	0.087	0.009	0.022	0.015	0.033	0.044	0.121	0.091	0.144	0.082	0.054	0.023
FeO	1.329	1.229	1.362	1.445	0.554	0.577	0.563	0.623	0.639	0.453	0.463	0.445	0.437	0.452	0.997	1.043
MnO	0.903	0.778	0.803	0.987	0.378	0.343	0.393	0.376	0.400	0.367	0.340	0.330	0.351	0.336	0.432	0.456
MgO	0.000	0.009	0.023	0.022	0.008	0.000	0.000	0.000	0.007	0.000	0.032	0.022	0.027	0.031	0.000	0.000
CaO	0.509	0.484	0.488	0.456	0.310	0.295	0.311	0.289	0.311	0.111	0.126	0.133	0.101	0.143	0.322	0.341
Total	98.894	98.557	98.997	99.260	99.243	98.860	98.979	98.996	99.427	98.876	98.734	98.752	98.674	98.629	99.565	99.861
Ions on the basis of 4 O																
Zr	0.912	0.921	0.922	0.921	0.939	0.943	0.942	0.943	0.942	0.944	0.945	0.946	0.945	0.946	0.919	0.919
Th	0.002	0.002	0.002	0.002	0.002	0.001	0.001	0.001	0.001	0.002	0.001	0.002	0.001	0.001	0.006	0.007
U	0.001	0.001	0.001	0.001	0.000	0.000	0.000	0.000	0.000	0.001	0.000	0.000	0.001	0.000	0.001	0.001
Hf	0.035	0.034	0.035	0.036	0.036	0.034	0.035	0.033	0.035	0.034	0.032	0.033	0.031	0.032	0.045	0.045
Al	0.004	0.003	0.002	0.004	0.003	0.000	0.001	0.001	0.001	0.002	0.004	0.003	0.005	0.003	0.002	0.001
Fe	0.035	0.032	0.036	0.038	0.014	0.015	0.015	0.016	0.017	0.012	0.012	0.012	0.011	0.012	0.026	0.027
Mn	0.024	0.021	0.021	0.026	0.010	0.009	0.010	0.010	0.011	0.010	0.009	0.009	0.009	0.009	0.012	0.012
Mg	0.000	0.000	0.001	0.001	0.000	0.000	0.000	0.000	0.000	0.000	0.001	0.001	0.001	0.001	0.000	0.000
Ca	0.017	0.016	0.016	0.015	0.010	0.010	0.010	0.010	0.010	0.004	0.004	0.004	0.003	0.005	0.011	0.011
Sum of A-Site	1.029	1.031	1.037	1.046	1.015	1.013	1.015	1.014	1.018	1.007	1.010	1.010	1.009	1.010	1.022	1.024
Si	0.989	0.994	0.997	0.993	1.001	1.002	1.001	1.003	0.999	1.004	1.003	1.003	1.004	1.004	0.999	0.999
Ti	0.002	0.002	0.002	0.003	0.002	0.002	0.002	0.001	0.002	0.002	0.001	0.001	0.001	0.001	0.004	0.002
Sum of B-Site	0.991	0.996	1.000	0.996	1.003	1.004	1.003	1.004	1.002	1.006	1.004	1.004	1.005	1.005	1.003	1.002

Table 10. Electron microprobe analysis of zircon (continued).

	Ravine				North Percy Peak					Government Pit				
Wt % oxides														
ZrO2	59.975	59.893	60.032	60.008	60.037	60.082	60.101	60.005	60.102	60.012	60.211	60.187	60.055	60.041
SiO2	31.782	31.734	31.784	31.976	31.876	31.910	31.899	31.967	31.887	31.773	31.897	31.854	31.900	31.884
TiO2	0.119	0.104	0.092	0.150	0.135	0.099	0.131	0.116	0.098	0.078	0.083	0.090	0.064	0.053
ThO2	0.945	0.934	0.874	0.943	0.117	0.101	0.094	0.084	0.088	0.132	0.110	0.096	0.107	0.122
UO2	0.125	0.154	0.091	0.097	0.110	0.084	0.067	0.072	0.091	0.088	0.081	0.110	0.088	0.076
HfO2	5.009	4.984	5.211	4.553	4.987	4.888	4.723	4.524	4.600	5.211	5.311	5.067	5.212	4.999
Al2O3	0.083	0.081	0.090	0.117	0.088	0.100	0.091	0.073	0.110	0.064	0.043	0.054	0.037	0.033
FeO	1.114	0.833	0.982	0.987	1.760	1.550	1.487	1.612	1.443	0.998	1.100	0.877	0.900	0.786
MnO	0.436	0.399	0.412	0.544	0.546	0.554	0.487	0.507	0.487	0.645	0.567	0.609	0.711	0.723
MgO	0.000	0.000	0.000	0.033	0.000	0.009	0.008	0.000	0.000	0.000	0.000	0.000	0.007	0.000
CaO	0.326	0.298	0.284	0.311	0.675	0.712	0.733	0.688	0.709	0.554	0.609	0.618	0.597	0.603
Total	99.914	99.414	99.852	99.719	100.331	100.089	99.821	99.648	99.615	99.555	100.012	99.562	99.678	99.320
Ions on the basis of 4 O														
Zr	0.918	0.921	0.920	0.917	0.913	0.914	0.916	0.915	0.917	0.919	0.918	0.920	0.918	0.920
Th	0.007	0.007	0.006	0.007	0.001	0.001	0.001	0.001	0.001	0.001	0.001	0.001	0.001	0.001
U	0.001	0.001	0.001	0.001	0.001	0.001	0.000	0.001	0.001	0.001	0.001	0.001	0.001	0.001
Hf	0.045	0.045	0.047	0.041	0.044	0.044	0.042	0.040	0.041	0.047	0.047	0.045	0.047	0.045
Al	0.003	0.003	0.003	0.004	0.003	0.004	0.003	0.003	0.004	0.002	0.002	0.002	0.001	0.001
Fe	0.029	0.022	0.026	0.026	0.046	0.040	0.039	0.042	0.038	0.026	0.029	0.023	0.024	0.021
Mn	0.012	0.011	0.011	0.014	0.014	0.015	0.013	0.013	0.013	0.017	0.015	0.016	0.019	0.019
Mg	0.000	0.000	0.000	0.002	0.000	0.000	0.000	0.000	0.000	0.000	0.000	0.000	0.000	0.000
Ca	0.011	0.010	0.010	0.010	0.023	0.024	0.025	0.023	0.024	0.019	0.020	0.021	0.020	0.020
Sum of A-Site	1.026	1.019	1.023	1.022	1.045	1.042	1.039	1.038	1.038	1.032	1.033	1.029	1.030	1.027
Si	0.998	1.001	0.999	1.002	0.994	0.996	0.997	1.000	0.998	0.998	0.998	0.999	1.000	1.002
Ti	0.003	0.002	0.002	0.004	0.003	0.002	0.003	0.003	0.002	0.002	0.002	0.002	0.002	0.001
Sum of B-Site	1.001	1.003	1.001	1.006	0.997	0.998	1.000	1.002	1.000	1.000	1.000	1.001	1.002	1.003

Table 10. Electron microprobe analysis of zircon (continued).

	Redstone Quarry					Blackcap				
Wt % oxides										
ZrO2	61.539	61.671	61.628	61.566	61.600	60.076	60.101	60.094	60.005	60.051
SiO2	32.398	32.444	32.412	32.621	32.655	31.953	31.966	31.982	31.911	31.871
TiO2	0.120	0.114	0.105	0.100	0.092	0.150	0.091	0.112	0.095	0.089
ThO2	1.338	1.311	1.291	1.118	1.230	0.654	0.555	0.583	0.546	0.511
UO2	0.115	0.089	0.091	0.091	0.078	0.098	0.101	0.081	0.084	0.090
HfO2	3.009	3.012	2.981	3.009	3.072	4.217	4.119	4.124	4.006	4.232
Al2O3	0.132	0.114	0.101	0.104	0.110	0.098	0.034	0.056	0.072	0.032
FeO	0.909	1.023	1.012	1.004	0.982	1.443	1.336	1.244	1.430	1.277
MnO	0.421	0.400	0.393	0.383	0.375	0.423	0.433	0.456	0.409	0.410
MgO	0.067	0.045	0.041	0.050	0.023	0.000	0.000	0.000	0.006	0.000
CaO	0.387	0.411	0.282	0.301	0.281	0.809	0.774	0.784	0.832	0.764
Total	100.435	100.634	100.337	100.347	100.498	99.921	99.510	99.516	99.396	99.327
Ions on the basis of 4 O										
Zr	0.929	0.929	0.931	0.928	0.927	0.915	0.918	0.917	0.917	0.919
Th	0.009	0.009	0.009	0.008	0.009	0.005	0.004	0.004	0.004	0.004
U	0.001	0.001	0.001	0.001	0.001	0.001	0.001	0.001	0.001	0.001
Hf	0.027	0.027	0.026	0.027	0.027	0.038	0.037	0.037	0.036	0.038
Al	0.005	0.004	0.004	0.004	0.004	0.004	0.001	0.002	0.003	0.001
Fe	0.024	0.026	0.026	0.026	0.025	0.038	0.035	0.033	0.037	0.034
Mn	0.011	0.010	0.010	0.010	0.010	0.011	0.011	0.012	0.011	0.011
Mg	0.003	0.002	0.002	0.002	0.001	0.000	0.000	0.000	0.000	0.000
Ca	0.013	0.014	0.009	0.010	0.009	0.027	0.026	0.026	0.028	0.026
Sum of A-Site	1.021	1.022	1.018	1.015	1.013	1.037	1.033	1.032	1.037	1.033
Si	1.003	1.002	1.004	1.008	1.008	0.998	1.001	1.001	1.000	1.001
Ti	0.003	0.003	0.002	0.002	0.002	0.004	0.002	0.003	0.002	0.002
Sum of B-Site	1.006	1.005	1.006	1.010	1.011	1.002	1.003	1.004	1.002	1.003

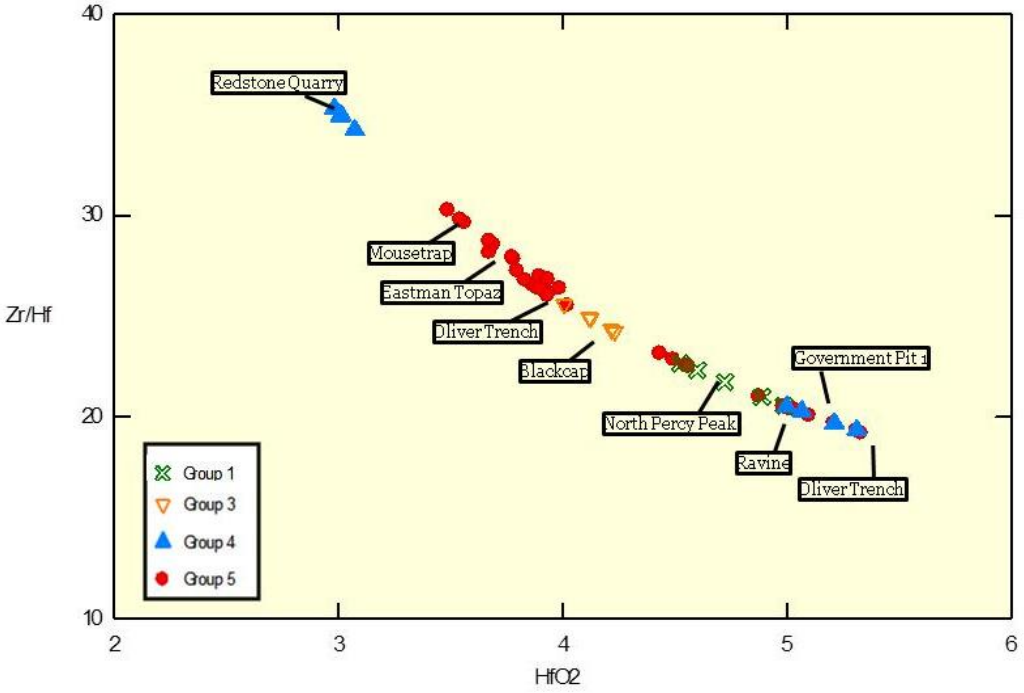

Figure 49. Zr/Hf apfu versus HfO_2 wt.% for zircon.

Petrographic descriptions

The thin sections were used to perform statistical point counts. Point counting is the process of observing the thin section under a petrographic microscope and identifying each mineral in the crosshairs as the slide is moved in small increments. Three hundred representative points were identified for each thin section (Table 10). Overall, all of the miarolitic pegmatites sampled are predominantly composed of quartz and potassium feldspar (combined total of over 75% of the point counts), excluding Blackcap (Figure 50). Blackcap is interesting because while there are no potassium feldspar, albite constitutes for over 60% of the point counts. This albite may be a replacement unit.

The thin sections were also used to observe the varying textures among the miarolitic pegmatite samples (Figures 51-56). All thin section photomicrographs were taken with crossed nicols, and the length of the field of view = 4.5 mm. The grains observed in all of the samples collected are anhedral to subhedral and millimeter to centimeter in size.

Table 11. Point counts from petrographic thin sections.

Group	Locality	Quartz	K-Spar	Albite	Biotite	Musc	Zircon	Opaques	Total
Group 1	**N Percy Peak**	103	122	46	27			2	300
	N Percy Peak	97	168	30	5				300
Group 2	**N Sugar Loaf**	114	142	39	5				300
	N Sugar Loaf	84	134	60	20	2			300
Group 3	**W Hurricane**	111	168	2	19				300
	W Hurricane	88	204		5			3	300
	E Hurricane	99	180	3	17		1		300
	Blackcap	81		200		10		9	300
Group 4	**Gov Pit**	89	196	13	2				300
	Gov Pit	109	174	16	1				300
	Gov Pit	89	157	33	21				300
	Brook Digg	210	27	40	23				300
	Redstone Qu	116	148	12	24				300
Group 5	**Oliver Trench**	53	205	17	25				300
	Oliver Diggings	142	100	31	27				300
	Large Boulder	113	115	31	41				300
Group 6	**Raccoon Gulch**	116	174	10					300
	Raccoon Gulch	70	207	11		12			300
Extra	**Moat Mnt**	109	177	4	5	5			300
	Moat Mnt	75	158	20	47				300
	Moat Mnt	70	197	21	12				300
	Moat Mnt	89	197	2	12				300
	Moat Mnt	121	174	2	3				300

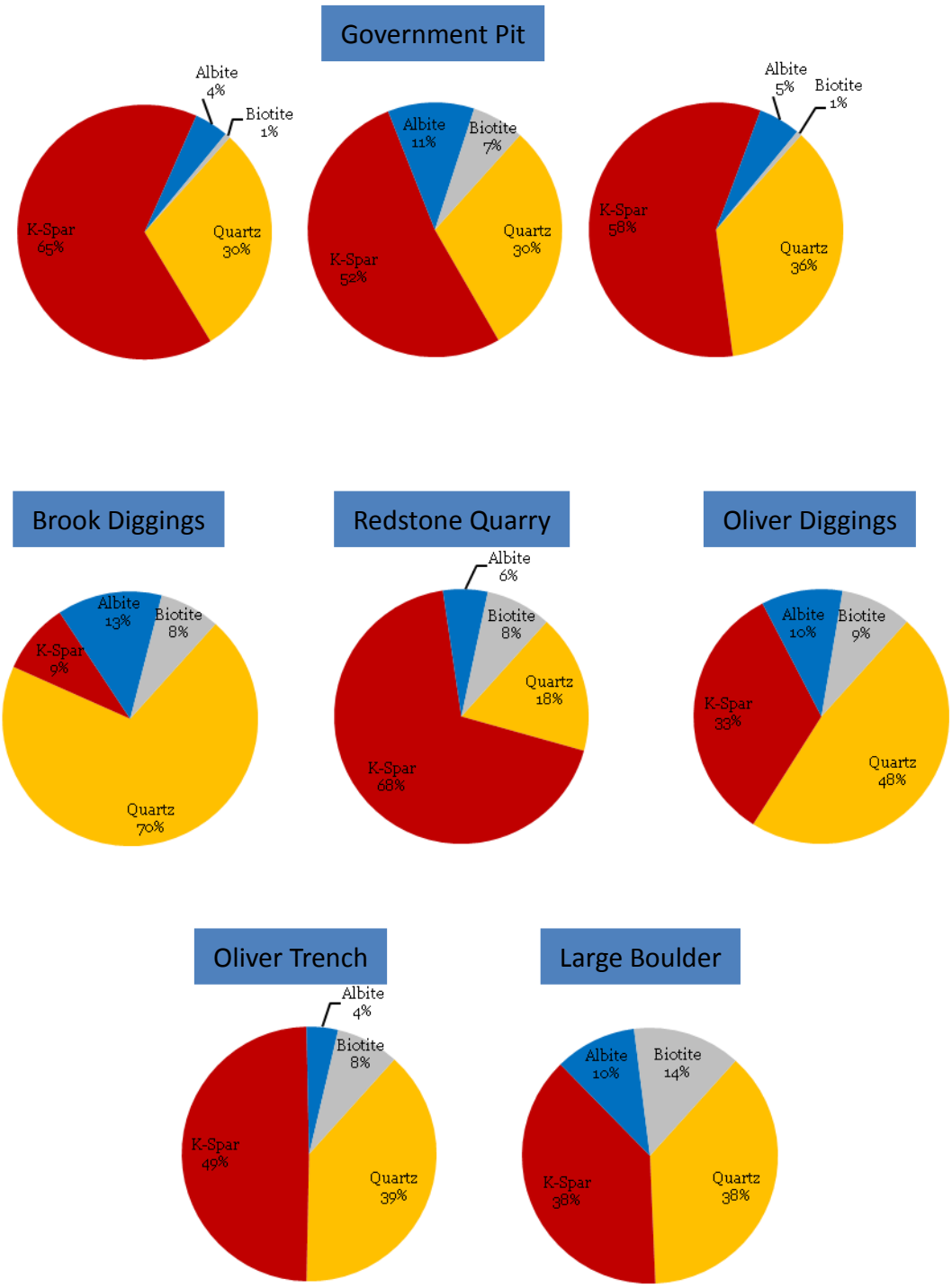

Figure 50. Graphical representation of the point counts from Table 10.

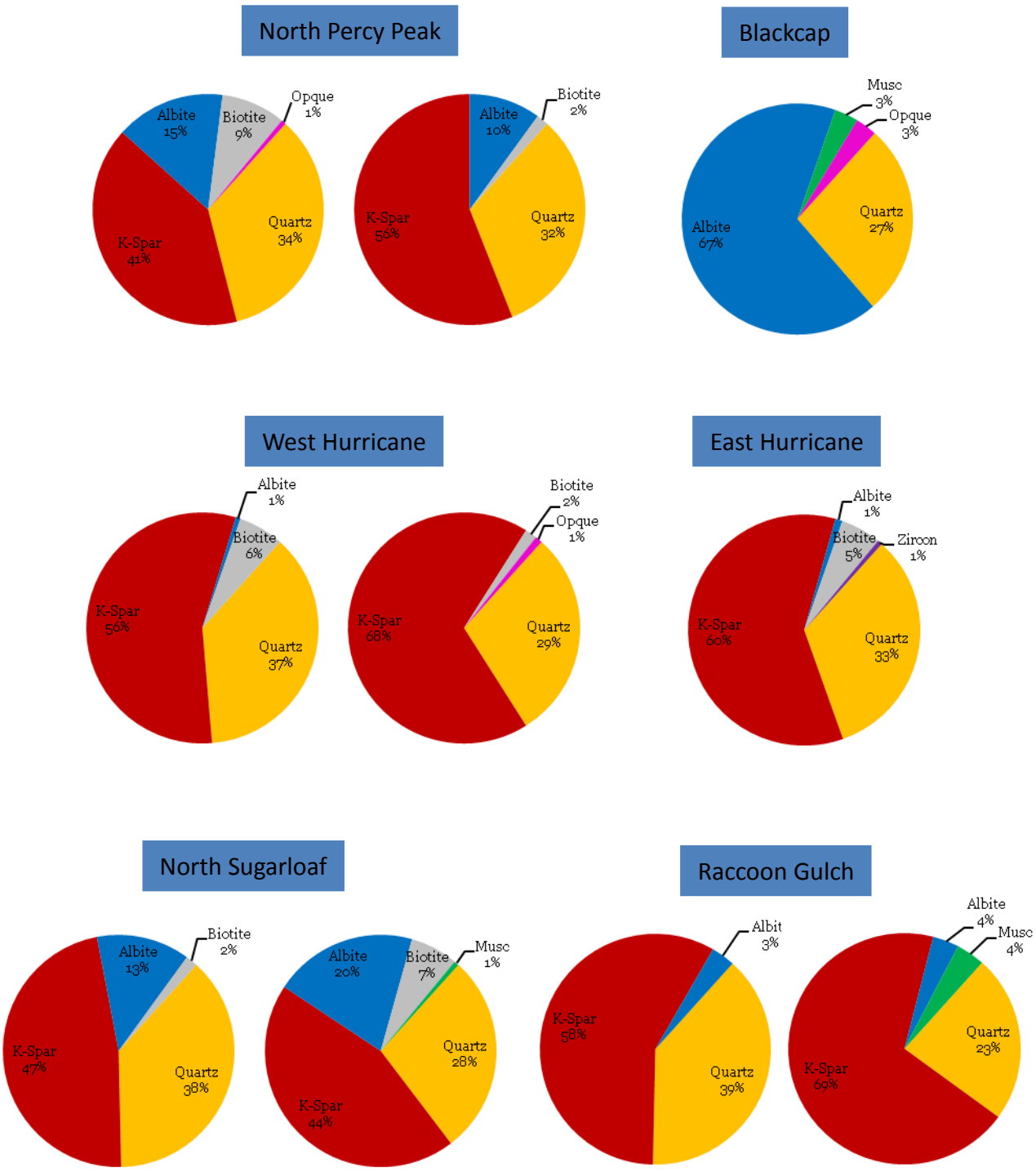

Figure 50 (continued). Graphical representation of the point counts from Table 10.

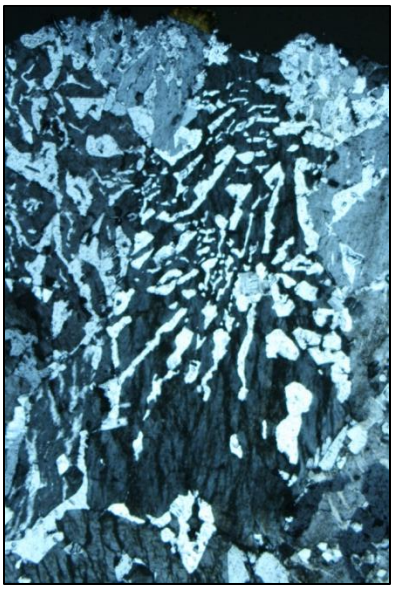

Figure 51. Thin section photomicrograph from Brook Diggings showing myrmekitic texture of quartz and plagioclase.

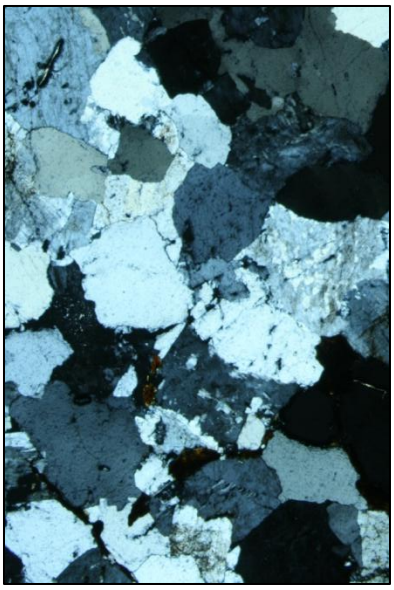

Figure 52. Thin section photomicrograph from Oliver Diggings showing equigranular texture of quartz and potassium feldspar.

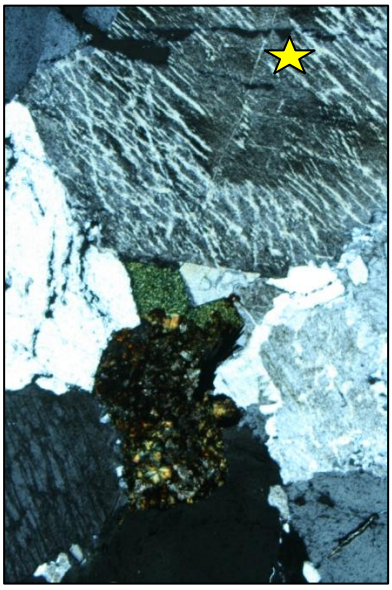

Figure 53. Thin section photomicrograph from Large Boulder near Oliver Diggings showing a zoned, subhedral potassium feldspar grain (star).

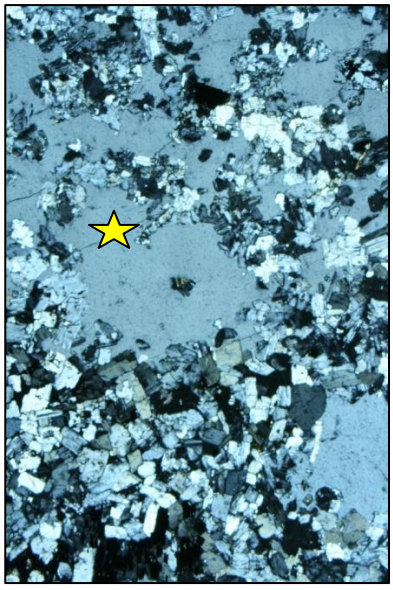

Figure 54. Thin section photomicrograph from Blackcap showing inequigranular texture of quartz phenocrysts (star) surrounded by a matrix of quartz and plagioclase.

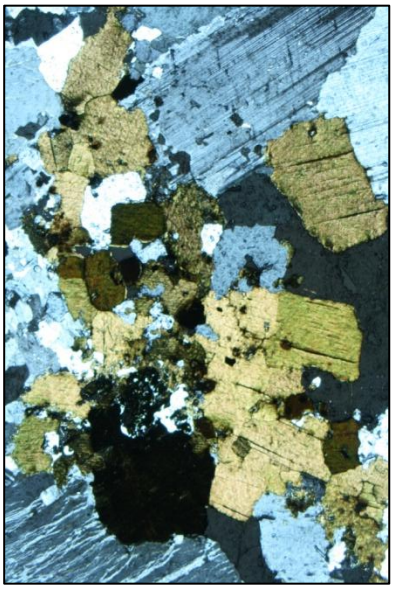

Figure 55. Thin section photomicrograph from West Hurricane showing a cluster of biotite grains.

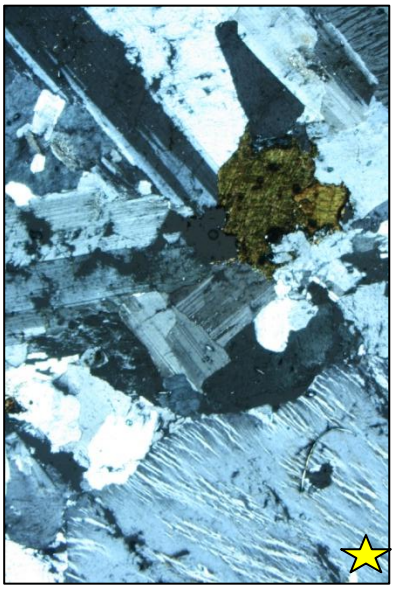

Figure 56. Thin section photomicrograph from North Sugarloaf a coarse perthite grain (star).

Whole rock "wall zone analogue" analysis

According to the Na_2O+K_2O versus SiO_2 plot, all of the miarolitic pegmatites sampled from the WMIP are granitic in composition (Figure 57). Major, trace, and REE element concentrations of the sampled miarolitic pegmatites from XRF analysis are listed in Table 11.

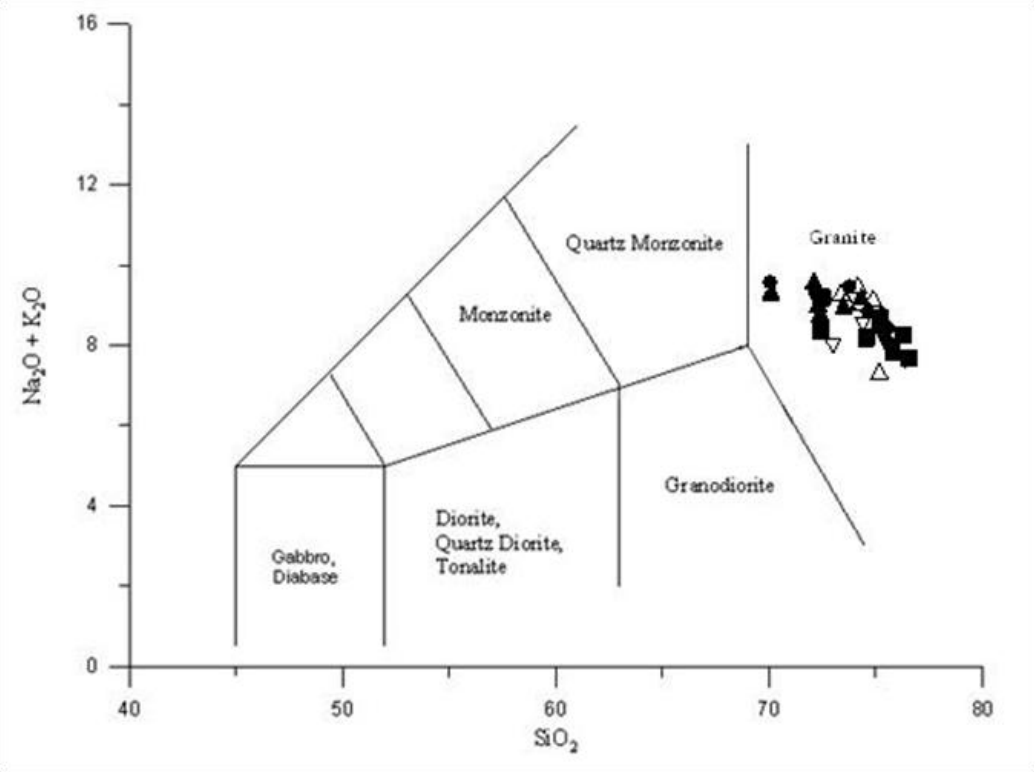

Figure 57. Total alkali wt.% versus silica wt.% diagram showing the rock type of the miarolitic pegmatite samples (Le Maitre 1989).

Table 12. X-ray fluorescence analysis of all whole rock samples.

	Raccoon Gulch							Government Pit		Oliver Trench			Oliver Diggings	Large boulder	Brook Diggings	
	1.1	1.1	1.12	1.13	1.2	1.4	1.9	2.1	2.3	3.1	3.2	3.3	4.1	5.1	6.1	6.2
Wt.% oxides																
SiO2	76.08	76.57	72.75	75.48	76.84	74.83	72.64	70.33	73.77	74.09	75.74	75.49	75.64	70.33	72.35	74.59
TiO2	0.28	0.14	0.16	0.12	0.15	0.23	0.18	0.23	0.15	0.08	0.10	0.15	0.08	0.24	0.10	0.06
Al2O3	11.79	11.96	13.84	12.88	11.51	12.30	12.60	14.02	12.93	13.11	12.37	12.00	12.64	14.29	12.78	13.13
Fe2O3	1.24	0.99	1.50	0.60	0.78	1.79	3.64	2.85	1.84	1.10	1.59	2.07	1.34	3.11	1.77	1.04
MnO	0.07	0.04	0.04	0.03	0.00	0.02	0.07	0.06	0.05	0.01	0.03	0.03	0.02	0.07	0.03	0.01
MgO	0.02	0.00	0.04	0.00	0.00	0.03	0.02	0.01	0.00	0.00	0.00	0.00	0.00	0.00	0.00	0.00
CaO	0.41	0.19	0.20	0.15	0.25	0.57	0.10	1.08	0.80	0.26	0.17	0.25	0.16	0.32	0.57	0.35
Na2O	3.38	3.17	4.03	3.30	3.67	3.65	3.12	3.65	3.21	3.19	3.78	3.77	3.64	3.53	2.66	3.55
K2O	4.52	5.13	5.23	5.45	4.05	4.59	5.29	5.69	5.75	6.32	4.50	4.72	5.16	6.09	6.94	5.66
P2O5	0.04	0.02	0.03	0.02	0.02	0.03	0.03	0.04	0.02	0.01	0.03	0.04	0.01	0.04	0.01	0.01
LOI	2.07	1.72	2.08	1.89	2.66	1.85	2.22	1.90	1.38	1.75	1.62	1.32	1.23	1.79	2.69	1.54
Total	99.90	99.93	99.90	99.92	99.93	99.89	99.91	99.86	99.90	99.92	99.93	99.84	99.92	99.81	99.90	99.94
Trace elements (ppm)																
Zn	13	12	22	3	15	28	57	108	70	12	32	119	18	82	65	27
Rb	273	277	315	318	239	356	380	314	291	438	393	502	358	469	464	338
Sr	25	29	36	27	23	21	22	49	45	10	8	6	15	45	12	15
Zr	405	134	279	171	141	288	124	527	316	154	100	531	129	626	96	71

Table 12. X-ray fluorescence analysis of all whole rock samples (continued).

	Redstone Quarry		West Hurricane			East Hurricane		Blackcap	North Sugarloaf			North Percy Peak			Ravine	Mousetrap	Eastman Topaz
	7.1	7.2	8.1	8.2	8.3	9.1	9.2	10.1	11.1	11.2	11.3	12.1	12.2	12.3	13.1	14.1	15.1
Wt.% oxides																	
SiO2	72.57	72.64	74.43	73.87	75.15	73.63	74.49	75.44	75.26	75.45	72.42	73.26	76.66	74.67	74.97	75.94	75.90
TiO2	0.19	0.28	0.09	0.16	0.17	0.15	0.14	0.11	0.12	0.01	0.16	0.30	0.16	0.16	0.02	0.13	0.05
Al2O3	13.31	13.17	12.45	12.44	12.65	12.53	12.31	12.46	12.64	13.75	13.49	12.54	11.81	13.10	13.53	11.78	12.81
Fe2O3	2.50	2.66	1.65	2.16	2.28	2.34	2.21	2.08	1.48	0.10	1.85	2.97	1.52	1.60	0.68	2.03	1.29
MnO	0.05	0.05	0.04	0.05	0.04	0.03	0.04	0.01	0.12	0.00	0.03	0.11	0.03	0.04	0.01	0.04	0.02
MgO	0.00	0.15	0.00	0.00	0.14	0.00	0.00	0.00	0.00	0.00	0.00	0.21	0.06	0.06	0.00	0.00	0.00
CaO	0.92	0.72	0.19	0.25	0.31	0.31	0.11	0.00	0.08	0.24	0.34	0.53	0.34	0.43	0.16	0.19	0.34
Na2O	3.48	3.97	4.10	4.28	4.38	4.42	4.44	7.09	3.50	6.55	3.94	3.76	3.14	3.96	4.21	3.50	4.11
K2O	5.55	4.83	5.40	4.85	4.79	4.90	4.66	0.24	5.28	2.00	5.35	4.33	4.60	4.67	4.66	4.58	4.36
P2O5	0.04	0.07	0.02	0.01	0.02	0.02	0.02	0.02	0.02	0.01	0.02	0.07	0.03	0.04	0.01	0.02	0.02
LOI	1.25	1.32	1.47	1.80	0.00	1.47	1.43	2.03	1.39	1.82	2.27	1.80	1.55	1.18	1.64	1.66	1.02
Total	99.86	99.86	99.84	99.87	99.93	99.80	99.85	99.48	99.89	99.93	99.87	99.88	98.35	98.73	98.25	98.21	98.90
Trace elements (ppm)																	
Zn	72	44	87	94	77	114	105	135	18	0	59	37	15	21	45	46	46
Rb	295	391	520	289	248	363	361	25	322	259	536	329	293	328	540	300	471
Sr	43	88	BD	BD	4	3	BD	BD	28	7	17	51	51	58	BD	16	BD
Zr	466	434	553	700	814	1146	748	3678	180	131	361	385	197	200	127	480	102

Table 12. X-ray fluorescence analysis of all whole rock samples (continued).

	Raccoon Gulch							Government Pit		Oliver Trench			Oliver Diggings	Large boulder	Brook Diggings	
	1.1	1.1	1.12	1.13	1.2	1.4	1.9	2.1	2.3	3.1	3.2	3.3	4.1	5.1	6.1	6.2
Trace elements (ppm)																
Ba	140.21	226.29	310.60	205.80	119.72	126.75	169.69	313.34	297.65	20.41	27.05	47.91	45.19	383.74	44.23	49.20
La	146.23	45.85	80.44	65.12	49.00	88.35	49.74	141.82	73.29	9.32	20.29	83.28	12.19	183.27	12.17	3.19
Ce	360.53	130.91	206.28	139.22	124.16	223.42	106.09	348.79	180.58	31.47	54.27	185.84	33.85	329.60	32.74	11.16
Pr	34.34	11.77	17.79	12.95	13.20	22.44	10.91	35.57	19.02	3.94	5.66	20.26	3.62	42.27	4.21	1.78
Nd	107.71	37.78	52.79	34.17	44.64	76.24	36.44	119.19	63.87	12.52	16.41	62.26	10.43	144.41	15.55	7.36
Sm	17.76	7.27	15.47	4.57	9.65	15.51	8.46	23.04	12.86	3.92	4.20	14.50	2.58	28.51	5.20	4.01
Eu	0.54	0.55	0.56	0.39	0.44	0.49	0.48	1.57	1.34	0.28	0.07	0.06	0.34	2.03	0.40	0.50
Gd	24.26	9.08	11.18	13.24	10.96	14.67	10.13	31.79	17.96	4.71	5.45	16.86	3.67	29.43	5.44	3.99
Y	68.59	39.77	44.21	22.08	44.20	81.19	46.38	90.32	56.46	39.80	38.39	103.49	26.52	108.04	59.68	45.61
Dy	19.49	10.58	10.73	6.19	13.58	16.97	10.68	20.74	12.84	8.24	8.41	21.31	5.65	24.60	8.86	9.15
Ho	2.96	1.68	1.76	0.88	2.04	3.01	1.90	3.36	2.09	1.54	1.70	3.66	1.08	4.00	1.85	1.87
Er	8.78	5.09	5.35	2.54	6.03	8.99	5.26	8.88	5.57	4.51	4.96	9.69	3.25	10.10	5.49	5.43
Lu	1.57	0.90	0.95	0.53	1.07	1.49	0.90	1.41	0.91	0.88	0.73	1.48	0.54	1.50	0.84	0.74
Yb	10.18	5.75	5.91	3.58	7.12	9.85	6.61	11.00	6.99	6.44	5.36	11.33	3.91	11.39	6.50	5.89
Tb	3.55	1.50	1.87	2.11	1.89	2.40	1.90	4.83	3.05	1.51	1.39	4.47	1.14	5.31	1.25	1.19
V	8.16	4.38	4.59	5.10	3.06	6.26	9.63	2.69	1.96	1.70	6.05	14.16	2.06	4.24	0.91	1.12
Cr	2.22	2.62	2.24	4.22	2.64	1.93	5.45	1.92	1.79	2.69	7.09	12.79	2.22	5.06	1.48	3.05
Nb	156.37	121.00	119.68	112.42	127.16	145.55	192.01	166.13	101.31	148.52	186.88	423.58	128.67	154.72	196.99	198.80
Hf	30.08	12.41	16.06	17.15	18.71	16.81	7.51	23.14	16.52	14.38	8.28	28.45	9.59	22.40	7.29	6.89
Ta	14.43	9.78	12.35	15.90	13.13	21.47	16.86	9.39	6.72	14.29	12.70	23.86	11.46	10.16	13.11	14.44
Pb	32.44	40.82	57.25	23.96	28.89	55.40	23.69	323.86	54.78	82.75	69.15	80.53	77.83	68.76	85.99	85.77
Th	60.58	39.71	39.06	27.31	46.37	57.43	43.08	47.93	26.50	73.64	119.04	71.48	68.23	52.24	51.89	37.72
U	13.37	12.42	13.33	7.54	11.82	20.86	16.57	16.30	11.74	31.01	34.66	27.01	13.58	13.88	25.87	22.46

Table 12. X-ray fluorescence analysis of all whole rock samples (continued).

	Redstone Quarry		West Hurricane			East Hurricane		Blackcap	North Sugarloaf			North Percy Peak			Ravine	Mousetrap	Eastman Topaz
	7.1	7.2	8.1	8.2	8.3	9.1	9.2	10.1	11.1	11.2	11.3	12.1	12.2	12.3	13.1	14.1	15.1
Trace elements (ppm)																	
Ba	367.15	291.09	38.32	19.62	33.37	29.29	36.98	20.22	181.98	10.43	93.63	229.93	238.55	236.90	14.35	83.66	27.10
La	93.23	127.59	58.66	113.26	75.04	141.22	125.29	13.65	43.15	41.39	109.30	56.21	11.42	31.97	23.17	68.63	17.04
Ce	210.23	258.16	142.37	257.54	171.29	314.39	276.68	53.61	98.52	145.68	218.19	172.20	33.19	105.33	82.01	194.90	76.18
Pr	22.85	23.50	16.99	25.62	20.62	35.37	29.16	19.65	10.18	17.55	18.98	11.77	2.97	6.40	7.52	17.24	5.58
Nd	79.32	70.30	51.92	79.24	58.62	105.29	85.76	19.54	33.28	57.40	62.47	33.48	7.61	17.96	25.36	55.95	19.23
Sm	16.00	10.97	13.06	12.55	10.47	19.71	14.54	5.91	7.89	16.06	14.03	5.64	0.23	2.91	7.63	11.22	5.80
Eu	1.88	0.93	0.08	0.22	0.11	0.22	0.09	0.05	0.27	0.04	0.53	0.50	0.19	0.23	0.03	0.57	0.07
Gd	17.09	14.88	16.16	17.48	14.89	26.79	20.10	6.59	8.94	15.40	16.16	9.06	2.14	4.96	9.28	13.05	7.78
Y	64.40	43.93	86.08	32.80	34.92	83.79	47.67	80.79	47.00	85.34	70.59	24.43	13.51	14.20	89.28	50.92	60.29
Dy	15.17	10.01	22.65	10.42	17.64	27.39	15.90	53.95	10.52	19.22	14.21	6.58	3.43	3.48	13.71	12.36	10.51
Ho	2.48	1.61	3.30	1.42	2.07	3.61	2.08	6.30	1.91	3.53	2.58	0.98	0.56	0.64	2.82	2.18	2.18
Er	6.40	4.57	8.40	3.81	4.91	9.13	5.52	17.92	5.53	11.46	7.10	3.04	1.81	1.83	8.66	6.13	7.09
Lu	1.01	0.86	1.16	0.68	0.91	1.43	0.98	3.28	0.91	2.94	1.10	0.68	0.42	0.50	1.74	0.87	1.14
Yb	7.52	5.80	8.82	4.95	6.06	10.04	6.61	23.33	6.35	20.75	8.26	4.19	2.65	2.94	12.66	6.35	8.02
Tb	3.44	2.62	5.99	3.43	6.26	8.82	5.55	18.68	2.12	3.08	2.68	1.98	0.93	1.10	2.07	2.77	1.75
V	4.30	8.85	11.25	0.72	8.29	8.58	9.12	9.89	10.88	2.90	1.08	16.30	12.90	14.14	2.75	7.11	14.81
Cr	5.73	5.97	9.18	1.29	8.61	8.13	9.17	8.61	8.16	3.50	1.36	6.12	8.18	7.88	3.63	6.17	19.28
Nb	121.14	123.81	312.70	200.78	164.26	243.92	178.11	#####	187.15	75.36	183.71	148.41	105.17	95.70	173.55	165.33	158.58
Hf	16.92	14.84	46.63	23.14	47.07	59.59	35.58	199.42	12.17	14.79	13.71	15.76	8.82	8.68	11.94	18.65	10.12
Ta	8.33	10.74	26.67	12.62	11.61	18.84	12.85	130.02	16.65	32.40	11.13	16.05	9.88	12.16	53.78	11.22	18.41
Pb	66.15	42.20	198.05	28.42	13.04	31.35	42.02	58.62	27.87	80.24	97.39	50.63	37.19	45.83	118.13	59.04	104.83
Th	40.66	148.32	78.07	42.89	37.67	64.95	39.87	374.79	59.13	42.73	76.93	151.89	57.08	91.12	49.48	53.65	68.31
U	14.36	28.10	39.68	16.11	18.63	29.73	21.50	105.09	21.93	63.70	19.69	24.02	19.00	15.48	34.00	19.69	40.42

Major elements

All the miarolitic pegmatite samples have a high SiO_2 content narrowly ranging from 76.08-76.84 wt.%. High-silica rocks are subdivided into peralkaline, peraluminous, and metaluminous groups on the basis of alkali index. When plotted on the Shand's Index diagram, the majority of the samples are peraluminous. All samples are also Al-rich ranging from 11.51-14.29 wt.% Al_2O_3 and Fe-rich with up to 3.64 wt.% Fe_2O_3. All the samples are Mg-depleted with MgO <0.21 wt.% (Table 11).

Shand's index

The Shand's index plot depicts the aluminum saturation index (ASI) of whole rock samples by determining their molar ratio of A/CNK (Maniar & Piccoli 1989). All the samples plot around the boundary of peralkaline, metaluminous, and peraluminous with the majority plotting in the peraluminous field, indicating these samples are Al-rich (Figure 58). Classifying these miarolitic pegmatites as peraluminous is supported by the findings of topaz in the sample areas and the fact that they are silica-rich with >70 wt.% SiO_2 (Frost & Frost 1997).

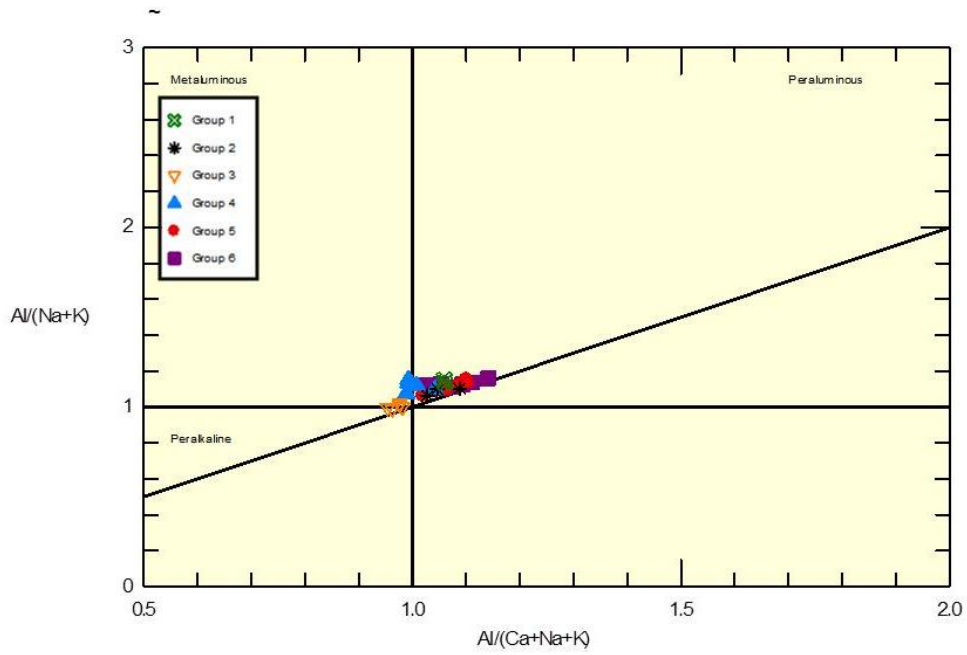

Figure 58. Shand's index depicting the Al saturation in the whole rock samples of the miarolitic pegmatites based on ppm (Maniar & Piccoli 1989).

R_1, R_2 discriminatio

n diagram

De la Roche et al. (1980) introduced a technique to characterize igneous rocks as alkaline or subalkaline with the R_1, R_2 discrimination diagram. Using the whole rock XRF data, all the samples from the WMIP plot in the subalkaline field, indicating they are Si-rich (>70 wt.% SiO_2) (Figure 59).

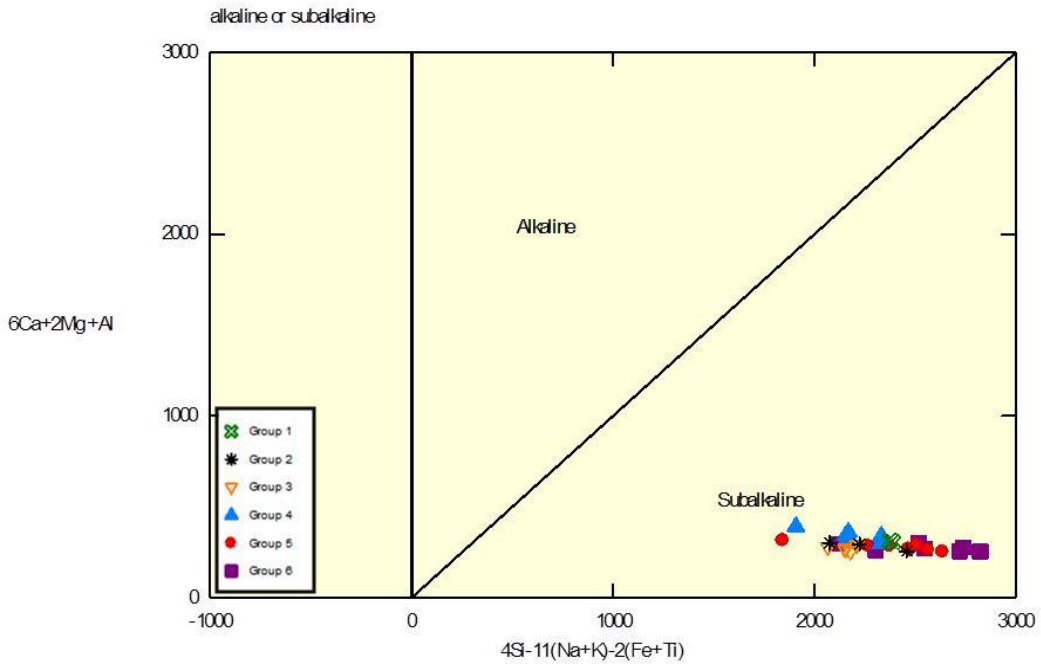

Figure 59. R_1, R_2 discrimination diagram based on ppm (De la Roche et al. 1980).

Calc-Alkalic/Tholeiitic affiliation plot

Subalkaline rocks are subdivided into either a calc-alkalic (Fe-poor) or tholeiitic (Fe-rich) affiliation using this plot (Namur 2011). All of the miarolitic pegmatite samples plot in the tholeiitic field indicating they are Fe-rich (Figure 60), which is expected because peraluminous A-type granites are typically Fe-rich (Frost &Frost 1997). This subdivision supports that these miarolitic pegmatites are rift related, because tholeiites typically form at continental rift areas.

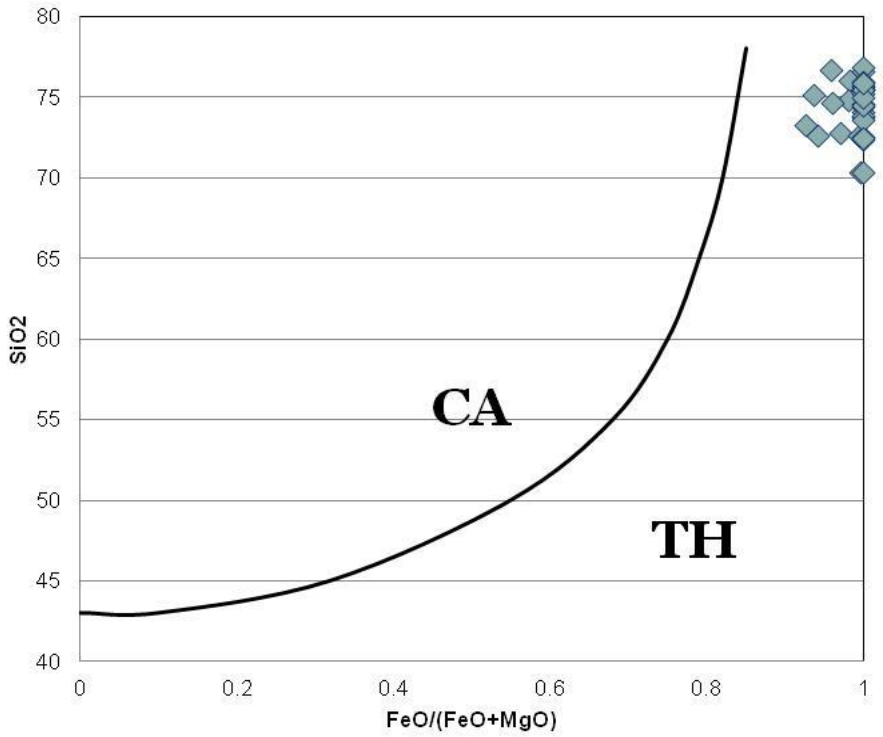

Figure 60. Calc-alkalic/tholeiitic affiliation plot based on wt.% (Namur 2011).

K/Rb versus Rb

This Rb versus K/Rb plot serves as a good indicator of the degree of geochemical evolution of these miarolitic pegmatites. As Rb increases and the ratio of K/Rb decreases, the degree of geochemical evolution increases. All the samples show an elevated Rb concentration (>239 ppm) indicating all the miarolitic pegmatites sampled from the WMIP are highly evolved (Figure 61). The localities with the highest Rb (>471 ppm) concentration and essentially the highest degree of geochemical fractionation are Ravine, Oliver Trench, West Hurricane, North Sugarloaf, and Eastman Topaz. Overall, the groups are slightly scattered, possibly indicating that closely related pegmatitic rocks have varying degrees of geochemical evolution.

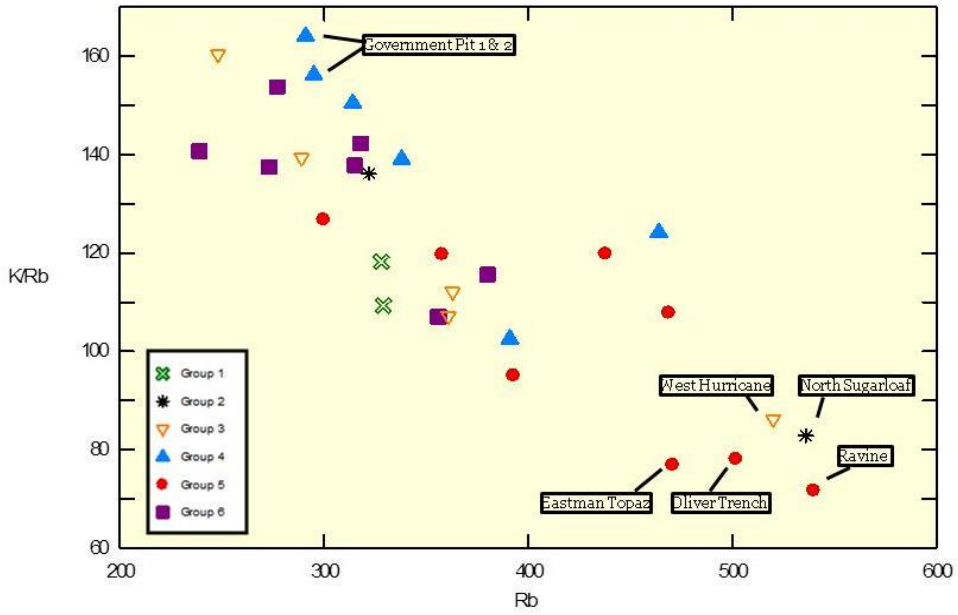

Figure 61. K/Rb versus Rb for whole rock analysis of all samples based on ppm.

Trace elements

These miarolitic pegmatite samples show an overall enrichment in REE and some trace elements. All of the samples are Ce-rich (up to 360.53 ppm) and Ta-poor (as low as 6.72 ppm) as would be expected for this NYF-system. All of the samples show a slight to strong Eu anomaly ranging from 0.03-2.03 ppm (Table 11).

Whole rock REE abundance

The Ce-La-Nd ternary shows all the samples are Ce-dominant (Figure 62). The Ce-La-Y ternary again shows most of the samples are Ce-dominant, although the Ravine, Brook Diggings, and Oliver Trench are Y-dominant (Figure 63). The Ti-Nb-Ta ternary shows that none of the samples have a significant Ta enrichment consistent with the idea that these miarolitic pegmatites are NYF-systems formed in an anorogenic setting (Figure 64).

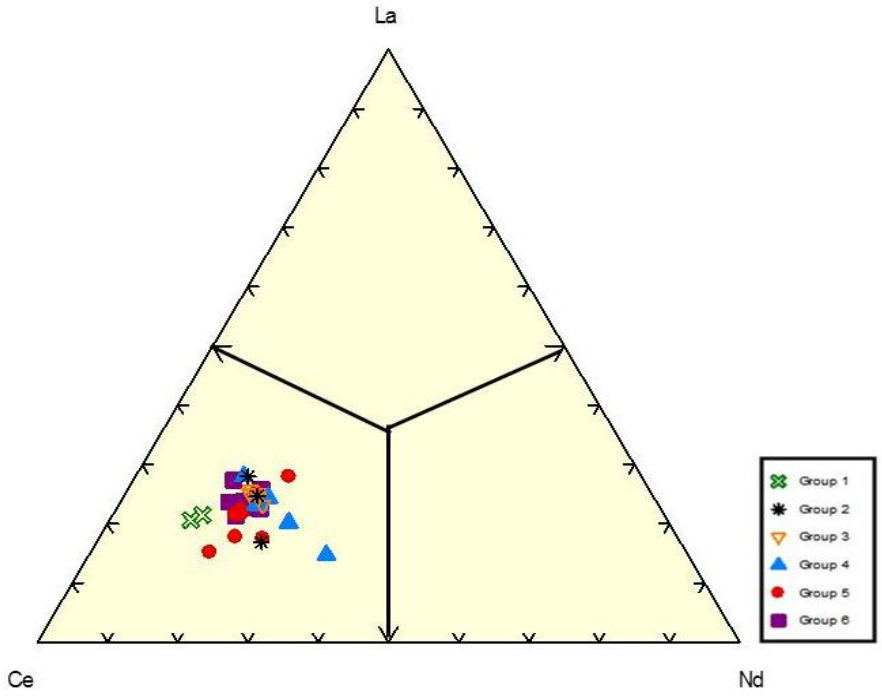

Figure 62. Ce-La-Nd ternary showing trace element abundance from whole rock analysis of all samples based on ppm.

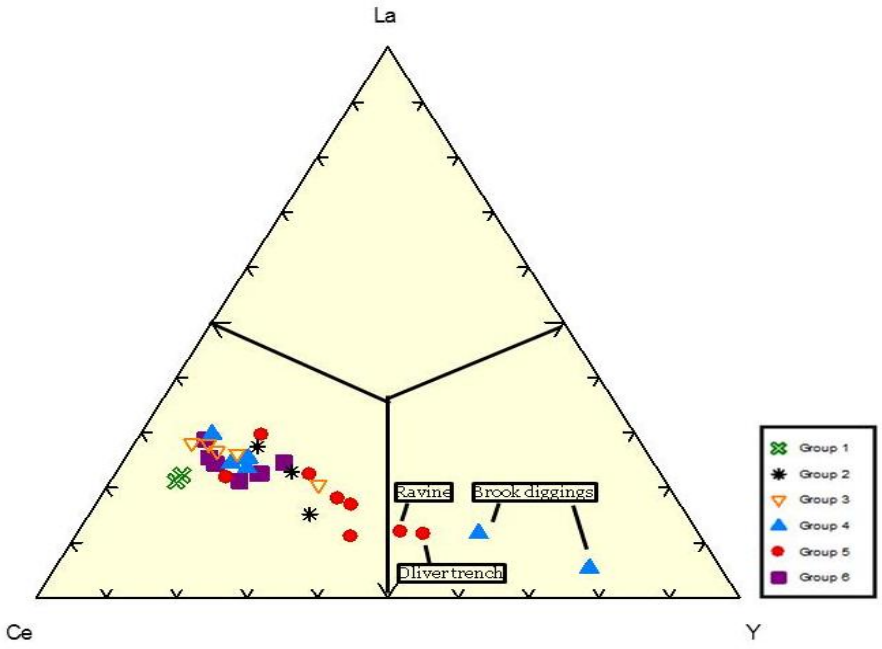

Figure 63. Ce-La-Y ternary showing trace element abundance from whole rock analysis of all samples based on ppm.

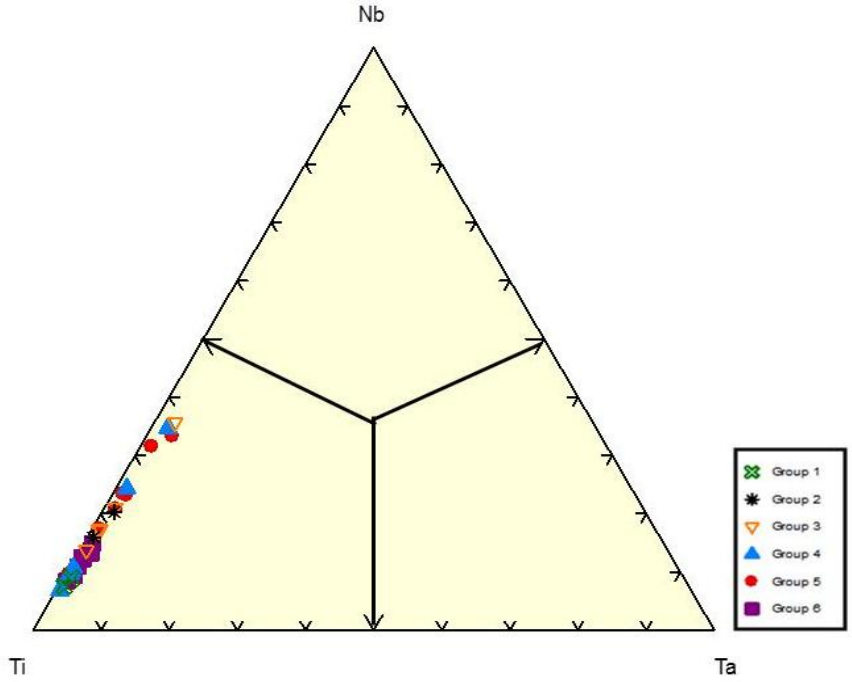

Figure 64. Ti-Nb-Ta ternary showing trace element abundance from whole rock analysis of all samples based on ppm.

Chondrite-normalized REE diagram

The chondrite-normalized REE diagram (Sun & McDonough 1989) shows that all of the miarolitic pegmatites have very similar overall patterns (Figure 65). The majority of the samples show a light REE (LREE) -enrichment with a slight Tb spike. The pronounced negative Eu anomaly suggests that plagioclase fractionation and alkali feldspar has played a significant role in the formation of these miarolitic pegmatites.

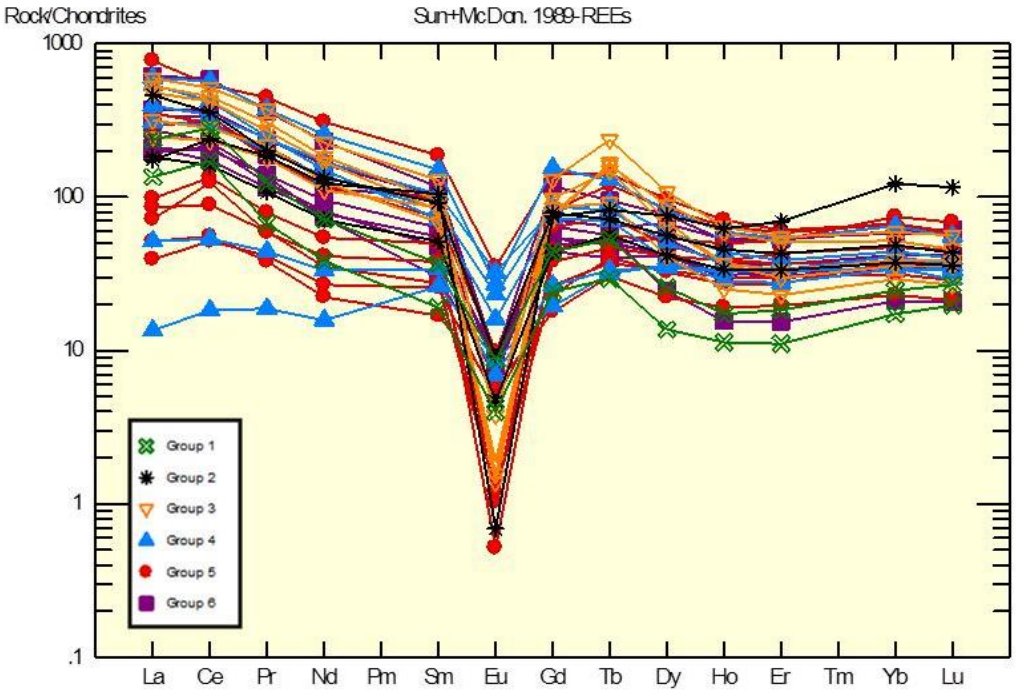

Figure 65. Whole rock chondrite normalized REE diagram depicting the REE enrichments and depletions for all the sampled miarolitic pegmatites based on ppm (Sun & McDonough 1989).

Spider diagram

The spider diagram (Sun & McDonough 1989) shows strong trace element pattern similarities amongst the samples suggesting that these miarolitic pegmatites are all petrogenetically related to the same province. All the samples are enriched in Rb, Dy, U, Th,and Pb, and depleted in Ba, Y, Sr, P, and Ti (Figure 66). Overall, all the samples are LREE-enriched. The wide variations in enrichments and depletions indicate all of the miarolitic pegmatites sampled are geochemically evolved.

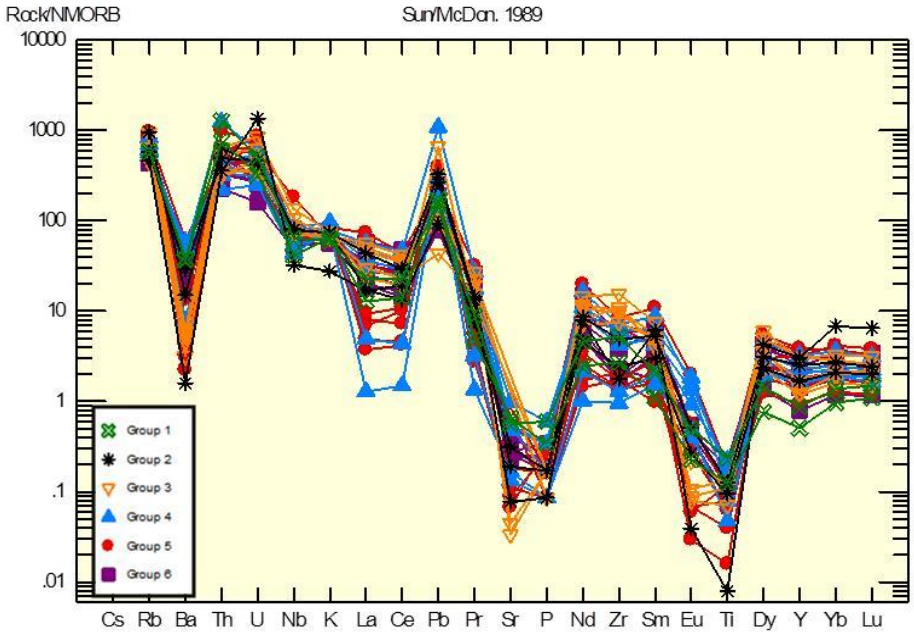

Figure 66. Trace element abundances from XRF whole rock analysis based on ppm (Sun & McDonough 1989).

Tectonic discrimination diagrams

Igneous rocks form in a wide variety of tectonic settings, including mid-ocean ridges (ORG), volcanic arcs (VAG), syn-collisional settings (syn-COLG), and within plate settings (WPG). The tectonic setting can be determined using the trace element abundances with tectonic discrimination diagrams (Pearce et al. 1984). All the miarolitic pegmatites sampled consistently fall in the WPG field of the various tectonic discrimination diagrams (Figures 67-70) suggesting again these miarolitic pegmatites were formed anorogenically due to extensional crustal thinning as a result of rifting.

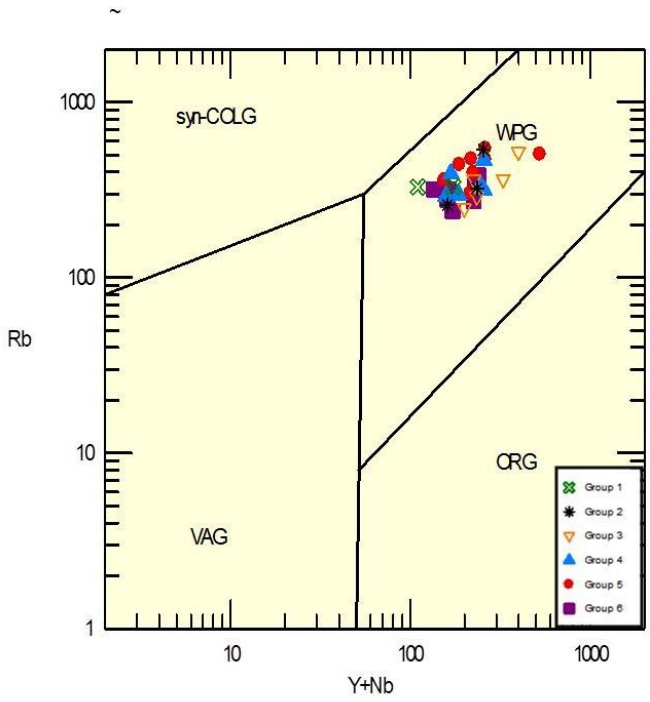

Figure 67. Rb versus Y+Nb tectonic discrimination diagram for all samples based on ppm (Pearce et al. 1984).

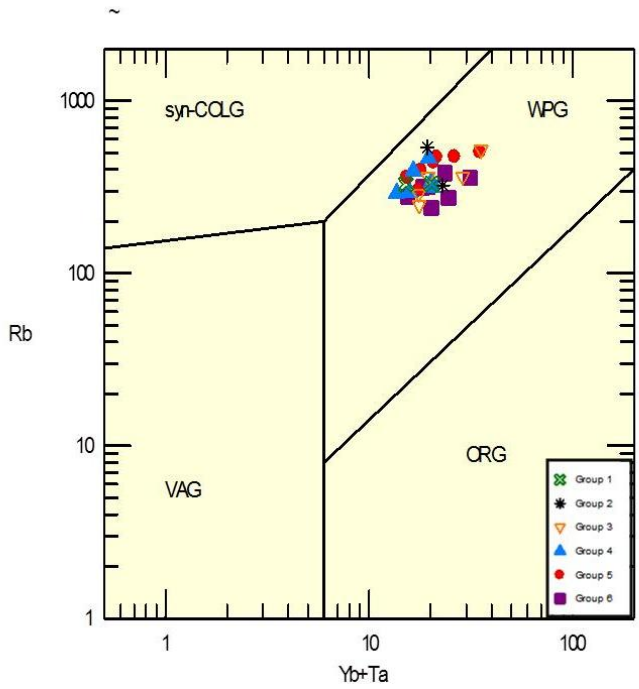

Figure 68. Rb versus Yb+Ta tectonic discrimination diagram for of all samples based on ppm (Pearce et al. 1984).

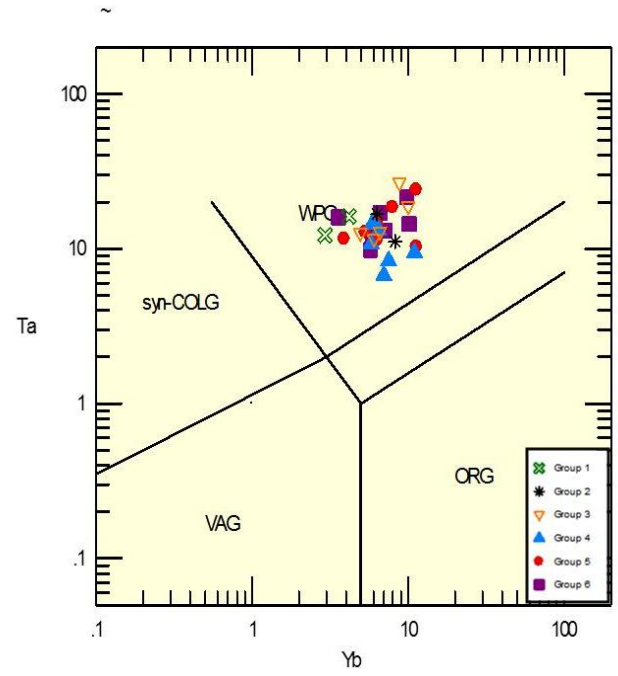

Figure 69. Ta versus Yb tectonic discrimination diagram for all samples based on ppm (Pearce et al. 1984).

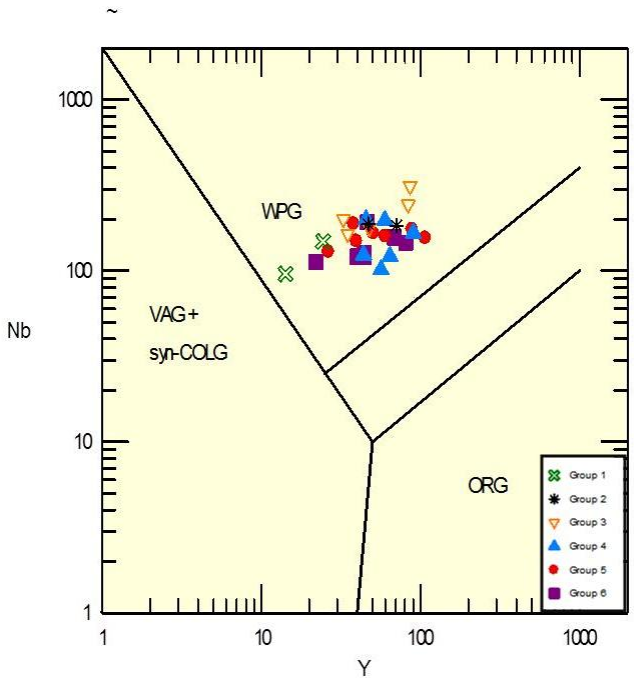

Figure 70. Nb versus Y tectonic discrimination diagram for all samples based on ppm (Pearce et al. 1984).

Tectonic discrimination ternaries

Anorogenic granites can be subdivided into A_1-type and A_2-type using the Y-Nb-Ga*3 and Y-Nb-Zr tectonic disrcimination ternaries (Eby 2006). A_1-type granites are associated with rifting while A_2-type granites are associated with post-collisional settings. Based on the trace element abundances, all the sampled miarolitic pegmatites fall in the A_1-type granite field indicating they are associated with an anorogenic, crustal-thinning rift event (Figures 51-52).

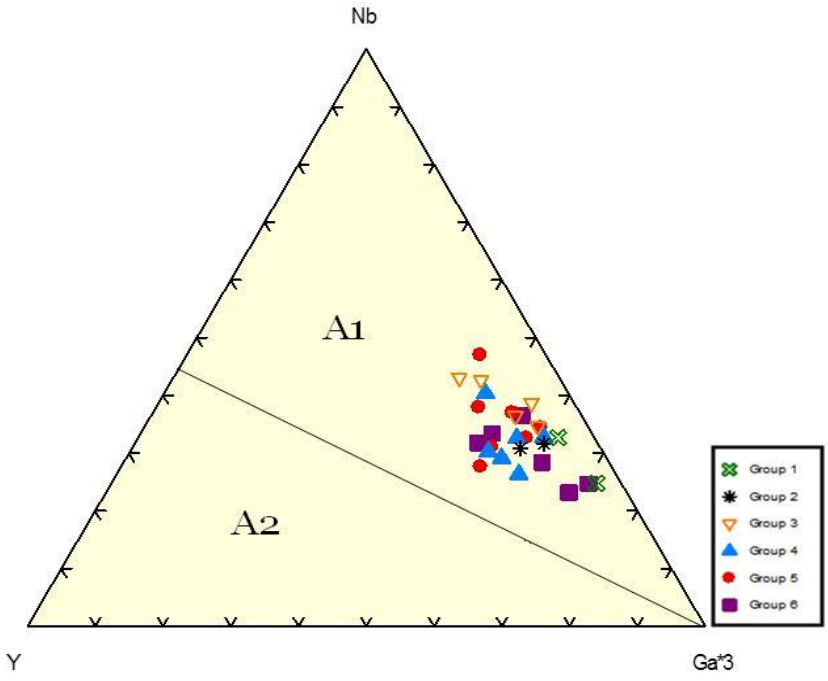

Figure 71. Y-Nb-Ga*3 tectonic discrimination ternary for whole rock analyses of all samples based on ppm (Eby 2006).

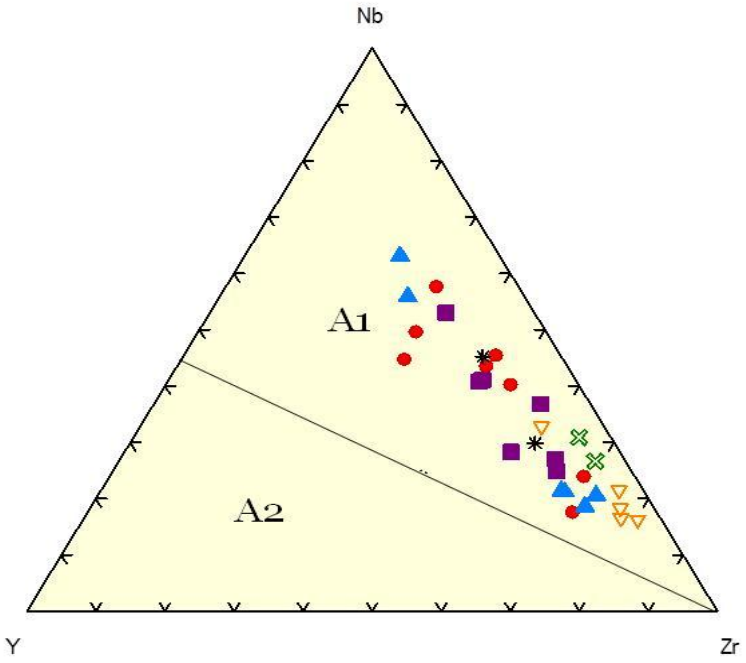

Figure 72. Y-Nb-Zr tectonic distinction ternary for whole rock analyses of all samples based on ppm (Eby 2006).

CONCLUSIONS

The WMIP, located in central New Hampshire, is a miarolitic pegmatite system that was emplaced during a rifting event that began 200 Ma ago and lasted nearly 100 Ma. In Figure 1, the rounded black and white blobs that represent the province lie in a roughly North-South trending line. This line marks the center of the rifting event that allowed these magma bodies to intrude to shallow depths. Since their emplacement, massive layers of overlying rock have been eroded and with the help of pegmatite enthusiasts and some dynamite, portions of this province are now exposed. To conduct this composite geochemical study of the WMIP, samples were collected from 15 different miarolitic pegmatites, the northernmost portion to the southern portion of the province. Most of the samples were collect from the central and largest unit, the WMB.

These sampled granitic bodies are referred to as "miarolitic pegmatites" as opposed to simply "pegmatites" because they fail to fit the physical definition of a pegmatite. It is suggested that these miarolitic pegmatites formed as a result of volatile decompression of a fractionated melt. With decreasing depth, the volatiles within the melt begin to exsolve and form vapor bubbles, into which crystals, that are often euhedral, can form (Simmons 2007). Unlike many pegmatites, these miarolitic pegmatites lack internal zonation, have a small range of grain size (mm to cm grains), and an overall small size.

Geochemical data confirmed that all of the sampled miarolitic pegmatites are in fact petrogenetically related to the same province and can be classified as Rare-Element, NYF-type systems (Černý & Ercit 2005). They can be further classified as peraluminous, A_1-type miarolitic pegmatites with a within plate granite signature. These miarolitic pegmatites are enriched in REE as indicated by the presence of allanite-(Ce), "bastnaesite", "euxenite/aeschynite", members of the ferberite/huebnerite series, ferrocolumbite, fergusonite-(Y), members of the ilmenite/pyrophanite series, "monazite", "samarskite", and thorite/thorogummite minerals.

There are two possible explanations for how these rift-related miarolitic pegmatites formed. The first is that a hotspot ponded at the base of the lithosphere and melted crustal material that was previously depleted in LCT components and the second is fractional crystallization of mafic mantle derived melts with limited crustal interaction. The data appears to supports the second explanation considering these miarolitic pegmatites have a high iron-enrichment, a magnesium-depletion, and a strong Eu anomaly indicating plagioclase has been removed from the system (Frost & Frost 1997).

The whole rock data shows an elevated Rb concentration (Figure 98) and a strong negative Eu anomaly (Figure 102) coupled with a wide range of elemental enrichments and depletions shown in the spider diagram and the chondrite-normalized diagram (Figure 102-103). This suggests all of the miarolitic pegmatites sampled from

the WMIP are geochemically evolved and will continue to provide beautiful specimens for collectors and rock hounds.

REFERENCES

Billings, M. P. (1943). Ring dikes and their origin. *New York Academy of Science Transaction Series III* 5, 131-141.

Černý, P., & Ercit, T.S. (2005): The classification of granitic pegmatites revisited. *The Canadian Mineralogist* 43, 2005-2026.

Chapman, C. A. (1976): Structural evolution of the White Mountain magma series. *Geological Society of America Memoir* 146, 281-300.

Creasy, J. W. & Eby, G. N. (1993): Ring dikes and plutons: A deeper view of calderas as illustrated by the White Mountain igneous province, New Hampshire. Field Trip Guidebook for the Northeastern United States: 1993 *Boston GSA* 1, N1-N25.

De la Roche, H., et al. (1980): A classification of volcanic and plutonic rocks using R_1,R_2-diagrams and major element analysis— its relationships with current nomenclature. *Chemical Geology* 29, 183–210.

Eby, G. N. (2006): Distinctions between A-type granites and petrogenetic pathways. Symposium on Magmatism, Crustal Evolution, and Metallogenesis of the Amazonian Craton, Abstracts Volume and Field Trips Guide. Belém, 48.

Eby, G. N. (2002): Geochemistry and petrogenesis of the Ossipee ring complex: a model for magmatism in the younger White Mountain Igneous Province. *Geological Society of America*, Abstracts with Programs 34, 1, A-70.

Eby, G. N. (1995): White Mountain magma series. Third Hutton Symposium on Granites and Related Rocks, Pre-Conference Field Trip Guide, Part 1, University of Massachusetts, Lowell, MA, 27 p.

Eby, G. N. (1992): Chemical subdivision of the A-type granitoids: petrogenetic and tectonic implications. *Geology* 20, 641-644.

Eby, G. N. & Kennedy, B. (2004): The Ossipee ring complex, New Hampshire. In Hanson, L. Guidebook to Field Trips from Boston, MA to Saco Bay, ME. New England Intercollegiate Geologic Conference, Salem, MA, 61-72.

Eby, G. N., et al. (1992): Geology, geochronology, and geochemistry of the White Mountain batholith, New Hampshire. *Geological Society of America* Special Paper 268, 379-397.

Frost, C. D. & Frost, B. R. (1997): High-K, iron-enriched rapakivi-type granites: the tholeiite connection. *Geology* 25, 647–650.

Loiselle, M. C. & Wones, D. S. (1979): Characteristics and origin of anorogenic granites. *Geological Society of America*, Abstracts with Programs 11, 468.

Maniar, P. D. & Piccoli, P. M. (1989): Tectonic discrimination of granitoids. *Geological Society of America Bulletin* 101, 635–643.

McHone, J.G. & Butler, J.R. (1984): Mesozoic igneous provinces of New England and the opening of the North Atlantic Ocean. *Geological Society of America Bulletin* 95, 757-765.

Meyers, P.E., et al. (1984): The Wausau Syenite Complex, Central Wisconsin, *30th Annual Institute on Lake Superior Geology, Guidbook*, Field Trip #3, 58.

Namur, O., et al. (2011): Differentiation of tholeiitic basalt to A-type granite in the Sept Iles layered intrusion, Canada. *Journal of Paleontology* 52, 487-539.

Pearce, J.A., et al. (1984): Trace element discrimination diagrams for the tectonic interpretation of granitic rocks. *Journal of Petrology* 25, 956-983.

Sharp, J. A., & Simmons, G. (1978): Geologic/geophysical models of intrusives of the White Mountain magma series (WMMS). *Geological Society of America Abstracts with Programs* 10, 85.

Simmons, W.B. (2007): Gem bearing pegmatites. *Canadian Mineralogist*, special publication, 196-206.

Simmons, W.B., et al. (1987): Geochemistry and evolution of the South Platte granite-pegmatite system, Jefferson County, Colorado. *Geochimica et Cosmochimica Acta* 51, 455-471.

Sun, S.S. and McDonough, W.F. (1989): Chemical and isotopic systematics of oceanic basalts; implications for mantle composition and processes. *Geological Society of London* 42, 313-345.

Wise, M.A. (1999). Characterization and classification of NYF-type pegmatites. *Canadian Mineralogist*, 37, 802-803.

Appendix

Table A-1. DCP Whole Rock Analyses

	mass (mg)	vol (l)	ppm Li				ppm Rb			
1 ppm standard			**1.01**				**0.991**			
line used			**610.367**				**780.023**			
count time I sec			**20**				**20**			
calibration range, ppm			**10-0.01**				**10-0.01**			
PMT voltage			**10000**				**10000**			
sample ID				**Li wt %**	**Li_2O wt %**	**ppm**		**Rb wt %**	**Rb_2O wt %**	**ppm**
1.1	200.00	0.035	0.054	0.001	0.002	9.450	2.170	0.038	0.035	379.750
1.2	198.20	0.035	0.009	0.000	0.000	1.589	1.570	0.028	0.025	277.245
1.4	204.00	0.035	0.115	0.002	0.004	19.730	2.330	0.040	0.037	399.755
1.7	201.00	0.035	0.069	0.001	0.003	12.015	10.000	0.174	0.159	1741.294
1.9	205.60	0.035	0.039	0.001	0.001	6.639	3.880	0.066	0.060	660.506
1.1O	202.50	0.035	0.175	0.003	0.007	30.247	2.700	0.047	0.043	466.667
1.12	202.90	0.035	0.039	0.001	0.001	6.727	2.660	0.046	0.042	458.847
1.13	199.10	0.035	0.115	0.002	0.004	20.216	3.010	0.053	0.048	529.131
2.1	197.30	0.035	0.416	0.007	0.016	73.796	3.660	0.065	0.059	649.265
2.3	197.80	0.035	0.295	0.005	0.011	52.199	3.140	0.056	0.051	555.612
3.1	198.50	0.035	0.130	0.002	0.005	22.922	4.940	0.087	0.080	871.033
3.2	200.40	0.035	0.250	0.004	0.009	43.663	3.680	0.064	0.059	642.715
3.3	202.90	0.035	0.235	0.004	0.009	40.537	4.840	0.083	0.076	834.894
4.1	203.30	0.035	0.039	0.001	0.001	6.714	3.730	0.064	0.059	642.154
5.1	198.80	0.035	0.386	0.007	0.015	67.958	4.790	0.084	0.077	843.310
6.1	202.60	0.035	0.265	0.005	0.010	45.780	4.910	0.085	0.078	848.223
6.2	200.70	0.035	0.115	0.002	0.004	20.055	2.640	0.046	0.042	460.389
7.1	202.70	0.035	0.295	0.005	0.011	50.937	2.190	0.038	0.035	378.145
7.1	203.50	0.035	0.301	0.005	0.011	51.769	2.210	0.038	0.035	380.098
7.2	200.90	0.035	0.431	0.008	0.016	75.087	2.660	0.046	0.042	463.415
8.1	199.20	0.035	0.265	0.005	0.010	46.561	4.370	0.077	0.070	767.821
8.2	203.60	0.035	0.446	0.008	0.017	76.670	2.540	0.044	0.040	436.640
8.3	199.50	0.035	0.311	0.005	0.012	54.561	1.760	0.031	0.028	308.772
9.1	201.40	0.035	0.295	0.005	0.011	51.266	1.990	0.035	0.032	345.829
9.2	201.30	0.035	0.386	0.007	0.014	67.114	2.250	0.039	0.036	391.207
10.1	199.80	0.035	0.069	0.001	0.003	12.087	0.051	0.001	0.001	8.934
11.1	201.30	0.035	0.084	0.001	0.003	14.605	1.800	0.031	0.029	312.966
11.2	201.50	0.035	0.085	0.001	0.003	14.764	1.380	0.024	0.022	239.702
11.3	202.00	0.035	0.536	0.009	0.020	92.871	3.050	0.053	0.048	528.465
12.1	202.50	0.035	0.521	0.009	0.019	90.049	1.590	0.027	0.025	274.815
12.2	202.40	0.035	0.310	0.005	0.012	53.607	1.800	0.031	0.028	311.265
12.3	204.20	0.035	0.235	0.004	0.009	40.279	2.020	0.035	0.032	346.229
13.1	201.90	0.035	0.175	0.003	0.007	30.337	4.270	0.074	0.068	740.218
14.1	201.40	0.035	0.250	0.004	0.009	43.446	2.140	0.037	0.034	371.897
15.1	207.00	0.035	0.551	0.009	0.020	93.164	3.200	0.054	0.049	541.063

Table A-1. DCP Whole Rock Analyses (continued).

	mass (mg)	vol (l)	ppm B				ppm Be			
1 ppm standard			0.954				0.986			
line used			249.687				234.861			
count time I sec			20				10			
calibration range, ppm			1-0.001				10-0.001			
PMT voltage			10000				10000			
sample ID				B wt %	B_2O wt %	ppm		Be wt %	BeO wt %	ppm
1.1	200.00	0.035	0.493	0.009	0.010	86.275	0.016	0.000	0.000	2.800
1.2	198.20	0.035	0.251	0.004	0.005	44.324	0.002	0.000	0.000	0.353
1.4	204.00	0.035	0.223	0.004	0.004	38.260	0.057	0.001	0.000	9.779
1.7	201.00	0.035	0.265	0.005	0.005	46.144	0.056	0.001	0.000	9.751
1.9	205.60	0.035	0.123	0.002	0.002	20.939	0.027	0.000	0.000	4.596
1.1O	202.50	0.035	0.109	0.002	0.002	18.840	0.005	0.000	0.000	0.864
1.12	202.90	0.035	0.507	0.009	0.010	87.457	0.022	0.000	0.000	3.795
1.13	199.10	0.035	0.365	0.006	0.007	64.164	0.010	0.000	0.000	1.758
2.1	197.30	0.035	0.279	0.005	0.006	49.493	0.037	0.001	0.000	6.564
2.3	197.80	0.035	0.351	0.006	0.007	62.108	0.013	0.000	0.000	2.300
3.1	198.50	0.035	0.024	0.000	0.000	4.232	0.002	0.000	0.000	0.353
3.2	200.40	0.035	0.081	0.001	0.002	14.147	0.054	0.001	0.000	9.431
3.3	202.90	0.035	0.223	0.004	0.004	38.467	0.076	0.001	0.000	13.110
4.1	203.30	0.035	0.251	0.004	0.005	43.212	0.012	0.000	0.000	2.066
5.1	198.80	0.035	0.152	0.003	0.003	26.761	0.014	0.000	0.000	2.465
6.1	202.60	0.035	0.004	0.000	0.000	0.691	0.002	0.000	0.000	0.346
6.2	200.70	0.035	0.152	0.003	0.003	26.507	0.023	0.000	0.000	4.011
7.1	202.70	0.035	0.194	0.003	0.004	33.498	0.033	0.001	0.000	5.698
7.1	203.50	0.035	0.184	0.003	0.004	31.646	0.023	0.000	0.000	3.956
7.2	200.90	0.035	0.152	0.003	0.003	26.481	0.039	0.001	0.000	6.794
8.1	199.20	0.035	0.138	0.002	0.003	24.247	0.130	0.002	0.001	22.841
8.2	203.60	0.035	0.100	0.002	0.002	17.191	0.050	0.001	0.000	8.595
8.3	199.50	0.035	0.223	0.004	0.004	39.123	0.010	0.000	0.000	1.754
9.1	201.40	0.035	0.123	0.002	0.002	21.375	0.076	0.001	0.000	13.208
9.2	201.30	0.035	0.180	0.003	0.004	31.297	0.051	0.001	0.000	8.867
10.1	199.80	0.035	0.294	0.005	0.006	51.502	0.045	0.001	0.000	7.883
11.1	201.30	0.035	0.365	0.006	0.007	63.462	0.003	0.000	0.000	0.522
11.2	201.50	0.035	0.265	0.005	0.005	46.030	0.084	0.001	0.001	14.591
11.3	202.00	0.035	0.223	0.004	0.004	38.639	0.014	0.000	0.000	2.426
12.1	202.50	0.035	0.265	0.005	0.005	45.802	0.054	0.001	0.000	9.333
12.2	202.40	0.035	0.365	0.006	0.007	63.118	0.005	0.000	0.000	0.865
12.3	204.20	0.035	0.237	0.004	0.005	40.622	0.044	0.001	0.000	7.542
13.1	201.90	0.035	0.365	0.006	0.007	63.274	0.019	0.000	0.000	3.294
14.1	201.40	0.035	0.379	0.007	0.008	65.864	0.002	0.000	0.000	0.348
15.1	207.00	0.035	0.294	0.005	0.006	49.710	0.100	0.002	0.001	16.908

Table A-1. DCP Whole Rock Analyses (continued).

	mass (mg)	vol (l)	ppm Ga			
1 ppm standard			**1.05**			
line used			**294.364**			
count time I sec			**20**			
calibration range, ppm			**0.01-1**			
PMT voltage			**10000**			
sample ID				**Ga wt %**	**Ga_2O_3 wt %**	**ppm**
1.1	200.00	0.035	0.463	0.008	0.006	81.025
1.2	198.20	0.035	0.522	0.009	0.007	92.180
1.4	204.00	0.035	0.451	0.008	0.006	77.377
1.7	201.00	0.035	0.412	0.007	0.005	71.741
1.9	205.60	0.035	0.565	0.010	0.007	96.182
1.1O	202.50	0.035	0.733	0.013	0.009	126.691
1.12	202.90	0.035	0.683	0.012	0.009	117.817
1.13	199.10	0.035	0.609	0.011	0.008	107.057
2.1	197.30	0.035	0.704	0.012	0.009	124.886
2.3	197.80	0.035	0.334	0.006	0.004	59.100
3.1	198.50	0.035	0.404	0.007	0.005	71.234
3.2	200.40	0.035	0.330	0.006	0.004	57.635
3.3	202.90	0.035	0.405	0.007	0.005	69.862
4.1	203.30	0.035	0.426	0.007	0.005	73.340
5.1	198.80	0.035	0.564	0.010	0.007	99.296
6.1	202.60	0.035	0.447	0.008	0.006	77.221
6.2	200.70	0.035	0.696	0.012	0.009	121.375
7.1	202.70	0.035	0.445	0.008	0.006	76.838
7.1	203.50	0.035	0.393	0.007	0.005	67.592
7.2	200.90	0.035	0.407	0.007	0.005	70.906
8.1	199.20	0.035	0.634	0.011	0.008	111.396
8.2	203.60	0.035	0.554	0.010	0.007	95.236
8.3	199.50	0.035	0.522	0.009	0.007	91.579
9.1	201.40	0.035	0.459	0.008	0.006	79.767
9.2	201.30	0.035	0.504	0.009	0.007	87.630
10.1	199.80	0.035	0.522	0.009	0.007	91.441
11.1	201.30	0.035	0.685	0.012	0.009	119.101
11.2	201.50	0.035	0.606	0.011	0.008	105.261
11.3	202.00	0.035	0.657	0.011	0.008	113.837
12.1	202.50	0.035	0.543	0.009	0.007	93.852
12.2	202.40	0.035	0.495	0.009	0.006	85.598
12.3	204.20	0.035	0.538	0.009	0.007	92.214
13.1	201.90	0.035	0.572	0.010	0.007	99.158
14.1	201.40	0.035	0.559	0.010	0.007	97.145
15.1	207.00	0.035	0.394	0.007	0.005	66.618

Table A-2. DCP analysis of amphibole.

			Li	Li wt %	Li_2O wt %	ppm	Rb	Rb wt %	Rb_2O wt %	ppm
1 ppm std	**mass (mg)**	**volume (l)**	**0.987**				**1.120**			
9.2a	201.400	0.035	1.890	0.033	0.071	328.451	0.547	0.010	0.009	95.060
9.2b	202.200	0.035	0.841	0.015	0.031	145.574	0.392	0.007	0.006	67.854

Table A-3. DCP analysis of biotite.

			Li	Li wt %	Li_2O wt %	ppm	Rb	Rb wt %	Rb_2O wt %	ppm
1 ppm std	**mass (mg)**	**volume (l)**	**0.987**				**1.120**			
2.3	193.800	0.035	2.580	0.047	0.100	465.944	7.050	0.127	0.116	1273.220
3.1	194.700	0.035	2.850	0.051	0.110	512.327	17.800	0.320	0.293	3199.795
5.1	190.800	0.035	1.150	0.021	0.045	210.954	4.280	0.079	0.072	785.115
6.2	89.000	0.035	0.996	0.039	0.084	391.685	5.760	0.227	0.207	2265.169
8.1	204.600	0.035	5.100	0.087	0.188	872.434	24.800	0.424	0.388	4242.424
9.1	155.200	0.035	0.737	0.017	0.036	166.205	27.200	0.613	0.561	6134.021

Table A-4. DCP analyses of amphibole.

			Li ppm	Li wt %	Li_2O wt %	ppm	Rb ppm	Rb wt %	Rb_2O wt %	ppm
1 ppm std	**mass (mg)**	**volume (l)**	**0.987**				**1.12**			
1.1	208.200	0.035	0.065	0.001	0.002	10.927	7.010	0.118	0.108	1178.434
2.3	193.200	0.035	0.100	0.002	0.004	18.116	2.040	0.037	0.034	369.565
3.1	203.900	0.035	0.841	0.014	0.031	144.360	7.680	0.132	0.121	1318.293
5.1	198.200	0.035	1.080	0.019	0.041	190.716	6.870	0.121	0.111	1213.169
6.2	202.600	0.035	0.841	0.015	0.031	145.286	7.590	0.131	0.120	1311.204
7.2	203.700	0.035	0.065	0.001	0.002	11.168	5.410	0.093	0.085	929.553
8.1	202.000	0.035	0.031	0.001	0.001	5.371	4.850	0.084	0.077	840.347
9.1	197.600	0.035	0.048	0.001	0.002	8.502	3.600	0.064	0.058	637.652
11.2	199.600	0.035	0.203	0.004	0.008	35.596	1.110	0.019	0.018	194.639
12.2	193.600	0.035	0.289	0.005	0.011	52.247	4.480	0.081	0.074	809.917
13.1	202.800	0.035	0.134	0.002	0.005	23.126	19.400	0.335	0.306	3348.126

Table A-5. Electron microprobe analysis of arfvedsonite, $NaNa_2(Fe_4^{2+}Fe^{3+})Si_8O_{22}(OH)_2$.

Simplified Formula: $AB_2C_5T_8O_{22}X_2$

	East Hurricane									
Wt. % oxides										
SiO2	50.213	50.099	50.431	50.387	50.339	50.218	50.118	50.216	50.385	50.221
TiO2	0.555	0.509	0.522	0.518	0.530	0.500	0.517	0.512	0.494	0.488
Al2O3	0.678	0.707	0.721	0.698	0.704	0.755	0.721	0.687	0.693	0.732
FeO	40.966	41.265	41.231	41.199	41.309	41.388	41.344	41.348	41.299	41.317
MnO	0.856	0.877	0.807	0.786	0.765	0.821	0.809	0.833	0.795	0.800
MgO	0.011	0.008	0.009	0.000	0.000	0.007	0.009	0.000	0.000	0.000
CaO	0.009	0.009	0.008	0.009	0.015	0.011	0.009	0.008	0.008	0.007
Zn	0.332	0.412	0.387	0.433	0.287	0.275	0.300	0.298	0.277	0.312
Na2O	0.034	0.022	0.012	0.023	0.027	0.019	0.015	0.023	0.031	0.022
K2O	1.478	1.500	1.443	1.487	1.512	1.476	1.443	1.412	1.419	1.438
F	3.098	3.006	2.987	3.004	2.956	2.774	2.673	2.712	2.567	2.600
Subtotal	98.230	98.414	98.558	98.544	98.444	98.244	97.958	98.049	97.968	97.937
-O=F	1.304	1.266	1.258	1.265	1.245	1.168	1.125	1.142	1.081	1.095
Total	96.926	97.148	97.300	97.279	97.199	97.076	96.833	96.907	96.887	96.842
Ions on the basis of 24 O + F										
Na	0.011	0.007	0.004	0.007	0.008	0.006	0.005	0.007	0.010	0.007
K	0.305	0.310	0.297	0.306	0.312	0.306	0.300	0.293	0.295	0.299
Sum of A-site	0.315	0.316	0.301	0.313	0.320	0.312	0.305	0.300	0.305	0.306
Mn	0.117	0.120	0.110	0.107	0.105	0.113	0.112	0.115	0.110	0.111
Mg	0.003	0.002	0.002	0.000	0.000	0.002	0.002	0.000	0.000	0.000
Ca	0.002	0.002	0.001	0.002	0.003	0.002	0.002	0.001	0.001	0.001
Zn	0.049	0.061	0.057	0.064	0.043	0.041	0.045	0.045	0.041	0.047
Sum of B-site	0.171	0.185	0.171	0.173	0.150	0.158	0.160	0.161	0.153	0.158
Fe	5.535	5.582	5.559	5.557	5.581	5.618	5.635	5.626	5.628	5.635
Al	0.129	0.135	0.137	0.133	0.134	0.144	0.139	0.132	0.133	0.141
Ti	0.067	0.062	0.063	0.063	0.064	0.061	0.063	0.063	0.061	0.060
Sum of C-Site	5.731	5.779	5.760	5.753	5.780	5.824	5.837	5.821	5.822	5.835
Si **(T-Site)**	8.113	8.105	8.132	8.128	8.134	8.153	8.170	8.172	8.212	8.191
F **(X-Site)**	1.583	1.538	1.523	1.532	1.510	1.424	1.378	1.395	1.323	1.341

* The analyzed samples have been heavily altered, thus the formulas do not balance properly.

Table A-6. Electron microprobe analysis of potassium feldspar, $KAlSi_3O_8$.

Simplified Formula: $A_1B_1C_3$

	Racoon Gulch				Government Pit						Oliver Trench				
Wt. % oxides															
SiO2	65.320	65.366	65.252	65.111	65.181	65.454	65.503	65.457	65.550	65.472	64.530	64.583	64.412	64.391	64.599
TiO2	0.006	0.009	0.005	0.007	0.007	0.004	0.006	0.004	0.008	0.005	0.009	0.012	0.008	0.012	0.006
Al2O3	18.273	18.325	18.400	18.385	18.367	18.430	18.452	18.440	18.378	18.451	18.232	18.316	18.200	18.233	18.265
FeO	0.127	0.089	0.095	0.112	0.082	0.078	0.104	0.088	0.093	0.073	0.028	0.030	0.036	0.028	0.022
MnO	0.011	0.007	0.009	0.011	0.004	0.011	0.006	0.007	0.006	0.000	0.000	0.000	0.000	0.000	0.000
MgO	0.000	0.000	0.000	0.008	0.000	0.000	0.000	0.000	0.000	0.000	0.000	0.000	0.000	0.000	0.000
CaO	0.102	0.125	0.094	0.095	0.110	0.344	0.334	0.314	0.337	0.289	0.100	0.088	0.093	0.077	0.110
BaO	0.006	0.000	0.008	0.007	0.000	0.005	0.000	0.006	0.007	0.005	0.008	0.006	0.011	0.006	0.007
Na2O	0.788	0.834	0.723	0.688	0.733	1.778	1.671	1.555	1.782	1.658	1.050	1.005	0.983	1.083	1.114
K2O	15.676	15.832	15.672	15.730	15.782	13.870	14.256	14.223	14.156	14.322	15.223	15.300	15.285	15.221	15.106
Total	100.309	100.587	100.258	100.154	100.266	99.974	100.332	100.094	100.317	100.275	99.180	99.340	99.028	99.051	99.229
Ions on the basis of 8 O															
Fe	0.005	0.003	0.004	0.004	0.003	0.003	0.004	0.003	0.004	0.003	0.001	0.001	0.001	0.001	0.001
Mn	0.000	0.000	0.000	0.000	0.000	0.000	0.000	0.000	0.000	0.000	0.000	0.000	0.000	0.000	0.000
Mg	0.000	0.000	0.000	0.001	0.000	0.000	0.000	0.000	0.000	0.000	0.000	0.000	0.000	0.000	0.000
Ca	0.005	0.006	0.005	0.005	0.005	0.017	0.016	0.015	0.017	0.014	0.005	0.004	0.005	0.004	0.005
Ba	0.000	0.000	0.000	0.000	0.000	0.000	0.000	0.000	0.000	0.000	0.000	0.000	0.000	0.000	0.000
Na	0.070	0.074	0.064	0.061	0.065	0.158	0.148	0.138	0.158	0.147	0.095	0.090	0.089	0.098	0.101
K	0.920	0.927	0.919	0.924	0.927	0.811	0.832	0.832	0.826	0.837	0.902	0.905	0.908	0.904	0.897
Sum of A-Site	1.000	1.011	0.993	0.996	1.001	0.989	1.001	0.989	1.005	1.001	1.003	1.001	1.002	1.006	1.004
Al **(B-Site)**	0.991	0.992	0.998	0.998	0.996	0.996	0.995	0.996	0.991	0.996	0.999	1.002	0.999	1.000	1.002
Si	3.004	3.001	3.001	3.000	3.000	3.001	2.998	3.001	3.000	2.998	2.998	2.997	2.999	2.997	3.006
Ti	0.000	0.000	0.000	0.000	0.000	0.000	0.000	0.000	0.000	0.000	0.000	0.000	0.000	0.000	0.000
Sum of C-Site	3.004	3.001	3.001	3.000	3.000	3.001	2.998	3.001	3.000	2.999	2.999	2.997	2.999	2.997	3.007

Table A-6. Electron microprobe analysis of potassium feldspar, $KAlSi_3O_8$ (continued).

Simplified Formula: $A_1B_1C_3$

	Large boulder near Oliver Diggings					Brook Diggings					Redstone Quarry					W Hurricane	
Wt. % oxides																	
SiO2	64.477	64.677	65.211	64.777	64.777	65.211	65.156	65.116	65.226	65.198	67.965	68.009	68.433	68.423	68.237	65.148	64.877
TiO2	0.036	0.021	0.019	0.022	0.017	0.015	0.009	0.013	0.013	0.014	0.000	0.000	0.000	0.000	0.000	0.004	0.006
Al2O3	18.224	18.311	18.277	18.223	18.312	18.418	18.309	18.305	18.322	18.430	19.166	19.233	19.367	19.243	19.311	18.103	18.083
FeO	0.036	0.040	0.033	0.032	0.035	0.015	0.013	0.010	0.012	0.011	0.066	0.056	0.039	0.044	0.050	0.443	0.454
MnO	0.007	0.005	0.000	0.007	0.000	0.000	0.000	0.000	0.000	0.000	0.009	0.009	0.000	0.006	0.000	0.009	0.012
MgO	0.000	0.000	0.008	0.000	0.000	0.000	0.000	0.000	0.000	0.000	0.000	0.000	0.000	0.000	0.000	0.000	0.000
CaO	0.090	0.085	0.067	0.096	0.087	0.055	0.051	0.063	0.056	0.054	0.103	0.105	0.111	0.109	0.121	0.110	0.109
BaO	0.000	0.000	0.000	0.000	0.000	0.000	0.000	0.000	0.000	0.000	0.000	0.000	0.000	0.000	0.000	0.006	0.007
Na2O	0.045	0.043	0.036	0.055	0.063	2.545	2.455	2.550	2.471	2.334	11.412	11.389	11.321	11.353	11.332	0.975	0.985
K2O	16.411	16.554	16.512	16.734	16.630	13.155	13.211	13.145	13.155	13.454	0.502	0.494	0.566	0.655	0.532	15.450	15.423
Total	99.326	99.736	100.163	99.946	99.921	99.414	99.204	99.202	99.255	99.495	99.231	99.304	99.850	99.841	99.592	#####	99.956
Ions on the basis of 8 O																	
Fe	0.001	0.002	0.001	0.001	0.001	0.001	0.001	0.000	0.000	0.000	0.003	0.002	0.002	0.002	0.002	0.017	0.018
Mn	0.000	0.000	0.000	0.000	0.000	0.000	0.000	0.000	0.000	0.000	0.000	0.000	0.000	0.000	0.000	0.000	0.000
Mg	0.000	0.000	0.001	0.000	0.000	0.000	0.000	0.000	0.000	0.000	0.000	0.000	0.000	0.000	0.000	0.000	0.000
Ca	0.004	0.004	0.003	0.005	0.004	0.003	0.003	0.003	0.003	0.003	0.005	0.005	0.006	0.005	0.006	0.005	0.005
Ba	0.000	0.000	0.000	0.000	0.000	0.000	0.000	0.000	0.000	0.000	0.000	0.000	0.000	0.000	0.000	0.000	0.000
Na	0.004	0.004	0.003	0.005	0.006	0.230	0.221	0.230	0.223	0.211	1.030	1.028	1.021	1.024	1.022	0.088	0.089
K	0.974	0.983	0.980	0.993	0.987	0.781	0.784	0.780	0.781	0.799	0.030	0.029	0.034	0.039	0.032	0.917	0.916
Sum of A-Site	0.984	0.993	0.989	1.005	0.999	1.014	1.009	1.014	1.007	1.012	1.067	1.065	1.062	1.071	1.062	1.028	1.028
Al **(B-Site)**	1.000	1.004	1.003	1.000	1.004	1.010	1.004	1.004	1.005	1.011	1.051	1.055	1.062	1.056	1.059	0.993	0.992
Si	3.001	3.010	3.035	3.015	3.015	3.035	3.032	3.030	3.036	3.034	3.163	3.165	3.185	3.184	3.176	3.032	3.019
Ti	0.001	0.001	0.001	0.001	0.001	0.001	0.000	0.000	0.000	0.000	0.000	0.000	0.000	0.000	0.000	0.000	0.000
Sum of C-Site	3.002	3.011	3.035	3.015	3.015	3.035	3.033	3.031	3.036	3.035	3.163	3.165	3.185	3.184	3.176	3.032	3.019

Table A-6. Electron microprobe analysis of potassium feldspar, $KAlSi_3O_8$.

Simplified Formula: $A_1B_1C_3$

	West Hurricane								East Hurricane								
Wt. % oxides																	
SiO2	65.001	64.777	64.837	64.900	64.687	64.677	68.032	68.094	64.677	68.032	64.609	64.655	68.100	64.622	64.711	64.709	64.663
TiO2	0.004	0.008	0.008	0.017	0.007	0.009	0.000	0.000	0.009	0.000	0.007	0.011	0.000	0.005	0.009	0.012	0.008
Al2O3	18.010	18.045	18.005	18.109	18.099	18.011	19.043	19.008	18.211	19.243	18.198	18.222	19.132	18.155	18.088	17.967	17.945
FeO	0.510	0.455	0.523	0.309	0.312	0.311	0.311	0.106	0.045	0.107	0.055	0.056	0.088	0.455	0.389	0.455	0.467
MnO	0.009	0.009	0.014	0.006	0.005	0.005	0.000	0.009	0.000	0.000	0.000	0.000	0.000	0.006	0.007	0.005	0.006
MgO	0.000	0.000	0.000	0.000	0.000	0.000	0.000	0.008	0.000	0.000	0.000	0.000	0.000		0.000	0.000	0.000
CaO	0.121	0.115	0.133	0.016	0.022	0.018	0.143	0.121	0.023	0.155	0.031	0.036	0.133	0.145	0.133	0.145	0.116
BaO	0.005	0.009	0.008	0.000	0.000	0.000	0.000	0.000	0.000	0.000	0.000	0.000	0.000	0.006	0.000	0.000	0.005
Na2O	0.934	0.565	0.549	0.544	0.500	0.567	11.132	11.208	0.445	11.232	0.388	0.422	11.311	0.556	0.488	0.512	0.554
K2O	15.332	15.306	15.256	15.934	15.981	15.918	0.543	0.546	15.918	0.543	16.209	16.276	0.443	16.015	16.000	16.033	15.944
Total	99.926	99.289	99.333	99.835	99.613	99.516	99.225	99.118	99.328	99.319	99.497	99.678	99.230	99.965	99.825	99.838	99.708
Ions on the basis of 8 O																	
Fe	0.020	0.018	0.020	0.012	0.012	0.012	0.012	0.004	0.002	0.004	0.002	0.002	0.003	0.018	0.015	0.018	0.018
Mn	0.000	0.000	0.001	0.000	0.000	0.000	0.000	0.000	0.000	0.000	0.000	0.000	0.000	0.000	0.000	0.000	0.000
Mg	0.000	0.000	0.000	0.000	0.000	0.000	0.000	0.001	0.000	0.000	0.000	0.000	0.000	0.000	0.000	0.000	0.000
Ca	0.006	0.006	0.007	0.001	0.001	0.001	0.007	0.006	0.001	0.008	0.002	0.002	0.007	0.007	0.007	0.007	0.006
Ba	0.000	0.000	0.000	0.000	0.000	0.000	0.000	0.000	0.000	0.000	0.000	0.000	0.000	0.000	0.000	0.000	0.000
Na	0.084	0.051	0.050	0.049	0.045	0.051	1.004	1.011	0.040	1.013	0.035	0.038	1.021	0.050	0.044	0.046	0.050
K	0.910	0.909	0.906	0.946	0.949	0.945	0.032	0.032	0.945	0.032	0.962	0.966	0.026	0.951	0.950	0.952	0.946
Sum of A-Site	1.021	0.983	0.983	1.008	1.007	1.009	1.056	1.055	0.988	1.058	1.001	1.008	1.057	1.026	1.016	1.023	1.021
Al **(B-Site)**	0.988	0.990	0.988	0.993	0.993	0.988	1.045	1.043	0.999	1.056	0.998	1.000	1.049	0.996	0.992	0.986	0.984
Si	3.025	3.015	3.017	3.020	3.010	3.010	3.166	3.169	3.010	3.166	3.007	3.009	3.169	3.007	3.012	3.011	3.009
Ti	0.000	0.000	0.000	0.001	0.000	0.000	0.000	0.000	0.000	0.000	0.000	0.000	0.000	0.000	0.000	0.000	0.000
Sum of C-Site	3.025	3.015	3.018	3.021	3.011	3.010	3.166	3.169	3.010	3.166	3.007	3.009	3.169	3.008	3.012	3.012	3.010

Table A-6. Electron microprobe analysis of potassium feldspar, $KAlSi_3O_8$ (continued).

Simplified Formula: $A_1B_1C_3$

		Blackcap					North Sugarloaf									
Wt. % oxides																
SiO2	64.702	68.232	68.100	67.873	67.834	68.100	68.100	67.893	67.756	67.800	67.896	64.663	64.699	64.334	64.377	64.555
TiO2	0.009	0.000	0.000	0.000	0.000	0.000	0.000	0.000	0.000	0.000	0.000	0.004	0.006	0.006	0.004	0.009
Al2O3	18.004	19.132	19.032	18.945	18.834	18.900	19.244	19.322	19.212	19.121	19.211	18.430	18.411	18.313	18.323	18.200
FeO	0.455	0.451	0.477	0.445	0.468	0.563	0.045	0.048	0.044	0.041	0.051	0.000	0.009	0.006	0.094	0.088
MnO	0.006	0.000	0.000	0.000	0.000	0.000	0.000	0.000	0.000	0.000	0.000	0.000	0.000	0.000	0.000	0.000
MgO	0.000	0.000	0.000	0.000	0.000	0.000	0.000	0.000	0.000	0.000	0.000	0.000	0.000	0.000	0.000	0.000
CaO	0.143	0.133	0.122	0.116	0.139	0.134	0.055	0.060	0.056	0.063	0.052	0.066	0.045	0.056	0.049	0.055
BaO	0.000	0.000	0.000	0.000	0.000	0.000	0.000	0.000	0.000	0.000	0.000	0.006	0.006	0.004	0.000	0.006
Na2O	0.562	11.311	11.355	11.305	11.276	11.292	11.554	11.454	11.411	11.333	11.433	0.112	0.093	0.145	0.144	0.182
K2O	15.905	0.443	0.443	0.443	0.443	0.443	0.213	0.233	0.216	0.165	0.227	16.623	16.712	16.623	16.434	16.433
Total	99.786	99.710	99.536	99.138	99.003	99.443	99.218	99.033	98.713	98.534	98.876	99.904	99.981	99.487	99.425	99.528
Ions on the basis of 8 O																
Fe	0.018	0.018	0.019	0.017	0.018	0.022	0.002	0.002	0.002	0.002	0.002	0.000	0.000	0.000	0.004	0.003
Mn	0.000	0.000	0.000	0.000	0.000	0.000	0.000	0.000	0.000	0.000	0.000	0.000	0.000	0.000	0.000	0.000
Mg	0.000	0.000	0.000	0.000	0.000	0.000	0.000	0.000	0.000	0.000	0.000	0.000	0.000	0.000	0.000	0.000
Ca	0.007	0.007	0.006	0.006	0.007	0.007	0.003	0.003	0.003	0.003	0.003	0.003	0.002	0.003	0.002	0.003
Ba	0.000	0.000	0.000	0.000	0.000	0.000	0.000	0.000	0.000	0.000	0.000	0.000	0.000	0.000	0.000	0.000
Na	0.051	1.021	1.024	1.020	1.017	1.019	1.042	1.033	1.030	1.022	1.032	0.010	0.008	0.013	0.013	0.016
K	0.944	0.026	0.026	0.026	0.026	0.026	0.013	0.014	0.013	0.010	0.013	0.987	0.992	0.987	0.976	0.975
Sum of A-Site	1.020	1.071	1.075	1.069	1.069	1.074	1.060	1.052	1.047	1.037	1.050	1.000	1.003	1.003	0.995	0.998
Al **(B-Site)**	0.988	1.049	1.044	1.039	1.033	1.037	1.056	1.060	1.054	1.049	1.054	1.011	1.010	1.005	1.005	0.998
Si	3.011	3.175	3.169	3.159	3.157	3.169	3.169	3.160	3.153	3.155	3.160	3.009	3.011	2.994	2.996	3.004
Ti	0.000	0.000	0.000	0.000	0.000	0.000	0.000	0.000	0.000	0.000	0.000	0.000	0.000	0.000	0.000	0.000
Sum of C-Site	3.011	3.175	3.169	3.159	3.157	3.169	3.169	3.160	3.153	3.155	3.160	3.009	3.011	2.994	2.996	3.005

Table A-6. Electron microprobe analysis of potassium feldspar, $KAlSi_3O_8$ (continued).

Simplified Formula: $A_1B_1C_3$

	North Percy Peak										Ravine					Mousetrap	
Wt. % oxides																	
SiO2	64.877	65.011	64.677	65.011	64.556	65.088	65.151	65.038	65.145	65.178	65.211	64.877	64.755	64.656	64.877	64.877	64.844
TiO2	0.003	0.004	0.002	0.005	0.005	0.007	0.008	0.006	0.008	0.009	0.004	0.006	0.003	0.005	0.005	0.009	0.010
Al2O3	18.499	18.422	18.234	18.443	18.234	18.232	18.311	18.338	18.265	18.300	18.455	18.326	18.334	18.400	18.443	18.443	18.343
FeO	0.050	0.047	0.044	0.045	0.051	0.251	0.225	0.256	0.265	0.243	0.000	0.000	0.007	0.034	0.009	0.169	0.160
MnO	0.000	0.000	0.000	0.000	0.000	0.000	0.000	0.000	0.000	0.000	0.000	0.000	0.000	0.000	0.000	0.000	0.000
MgO	0.000	0.000	0.000	0.000	0.000	0.000	0.000	0.000	0.000	0.000	0.000	0.000	0.000	0.000	0.000	0.000	0.000
CaO	0.050	0.055	0.052	0.062	0.047	0.144	0.139	0.147	0.127	0.144	0.076	0.080	0.067	0.086	0.077	0.045	0.056
BaO	0.000	0.000	0.000	0.000	0.000	0.000	0.000	0.000	0.000	0.000	0.000	0.000	0.005	0.006	0.000	0.000	0.000
Na2O	0.644	0.589	0.594	0.644	0.596	0.960	0.930	1.003	0.940	0.990	1.410	1.445	1.383	1.450	1.367	0.230	0.330
K2O	15.878	15.774	15.767	15.623	15.523	15.311	15.311	15.122	15.322	15.443	14.744	14.678	14.566	14.554	14.334	14.334	16.421
Total	100.001	99.902	99.370	99.833	99.012	99.993	100.075	99.910	100.072	100.307	99.900	99.412	99.120	99.191	99.112	98.107	#####
Ions on the basis of 8 O																	
Fe	0.002	0.002	0.002	0.002	0.002	0.010	0.009	0.010	0.010	0.009	0.000	0.000	0.000	0.001	0.000	0.007	0.006
Mn	0.000	0.000	0.000	0.000	0.000	0.000	0.000	0.000	0.000	0.000	0.000	0.000	0.000	0.000	0.000	0.000	0.000
Mg	0.000	0.000	0.000	0.000	0.000	0.000	0.000	0.000	0.000	0.000	0.000	0.000	0.000	0.000	0.000	0.000	0.000
Ca	0.002	0.003	0.003	0.003	0.002	0.007	0.007	0.007	0.006	0.007	0.004	0.004	0.003	0.004	0.004	0.002	0.003
Ba	0.000	0.000	0.000	0.000	0.000	0.000	0.000	0.000	0.000	0.000	0.000	0.000	0.000	0.000	0.000	0.000	0.000
Na	0.058	0.053	0.054	0.058	0.054	0.087	0.084	0.090	0.085	0.089	0.127	0.130	0.125	0.131	0.123	0.021	0.030
K	0.943	0.936	0.936	0.927	0.921	0.909	0.909	0.898	0.910	0.917	0.875	0.871	0.865	0.864	0.851	0.851	0.975
Sum of A-Site	1.005	0.994	0.994	0.990	0.980	1.012	1.008	1.005	1.011	1.023	1.006	1.006	0.993	1.000	0.978	0.880	1.014
Al **(B-Site)**	1.015	1.010	1.000	1.012	1.000	1.000	1.004	1.006	1.002	1.004	1.012	1.005	1.006	1.009	1.012	1.012	1.006
Si	3.019	3.026	3.010	3.026	3.004	3.029	3.032	3.027	3.032	3.033	3.035	3.019	3.014	3.009	3.019	3.019	3.018
Ti	0.000	0.000	0.000	0.000	0.000	0.000	0.000	0.000	0.000	0.000	0.000	0.000	0.000	0.000	0.000	0.000	0.000
Sum of C-Site	3.019	3.026	3.010	3.026	3.005	3.029	3.032	3.027	3.032	3.034	3.035	3.019	3.014	3.009	3.019	3.020	3.018

Table A-6. Electron microprobe analysis of potassium feldspar, $KAlSi_3O_8$ (continued).

Simplified Formula: $A_1B_1C_3$

	Mousetrap			Eastman Topaz				
Wt. % oxides								
SiO2	64.789	66.998	67.656	67.898	67.987	64.777	64.877	64.986
TiO2	0.013	0.009	0.014	0.000	0.000	0.009	0.012	0.017
Al2O3	18.409	19.001	19.112	19.211	19.232	18.330	18.212	18.211
FeO	0.172	0.155	0.154	0.000	0.000	0.060	0.311	0.272
MnO	0.000	0.000	0.000	0.000	0.000	0.065	0.056	0.045
MgO	0.000	0.000	0.000	0.000	0.000	0.000	0.000	0.000
CaO	0.066	0.145	0.165	0.156	0.177	0.045	0.054	0.040
BaO	0.000	0.000	0.000	0.000	0.000	0.000	0.005	0.000
Na2O	0.340	11.223	11.184	11.223	11.334	0.845	0.566	0.654
K2O	16.330	0.340	0.454	0.545	0.448	15.560	15.767	15.677
Total	100.119	97.894	98.756	99.051	99.198	99.691	99.860	99.902
Ions on the basis of 8 O								
Fe	0.007	0.006	0.006	0.000	0.000	0.002	0.012	0.011
Mn	0.000	0.000	0.000	0.000	0.000	0.003	0.002	0.002
Mg	0.000	0.000	0.000	0.000	0.000	0.000	0.000	0.000
Ca	0.003	0.007	0.008	0.008	0.009	0.002	0.003	0.002
Ba	0.000	0.000	0.000	0.000	0.000	0.000	0.000	0.000
Na	0.031	1.013	1.009	1.013	1.023	0.076	0.051	0.059
K	0.969	0.020	0.027	0.032	0.027	0.924	0.936	0.931
Sum of A-Site	1.010	1.046	1.050	1.053	1.058	1.007	1.004	1.004
Al **(B-Site)**	1.010	1.042	1.048	1.054	1.055	1.005	0.999	0.999
Si	3.015	3.118	3.149	3.160	3.164	3.015	3.019	3.024
Ti	0.000	0.000	0.000	0.000	0.000	0.000	0.000	0.001
Sum of C-Site	3.016	3.118	3.149	3.160	3.164	3.015	3.020	3.025

VITA

Kristen Camp was born in New Orleans and raised in Slidell, Louisiana. She attended Salmen High School from 2000-2004. After receiving her diploma, she continued her education at the University of New Orleans, where she earned her Bachelor of Science in Geology with departmental and university honors in December, 2009.

Kristen conducted an undergraduate honors thesis under the guidance of William B. Simmons, Alexander U. Falster, and Karen Webber on the geochemistry and mineralogy of pegmatites associated with the Sebago batholith in Maine. She was so motivated by her advisors' passion for mineralogy and pegmatites that she returned for her master's degree. Upon completion of this thesis, her expected date of graduation with her Master of Science in Geology is December, 2011. The best way to contact Kristen is via email at kfcamp@uno.edu.